

# ENFOQUE



UTE  
REVISTA

Facultad Ciencias de la Ingeniería e Industrias  
eISSN:13906542



Volumen 15 • N°2 • Abril 2024

# Sumario

CHARACTERIZATION OF THE VEGETATION COMMUNITY AND ITS CONTRIBUTION TO A CARBON STOCK IN A DRY FOREST <i>Josselyn Muentes, Juan Manuel Moreira, César Chata, Antonella Alcívar, Iliana Zorrilla, Carlos A. Salas-Macías</i> .....	1
DISTRIBUTED CONGESTION CONTROL BASED ON UTILITY FUNCTION <i>Edison Segarra-Guzman, Patricia Ludeña-González</i> .....	9
CURRENT STATUS AND CHALLENGES OF IoT RESEARCH IN THE ECUADORIAN HEALTHCARE SECTOR: A SYSTEMATIC LITERATURE REVIEW <i>Cristina Vaca Orellana, and María Valle Dávila</i> .....	20
NUTRITIONAL PHYSIOLOGY OF <i>SPODOPTERA FRUGIPERDA</i> (J. E. SMITH) (LEPIDOPTERA: NOCTUIDAE) FED ON DIFFERENT WHEAT VARIETIES <i>Aqsa Amjad, Muhammad I. Ullah, Muhammad Arshad, Muhammad Z. Majeed, Rafia Umar, Nahdia Perveen, Muqadas Qadeer, Haroon Gul</i> .....	30
INVESTIGATION OF WIND EFFECTS ON UAV ADAPTIVE PID BASED MPC CONTROL SYSTEM <i>Andrés Santiago Martínez-León, Sergey Jatsun, Oksana Emelyanova</i> .....	36
EVOLUTION OF THE POLYGON OF THE PROTECTED NATURAL AREA “PARQUE NACIONAL SISTEMA ARRECIFAL VERACRUZANO” DUE TO THE EXPANSION OF THE PORT OF VERACRUZ, MEXICO <i>Xóchitl Citlalli Hernández-Silva, María del Refugio Castañeda-Chávez, Mario Díaz-González, Ángel Morán-Silva, Fabiola Lago-Reynoso, Olaya Pirene Castellanos-Onorio, Jesús Montoya-Mendoza, Manuel Alberto Susunaga-Mirada</i> .....	48

# Characterization of the Vegetation Community and its Contribution to a Carbon Stock in a Dry Forest

Josselyn Muentes<sup>1</sup>, Juan Manuel Moreira<sup>2</sup>, César Chata<sup>3</sup>,  
Antonella Alcívar<sup>4</sup>, Iliana Zorrilla<sup>5</sup>, Carlos A. Salas-Macías<sup>6</sup>

**Abstract** — The dry forest ecosystem is characterized by their rich biodiversity and adaptations to arid conditions. This study focused on determining the composition and structure of the vegetation, examining species interactions, and estimating carbon stored in its aboveground biomass (AGB) using an allometric equation proposed for mixed dry forests. We used 10 plots of 10 x 20 m to record data on trees with a diameter at breast height (DBH)  $\geq$  5 cm. Taxonomic classification was initially obtained using experts and specialized databases. Ecological importance was assessed through the Importance Value Index (IVI), and species association was determined using the Indicator Value Index (IndVal%). We identified 148 individuals of 21 species, 19 genera, and 12 families in four groups with strong associations, with *C. Trischistandra* standing out for its high IVI. The Kruskal-Wallis test did not show significant differences in carbon stored between plots, and was estimated a storage potential of 70.47 Mg C ha<sup>-1</sup>. This research highlights the importance of key species in carbon capture, which is crucial for mitigating climate change. Effective management of these species could have a positive impact on the conservation of the dry forest ecosystem and the fight against global warming. This analysis provides a deep understanding of the structure of this ecosystem.

**Keywords**— Allometry; Tree Diversity; Conservation; Carbon Estimation; Diameter Structure.

**Resumen** — El ecosistema del bosque seco se caracteriza por su rica biodiversidad y adaptaciones a condiciones áridas. Este estudio se centró en determinar la composición y estructura de la vegetación, examinar las interacciones entre las especies y estimar el carbono almacenado en su biomasa aérea (AGB), se usó una ecuación alométrica propuesta para bosques secos mixtos. Utilizamos 10 parcelas de 10 x 20 m para registrar datos sobre árboles con un diámetro a la altura del pecho (DAP)  $\geq$  5 cm. Inicialmente, la clasificación taxonómica se obtuvo consultando a expertos y bases de datos especializadas. La importancia ecológica se evaluó a través del Índice de Valor de Importancia (IVI) y la asociación de especies se determinó utilizando el Índice de Valor Indicador (IndVal%). Se identificaron 148 individuos de 21 especies, 19 géneros y 12 familias en cuatro grupos con fuertes asociaciones, destacándose *C. Trischistandra* por su alto IVI. El test de Kruskal-Wallis no mostró diferencias significativas en el carbono almacenado entre las parcelas y se estimó un potencial de almacenamiento de 70.47 Mg C ha<sup>-1</sup>. Esta investigación resalta la importancia de especies clave en la captura de carbono, lo cual es crucial para mitigar el cambio climático. El manejo efectivo de estas especies podría tener un impacto positivo en la conservación del ecosistema de bosque seco y en la lucha contra el calentamiento global. Este análisis brinda un entendimiento profundo de la estructura de este ecosistema.

**Palabras clave** — Alometría; Diversidad de árboles; Conservación; Estimación de carbono; Estructura de diámetro.

1 Carrera de Ingeniería Ambiental. Facultad de Ciencias Naturales y de la Agricultura. Universidad Estatal del Sur de Manabí. Jipijapa 130650, Ecuador, (e-mail: [josselyn.muentes@unesum.edu.ec](mailto:josselyn.muentes@unesum.edu.ec)). ORCID: <https://orcid.org/0000-0002-5362-8008>.

2 Jardín Botánico. Universidad Técnica de Manabí. Urbina 130105, Ecuador, (e-mail: [juan.moreira@utm.edu.ec](mailto:juan.moreira@utm.edu.ec)). ORCID: <https://orcid.org/0009-0005-3558-7272>.

3 Gobierno Autónomo Descentralizado Provincial de Manabí. Dirección de Ambiente y Riesgos. Manabí 130101, Ecuador, (e-mail: [cchata@manabi.gob.ec](mailto:cchata@manabi.gob.ec)). ORCID: <https://orcid.org/0009-0004-3064-5878>.

4 Carrera de Ingeniería Ambiental. Facultad de Ciencias Naturales y de la Agricultura. Universidad Estatal del Sur de Manabí. Jipijapa 130650, Ecuador, (e-mail: [maria.alcivar@unesum.edu.ec](mailto:maria.alcivar@unesum.edu.ec)). ORCID: <https://orcid.org/0000-0002-7950-146X>.

5 Maestría en Ecología, Gestión y Restauración del Medio Natural. Facultad de Biología. Universidad de Barcelona 08007, España, (e-mail: [iliana.zorrilla01@gmail.com](mailto:iliana.zorrilla01@gmail.com)). ORCID: <https://orcid.org/0009-0007-0093-9834>.

6 Departamento de Ciencias Agronómicas. Facultad de Ingeniería Agronómica. Universidad Técnica de Manabí. Km 15 vía Portoviejo-Santa Ana 131302, Ecuador, (e-mail: [carlos.salas@utm.edu.ec](mailto:carlos.salas@utm.edu.ec)). ORCID: <https://orcid.org/0000-0002-1641-1571>.

Manuscript Received: 15/08/2023

Revised: 15/11/2023

Accepted: 21/02/2024

DOI: <https://doi.org/10.29019/enfoqueute.990>

## I. INTRODUCTION

ACCORDING to six major international temperature datasets consolidated by the World Meteorological Organization [1], the last eight years have been the warmest on record globally. In 2022, the global average temperature exceeded pre-industrial levels (1850-1900) by approximately 1.15°C (ranging from 1.02°C to 1.27°C). These data are a cause for growing concern, especially considering the commitment established in the Paris Agreement to limit global warming to significantly below 2°C compared to pre-industrial levels and to strive for a 1.5°C limit by the year 2100. Unfortunately, 2022 marked the eighth consecutive year in which global annual temperatures have exceeded pre-industrial levels by at least 1°C, representing a significant challenge in achieving these crucial goals.

Forests play a crucial role in reducing greenhouse gas emissions (GHG) and mitigating climate change, as established by the United Nations Framework Convention on Climate Change (UNFCCC) [2]. Globally, forests store approximately 861 giga-

tons (Gt) of carbon, with 44 % in the soil, 42 % in live biomass, 8 % in dead wood, and 5 % in litter (equivalent to nearly a century of annual fossil fuel emissions). According to the World Bank [3], the carbon sink benefits of forests are diminished by deforestation and degradation, with 80 % of global deforestation being driven by agriculture. Between 2001 and 2021, emissions from deforestation and other forest disturbances were 8.8 gigatons Gt CO<sub>2</sub>e per year, while forest absorptions were -16.6 Gt CO<sub>2</sub>e per year, resulting in an average net sink of -7.7 Gt CO<sub>2</sub>e per year [4]. Forest biomass provides estimates of carbon stocks in forest vegetation, as approximately 50 % of it is composed of carbon. Over the last 22 years, forest absorptions in all climatic domains (tropical, subtropical, temperate, boreal) have exceeded emissions from forest disturbances [5].

In 2010, Ecuador had approximately 19.1 million hectares of natural forest, representing around 75 % of its total land area. However, by 2021, the country experienced a loss of 29.7 thousand hectares of natural forest, equivalent to an estimated release of 21.5 million tons of CO<sub>2</sub> into the atmosphere [6]. Four provinces (Sucumbíos, Orellana, Esmeraldas and Manabí) collectively accounted for 55 % of all tree cover loss during this period [7]. Taking Manabí as an example, it had 1.16 thousand hectares of natural forest at the beginning of the analyzed period, representing approximately 60 % of its territory. Unfortunately, by 2021, this province lost 473 hectares of natural forest, which is equivalent to the release of approximately 262 thousand tons of CO<sub>2</sub> [8]. Additionally, during the same period, Portoviejo also experienced significant tree cover loss. In 2010, the canton had 50.4 thousand hectares of forest, covering approximately 53 % of its land area. However, by 2022, the loss amounted to 9.46 hectares, with an estimated release of 5.01 kilotons of CO<sub>2</sub> into the atmosphere [9]. Currently, Ecuador hosts approximately 12.6 million hectares of native forest, representing around 50.73 % of its national territory. These data underscore the urgent need to take concrete measures to preserve and protect natural resources, as well as to comprehensively and effectively address the challenges associated with climate change in the country.

In the specific case of Ecuador, it was estimated that in the year 2000, the density of aboveground woody biomass was 253 tons per hectare, with a total aboveground biomass (AGB) of 4.54 gigatons. Subsequently, between 2001 and 2022, the country's forests showed annual emissions of 27.6 megatons of CO<sub>2</sub>e, while carbon removals reached -63.1 megatons of CO<sub>2</sub>e per year. This represents a net carbon sink of -35.5 megatons of CO<sub>2</sub>e per year [6]. These data are fundamental to understanding the role of forests as regulators of the carbon balance and their contribution to mitigating climate change [10].

Forest biomass is essential for estimating carbon stocks in forest vegetation and assessing changes in forest structure. The total biomass is derived from the difference between production through photosynthesis and consumption through respiration, making it a valuable measure to understand the state of forests [11]. However, it is important to highlight that forest biomass depends on its composition and structure. Therefore, preserving the integrity of forests and protecting them from deforestation and degradation is crucial to ensure their function as carbon sinks and make a significant contribution to the fight against climate change.

The main objective of this study was to determine the composition and structure of the vegetation, examining species interactions, and estimating carbon stored in its AGB using an allometric equation proposed for mixed dry forests. The resulting analysis intends to discuss the importance of the composition and structure of the ecosystem in terms of the carbon it can store. Subsequently, the results could serve as an important input for decision making for the conservation of tree species in the study area.

## II. METHODOLOGY

The study area is located in the forestal citadel at the southeastern of Portoviejo canton, in the province of Manabí, situated at coordinates -1.0187576 and -80.455844 (Figure 1). Field research was conducted during the period between July and August 2022. For data collection, 10 sampling plots measuring 10 x 20 m were established, resulting in a total area of 2 000 m<sup>2</sup>. In each plot, height and diameter at breast height (DBH) measurements were recorded for all trees with a DBH equal to or greater than 5 cm.

The taxonomic identification of species was carried out in two phases. Initially, valuable assistance was provided by local experts from the Jardín Botánico of the Universidad Técnica de Manabí (UTM), who contributed with their knowledge and experience to identifying the species present in the study area. Additionally, international databases such as WFO (The World Flora Online <http://www.worldfloraonline.org/>), International Plant Name Index (IPNI), Nomenclator from the Missouri Botanical Garden, and VAST (VAScular Trópicos / <https://www.tropicos.org/>) were used as complementary sources. These platforms provided precise and updated taxonomic information, ensuring rigor and accuracy in the classification of the studied species.

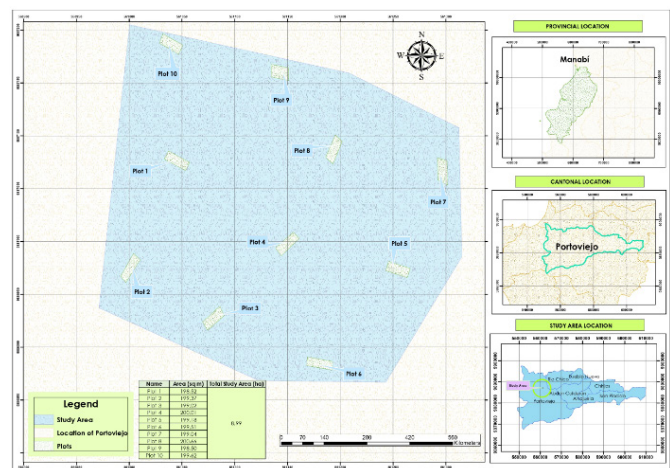


Fig. 1. Study area and plots.

### A. Composition and structure

A structural study was conducted based on taxonomic data encompassing four fundamental parameters to understand the ecology of the vegetation community:

**Abundance:** was analyzed the abundance of individuals per species in the sample. Were considered two types of abundan-

ce: absolute abundance ( $Ab_a$ ), which represents the total number of individuals per species, and relative abundance ( $Ab_r$ ), which shows the proportion of individuals of a species relative to the total number of individuals found in the study area.

Frequency: was determined the number of plots in which each species appears, evaluating both absolute frequency ( $Fr_a$ ) and relative frequency ( $Fr_r$ ). Relative frequency was calculated considering the number of plots in which a species appears in relation to the total number of inventoried plots.

Dominance: this parameter is related to the degree of coverage of species and was analyzed for both absolute dominance ( $Do_a$ ), which measures the basal area occupied by each species, and relative dominance ( $Do_r$ ), which shows the proportion of the absolute dominance of a species in relation to the absolute dominance of all species present.

Importance Value Index (IVI): proposed by Curtis & McIntosh [12], this index was calculated for each species by summing the relative abundance, relative frequency, and relative dominance. The IVI allows for comparing the ecological importance of each species within the forest, offering a comprehensive view of the composition, structure, site quality, and dynamics of the study area.

The exhaustive analysis of these parameters provided a complete understanding of the vegetation community in the studied forest. The evaluation of the IVI facilitated the understanding of the interaction between different species and their role in the ecological balance of the studied area.

Subsequently, using the absolute abundances of different species in each plot as input, a cluster analysis based on the Jaccard index was used to group the plots according to the similarity of their communities. From the obtained groups, the IndVal% was calculated along with the corresponding p-values for each species in each group of plots. IndVal% was used to measure the association of each species with a specific group, while p-values assessed the statistical significance of these associations.

Additionally, a diameter analysis was performed using 10 diameter classes with an interval of 18 cm to determine the structure of the forest under study.

### B. Carbon stored in AGB

The allometric equation proposed by [13] for mixed dry forests was applied to estimate the AGB of trees based on dendrometric variables. The variables used to feed the model were represented by total height (ht) in meters, diameter at breast height (DBH) in centimeters, and wood density ( $\rho$ ) in grams per cubic centimeter. To obtain wood density was used information from

the “Global wood density database” [14]. In cases where the data was not available was used the density of the genus, family [15], or an average of the individuals present in the plot.

Once the estimated AGB in kilograms of dry matter per tree was calculated, the total biomass per hectare ( $Mg\ ha^{-1}$ ) was determined. To achieve this, the biomass value obtained per plot was multiplied by a conversion factor that depended on the size of the plot. For the conversion of AGB to carbon were followed the guidelines established by the Intergovernmental Panel on Climate Change (IPCC) [16]. It was assumed that the carbon content in the AGB of each living tree is equivalent to 50 % of the AGB [17]. Thus, the amount of carbon in the AGB was obtained in megagrams per hectare ( $Mg\ C\ ha^{-1}$ ).

Once the data was collected, the Kruskal-Wallis test was used for the statistical analysis of the carbon values found per plot. This non-parametric test was chosen for its suitability to compare the means of three or more independent groups without assuming a normal distribution in the data. The Kruskal-Wallis test evaluated the null hypothesis that there are no significant differences in the amount of carbon stored among the plots of the dry forest. A typical significance level of 0.05 was established for the test.

## III. RESULTS

### A. Composition and structure

A total of 148 individuals belonging to 21 species within 19 genera and 12 families were identified (Table I). The *Fabaceae* family was the most diverse, with 44 individuals, followed by *Capparaceae* with 32 individuals, and *Malvaceae* with 25 individuals. Regarding abundance, it was determined that *C. Flexuosa* exhibited the highest absolute abundance (28 individuals) and relative abundance (19.18 %). This indicates that this species is dominant in terms of the number of individuals present in the study area. The species *E. Ruizii*, *C. Flexuosa* and *A. Macracantha* showed high relative frequency, suggesting that they are widely distributed in various plots within the dry forest area. On the other hand, *C. Trischistandra* displayed the highest absolute dominance ( $4.96\ m^2\ ha^{-1}$ ) and relative dominance (66.38 %), indicating that this species occupies a significant space within the forest and may have an important influence on the structure of the vegetation community. Furthermore, *C. Trischistandra* also stood out with the highest IVI value (77.39), suggesting that it plays a crucial role in the ecological balance of the dry forest.

TABLE I  
SPECIES, COMMON NAMES, GENUS, AND FAMILIES RECORDED IN THE STUDY AREA

Scientific name	Common name	Genus	Family
<i>Acacia macracantha</i> Humb. & Bonpl. ex Willd.	Guarango	Acacia	Fabacea
<i>Achatocarpus pubescens</i> C.H. Wright	Negrito	Achatocarpus	Achatocarpaceae
<i>Bauhinia aculeata</i> L.	Pata de vaca	Bauhinia	Fabaceae
<i>Bonellia sprucei</i> (Mez) B. Ståhl & Källersjö	Barbasco	Bonellia	Primulaceae

<i>Bursera graveolens</i> (Kunth) Triana & Planch.	Palo santo	Bursera	Burseraceae
<i>Caesalpinia coriaria</i> (Jacq.) Willd.	Cascol	Caesalpinia	Fabaceae
<i>Capparis flexuosa</i> (L.) L.	Sebastián	Capparis	Capparaceae
<i>Capparis inermis</i> Forssk.	Sebastián	Capparis	Capparaceae
<i>Capparis scabrida</i> Kunth	Zapote de perro	Capparis	Capparaceae
<i>Ceiba trischistandra</i> (A. Gray) Bakh.	Ceibo	Ceiba	Malvaceae
<i>Coccoloba ruiziana</i> Lindau	Patacón	Coccoloba	Polygonaceae
<i>Cochlospermum vitifolium</i> (Willd.) Spreng.	Bototillo	Cochlospermum	Bixaceae
<i>Colicodendron scabridum</i> (Kunth) Seem.	Zapote de perro	Colicodendron	Capparaceae
<i>Cordia lutea</i> Lam.	Moyuyo	Cordia	Cordiaceae
<i>Eriotheca ruizii</i> (K. Schum.) A. Robyns	Jaile	Eriotheca	Malvaceae
<i>Geoffroea spinosa</i> Jacq.	Seca	Geoffroea	Fabaceae
<i>Malpighia glabra</i> L.	Cerezo	Malpighia	Malpighiaceae
<i>Mimosa acantholoba</i> (Humb. & Bonpl. ex Willd.) Poir.	Litallo	Mimosa	Fabaceae
<i>Pithecellobium dulce</i> (Roxb.) Benth.	Tierra espino	Pithecellobium	Fabaceae
<i>Vasconcellea parviflora</i> A. DC.	Fosforito	Vasconcellea	Caricaceae
<i>Ziziphus thyrsoflora</i> Benth.	Ébano	Ziziphus	Rhamnaceae

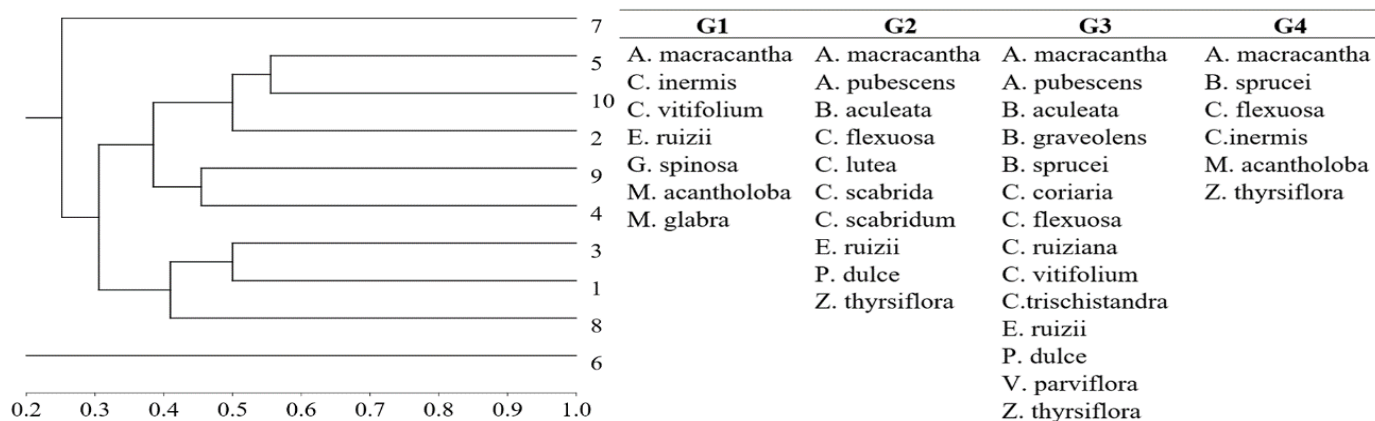


Fig. 2. Clustering of plots according to Jaccard index based on species similarity. Where: G1 = Group 1, G2 = Group 2, G3 = Group 3, G4 = Group 4.

Additionally, the species *E. Ruizii* and *C. Flexuosa* also exhibited considerable IVI values (36.87 and 33.54, respectively).

The clusters obtained through the cluster analysis and Jaccard index (Figure 2) result from the classification of the 10 plots based on the similarity of their species communities.

Group G1 consisted of:

- A. Macracantha*
- C. Inermis*
- C. Vitifolium*
- E. Ruizii*
- G. Spinosa*
- M. Acantholoba*
- M. Glabra*

Group G2 included:

- A. Macracantha*
- A. Pubescens*
- B. Aculeata*
- C. Flexuosa*
- C. Lutea*
- C. Scabrida*
- C. Scabridum*
- E. Ruizii*
- P. Dulce*
- Z. Thyrsoflora*

Group G3 comprised:

- A. Macracantha*
- A. Pubescens*

*B. Aculeata*  
*B. Graveolens*  
*B. Sprucei*  
*C. Coriaria*  
*C. Flexuosa*  
*C. Ruiziana*  
*C. Vitifolium*  
*C. Trischistandra*  
*E. Ruizii*  
*P. Dulce*

*V. Parviflora*  
*Z. Thyrsiflora*

Lastly, Group G4 consisted of:

*A. Macracantha*  
*B. Sprucei*  
*C. Flexuosa*  
*C. Inermis*  
*M. Acantholoba*  
*Z. Thyrsiflora*

TABLE II  
 INDICATOR VALUE INDEX (INDVAL%) ALONG WITH CORRESPONDING P-VALUES FOR EACH SPECIES IN EACH GROUP OF PLOTS

Species	Group 1		Group 2		Group 3		Group 4	
	indVal%	p	indVal%	p	indVal%	p	indVal%	p
<i>A. Macracantha</i>	5.814	0.691	7.752	0.670	4.186	0.905	75.580	0.060
<i>A. Pubescens</i>	0.000	1.000	47.620	0.112	17.140	0.413	0.000	1.000
<i>B. Aculeata</i>	0.000	1.000	25.640	0.241	9.231	0.483	0.000	1.000
<i>B. Graveolens</i>	0.000	1.000	0.000	1.000	20.000	0.498	0.000	1.000
<i>B. Sprucei</i>	0.000	1.000	0.000	1.000	20.000	0.262	66.670	0.037
<i>C. Coriaria</i>	0.000	1.000	0.000	1.000	20.000	0.490	0.000	1.000
<i>C. Flexuosa</i>	0.000	1.000	30.000	0.315	30.000	0.318	40.000	0.124
<i>C. Inermis</i>	100.000	0.099	0.000	1.000	0.000	1.000	0.000	1.000
<i>C. Lutea</i>	0.000	1.000	33.330	0.299	0.000	1.000	0.000	1.000
<i>C. Ruiziana</i>	0.000	1.000	0.000	1.000	20.000	0.507	0.000	1.000
<i>C. Scabrida</i>	0.000	1.000	33.330	0.299	0.000	1.000	0.000	1.000
<i>C. Scabridum</i>	0.000	1.000	33.330	0.302	0.000	1.000	0.000	1.000
<i>C. Vitifolium</i>	35.710	0.272	0.000	1.000	51.430	0.067	0.000	1.000
<i>C. Inermis</i>	0.000	1.000	0.000	1.000	0.000	1.000	100.000	0.100
<i>C. Trischistandra</i>	0.000	1.000	0.000	1.000	100.000	0.004	0.000	1.000
<i>E. Ruizii</i>	32.610	0.203	21.740	0.445	36.520	0.209	0.000	1.000
<i>G. Spinosa</i>	100.000	0.099	0.000	1.000	0.000	1.000	0.000	1.000
<i>M. Acantholoba</i>	25.000	0.196	0.000	1.000	0.000	1.000	75.000	0.100
<i>M. Glabra</i>	100.000	0.099	0.000	1.000	0.000	1.000	0.000	1.000
<i>P. Dulce</i>	0.000	1.000	20.830	0.398	7.500	0.546	0.000	1.000
<i>V. Parviflora</i>	0.000	1.000	0.000	1.000	20.000	0.509	0.000	1.000
<i>Z. Thyrsiflora</i>	0.000	1.000	52.630	0.062	1.579	0.938	39.470	0.316

Certain species showed significantly high IndVal% values in specific groups of plots, suggesting a strong association with those specific communities (Table II). In this regard, it was observed that although *A. Macracantha* does not exhibit very high values, it is associated with the other species present in all groups, with a predominant tendency towards Group 4. *C. Inermis*, *G. Spinosa*, and *M. Glabra* displayed IndVal% values of 100 % in Group 1, demonstrating that they can be considered indicators of those particular communities.

The species *C. Trischistandra* and *B. Sprucei* showed interesting patterns regarding their association with different groups of plots in the dry forest. On one hand, the IndVal% for *C. Trischistandra* in Group 3 was 100 %, indicating that it is highly represented in this group and shows a strong association with the other species present in it ( $p < 0.05$ ). On the other hand, *B. Sprucei* exhibited a similar behavior in terms of IndVal% (66.67 %) and p-value (0.037). In both cases, considering the p-value, it can be determined that these associations are not

random and are statistically significant. This suggests that both species may have specific characteristics that make them prefer the environmental conditions and coexisting species in each of the mentioned groups.

The diametric analysis resulted in a reverse J-shaped distribution (Figure 3) [18]. This distribution refers to the configura-

tion of the diameter structure of a forest, where there is a predominance of young and small-diameter individuals, followed by a marked decrease in density in intermediate diameters, and finally, an increase in the number of individuals as the diameter increases. This curve represents a typical pattern of natural regeneration and development of the forest community [19].

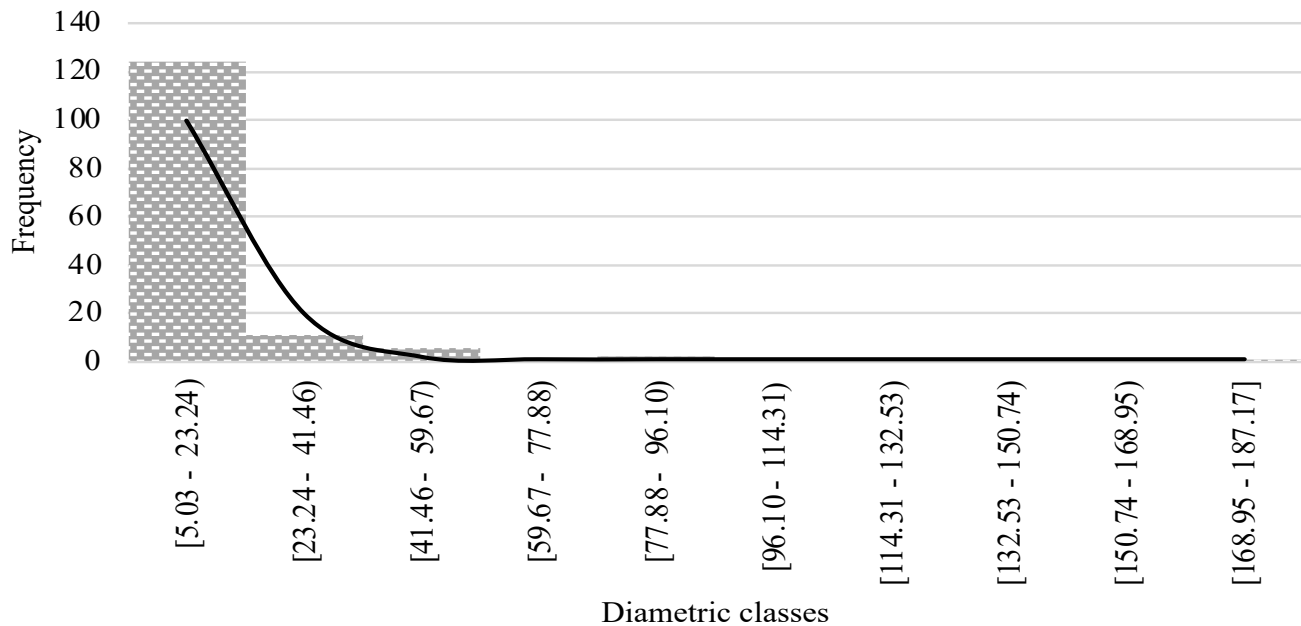


Fig. 3. Diameter structure of individuals present in the study area.

The origin of this distribution can be influenced by various factors, such as the history of natural or anthropogenic disturbances [20], the interaction between different strata of the forest and the regeneration capacity of the present species [21]. In any case, this type of distribution can indicate efficient biological functionality, strong recruitment capacity, a healthy state and a stable population [22].

In any case, the young individuals, which make up the lower diameter classes, are often the product of recent regeneration or succession events [23], which may be associated with selective logging or biotic factors. These conditions create open spaces where certain tree species establish and compete for resources, leading to a high density of small-sized young individuals [24].

As these trees mature and survive competition, they grow and become the individuals that form the wider part of the reverse J-shaped curve, i.e., the trees with intermediate diameters. At this stage, the process of self-thinning and interspecific competition becomes more noticeable, resulting in a thinning of tree density [25]. Some weaker trees may die or be outcompeted by more vigorous individuals adapted to the environment, contributing to the reduction of density in this zone of the curve.

Finally, in the right side of the reverse J-shaped curve, we find the largest and oldest trees. These individuals have overcome the earlier stages of development, withstood disturbances, and successfully competed for limited resources. Their presen-

ce indicates greater stability and longevity within the forest ecosystem [26].

Understanding the reverse J-shaped diametric distribution is essential for making informed decisions in sustainable forest management [27]. By analyzing this curve, forest managers can assess the regeneration status, evaluate the structure and health of the forest, and plan management strategies that promote proper regeneration, optimal growth of desirable species, and conservation of natural resources. Moreover, this knowledge enables addressing challenges such as the conservation of threatened species, mitigation of the effects of climate change and promotion of forest resilience to future disturbances [28].

### B. Carbon stored in AGB

The Kruskal-Wallis test did not yield sufficient evidence to claim the existence of statistically significant differences in the amount of carbon stored in the different plots of the dry forest. However, it was possible to observe that certain species store more carbon than others, primarily because they are more abundant in the plots, have larger diameters, heights or wood density (Figure 4). In this regard, it was determined that the study area can store  $70.47 \text{ Mg C ha}^{-1}$  in AGB. These values are somewhat higher than those found by the Ministry of the Environment [29] and [30] possibly due to the composition and structure of the forest.

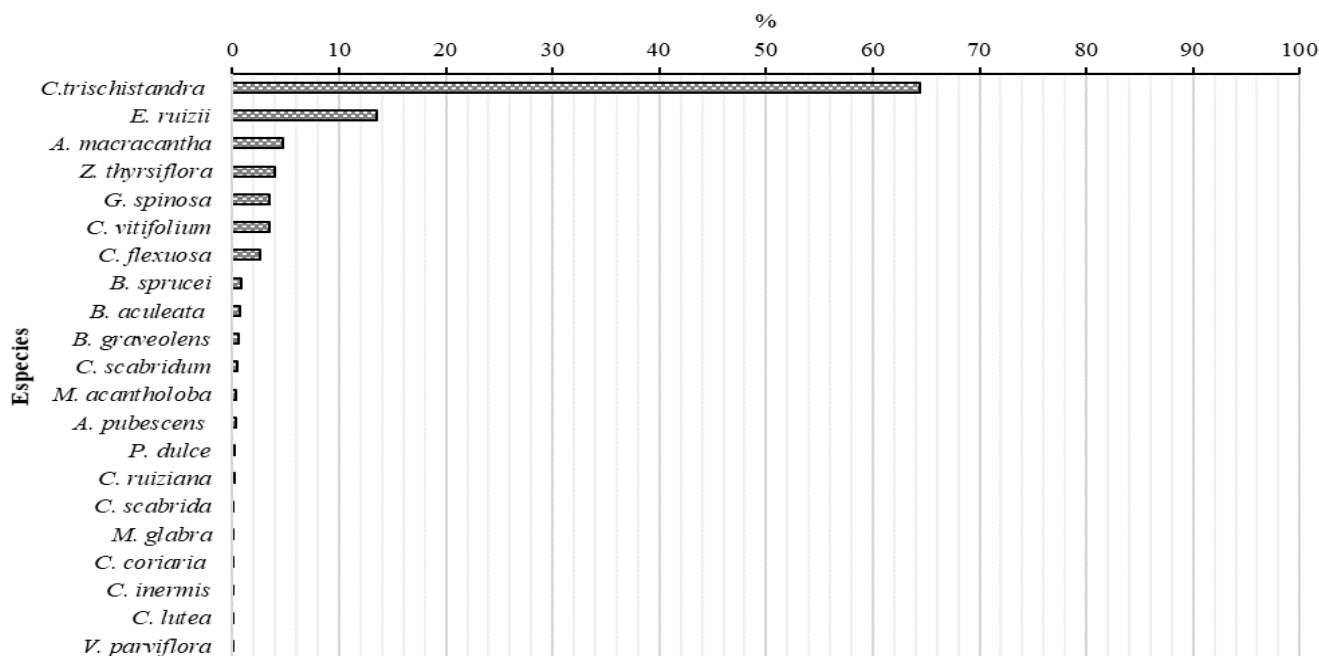


Fig. 4. Contribution of each species (%) to the total carbon stored in the study area.

#### IV. CONCLUSION

The results of the structural analysis in this study provide a detailed and revealing insight into the composition and structure of this ecosystem. Species with higher abundance, frequency, and dominance — as well as those with significant IndVal% values— are of particular relevance for understanding the dynamics and ecology of the dry forest. These findings help identify which species play key roles in the community and which may serve as indicators of specific conditions.

It is essential to note that the analysis of species clusters should consider not only the structural parameters of the forest but also relevant environmental factors. These factors can influence the distribution and coexistence of species, and their consideration is vital to fully comprehend the observed clustering patterns. The obtained results may vary based on spatial scale and study area, necessitating detailed analyses in different sites to gain a more comprehensive understanding of the variability in the plant community of the dry forest.

In this regard, the results of this study may have significant implications for estimating carbon stored in live AGB in the dry forest. Species with high IndVal% values and abundance could be significant contributors to the total AGB of the ecosystem. Therefore, the conservation and effective management of these species could have a positive impact on carbon capture and storage, which is relevant in the context of climate change and efforts to mitigate the effects of global warming.

#### V. REFERENCES

[1] OMM. (2023). *Los últimos ocho años han sido los más cálidos jamás registrados a nivel mundial*. [Online]. Available: <https://wmo.int/es/media/news/los-ultimos-ocho-anos-han-sido-los-mas-calidos-jamas-registrados-nivel-mundial>.

[2] FAO y PNUMA, “El estado de los bosques del mundo 2020. Los bosques, la biodiversidad y las personas”, ONU, Programa para el medio ambiente, Roma, 2020. Available: <http://doi.org/10.4060/ca8642es>

[3] Banco Mundial (18 Marzo 2016). Por qué los bosques son fundamentales para el clima, el agua, la salud y los medios de subsistencia. [Online]. Available: <https://www.bancomundial.org/es/news/feature/2016/03/18/why-forests-are-key-to-climate-water-health-and-livelihoods#:~:text=Los%20bosques%20son%20los%20principales,que%20contribuye%20al%20cambio%20clim%C3%A1tico>

[4] N. Harris, D. Gibbs, A. Baccini, R. Birdsey, S. de Bruin, M. Farina, L. Fatoyinbo, M. Hansen, M. Herold, R. Houghton, P. Potapov, D. Requeena, R. Roman, S. Saatchi, C. Slay, S. Turubanova, A. Tyukavina. “Global Maps of Twenty-First Century Forest Carbon Fluxes,” *Nature Climate Change*, vol. 11, pp. 234-240, 2021, doi: 10.1038/s41558-020-00976-6

[5] FAO, “Global Ecological Zones for FAO Forest Reporting: 2010 update”, *Food and Agriculture Organization of the United Nations*, Rome, 2012. Available: <https://www.fao.org/3/ap861e/ap861e00.pdf>

[6] Global Forest Watch. (2023). Forest-related greenhouse gas fluxes in Ecuador [Online]. Available: <https://gfw.global/3S71kT7>

[7] Global Forest Watch. (2023). Location of Tree Cover Loss in Ecuador [Online]. Available: <https://gfw.global/499SM4j>

[8] Global Forest Watch. (2023). Tree Cover Loss in Ecuador/Manabí [Online]. Available: <https://gfw.global/3NREGvp>

[9] Global Forest Watch. (2023). Tree Cover Loss in Manabí/Portoviejo [Online]. Available: <https://gfw.global/3S7PCGL>

[10] World Resources Institute, *Global Forest Review*. (2023). What is Carbon Dioxide Equivalent? [Online]. Available: <https://research.wri.org/gfr/biodiversity-ecological-services-indicators/greenhouse-gas-fluxes-forests>

[11] S. Brown, *Estimating Biomass and Biomass Change of Tropical Forests: a Primer. (FAO Forestry paper-134)*. Rome: Food and Agriculture Organization of the United Nations, 1997, ISBN 92-5-103955-0

[12] J. Curtis, R. McIntosh, “An Upland Forest Continuum in the Prairie-Forest Border Region of Wisconsin,” *Ecology*, vol. 32, no. 3, pp. 476-496, 1951, doi: 10.2307/1931725

[13] J. Chave, C. Andalo, S. Brown, M. Cairns, J. Chambers, D. Eamus, H. Fölster, F. Fromard, N. Higuchi, T. Kira, J.P. Lescure, B. Walker, H. Ogawa, H. Puig, B. Riera, T. Yakamura, “Tree Allometry and Improved Estimation of Carbon Stocks and Balance in Tropical Forests”, *Oecologia*, vol. 145, no. 1, pp. 81-99, 2005, doi: 10.1007/s00442-005-0100-x

[14] A. E. Zanne, G. Lopez-Gonzalez, D. A. Coomes, J. Ilic, S. Jansen, S. L. Lewis, R. B. Miller, N. G. Swenson, M. C. Wiemann, J. Chave,

- “Global Wood Density Database”, *Dryad*, vol. 235, 2009, doi: <https://doi.org/10.5061/dryad.234>
- [15] E. Honorio, T. Baker, *Manual para el monitoreo del ciclo del carbono en bosques amazónicos*. Lima: Instituto de Investigaciones de la Amazonia Peruana, 2010.
- [16] J. Penman, M. Gytarsky, T. Hiraishi, T. Krug, D. Kruger, R. Pipatti, L. Buendia, K. Miwa, T. Ngara, K. Tanabe, F. Wagner. “Good Practice Guidance for Land Use, Land-Use Change and Forestry”, IPCC, Japan: IGES, 2003. ISBN 4-88788-003-0. [https://www.ipcc.ch/site/assets/uploads/2018/03/GPG\\_LULUCF\\_FULLEN.pdf](https://www.ipcc.ch/site/assets/uploads/2018/03/GPG_LULUCF_FULLEN.pdf)
- [17] T. Barrett, “Storage and Flux of Carbon in Live Trees, Snags, and Logs in the Chugach and Tongass National Forests” *Pacific Northwest Research Station*, Portland, 2014. doi:10.2737/pnw-gtr-889.
- [18] O. Chadwick, L. Bruce, *Forest Stand Dynamics*, New York: John Wiley & Sons, 1996. ISBN 9780471138334
- [19] Z. Qiu, M. Zhang, K. Wang, F. Shi, “Vegetation Community Dynamics During Naturalized Developmental Restoration of Pinus Tabulaeformis Plantation in North Warm Temperate Xone” *Journal of Plant Ecology*, vol. 16, no. 4, 2023.
- [20] H. Cotler, P. Ortega-Larrocea, “Effects of Land Use on Soil Erosion in a Tropical Dry Forest Ecosystem, Chamela Watershed, Mexico” *CATENA*, vol. 65, no. 2, pp. 107-117, 2006, doi: 10.1016/J.CATENA.2005.11.004
- [21] N. T. Pao, K. Upadhaya, “Effect of Fragmentation and Anthropogenic Disturbances on Floristic Composition and Structure of Subtropical Broad Leaved Humid Forest in Meghalaya, Northeast India” *Applied Ecology and Environmental Research*, vol. 15, no. 4, 2017.
- [22] A. Berhanu, S. Demissew, W. Zerihun, M. Didita, “Woody Species Composition and Structure of Kuandisha Afromontane Forest Fragment, Northwestern Ethiopia”, *Journal of Forestry Research*, vol. 28, no. 2, pp. 343-355, 2017.
- [23] G. Tesfaye, D. Teketay, M. Fetene, “Regeneration of Fourteen Tree Species in Harena Forest, Southeastern Ethiopia” *Flora*, vol. 197, no. 6, pp. 461-474, 2002, doi: 10.1007/s11676-016-0329-8
- [24] J. Denslow, “Patterns of Plant Species Diversity During Succession Under Different Disturbance Regimes”, *Oecologia*, vol. 46, no. 1, pp. 18-21, 1980, doi: 10.1007/BF00346960
- [25] X. Li, S. D. Wilson, Y. Song, “Secondary Succession in Two Subtropical Forests” *Plant Ecology*, vol. 143, no. 1, pp. 13-21, 1999.
- [26] H. A. Meyer, “Structure, Growth, and Drain in Balanced Uneven-Aged Forests” *Journal of Forestry*, vol. 50, No. 2, pp. 85-92, 1952.
- [27] H. H. Koricho, G. Shumi, T. Gebreyesus, S. Song, F. Fufa, “Woody Plant Species Diversity and Composition in and Around Debre Libanos Church Forests of North Shoa Zone of Oromiya, Ethiopia”, *Journal of Forestry Research*, vol. 32, no. 5, pp. 1929-1939, 2021, doi: 10.1007/s11676-020-01241-4
- [28] M. C. Wilson, X. Y. Chen, R. T. Corlett, R. K. Didham, P. Ding, R. D. Holt, M. Holyoak, G. Hu, A. C. Hughes, L. Jiang, W. F. Laurance, J. Liu, S. L. Pimm, S. K. Robinson, S. E. Russo, X. Si, D. S. Wilcove, J. Wu, M. Yu, “Habitat Fragmentation and Biodiversity Conservation: Key Findings and Future Challenges” *Landscape Ecology*, vol. 31, no. 2, pp. 219-227, 2016, doi: 10.1007/s10980-015-0312-3
- [29] Ministerio del Ambiente, “Estadísticas de Patrimonio Natural del Ecuador continental” Quito, Ecuador, 2018. [Online]. Available: [https://proamazonia.org/wp-content/uploads/2019/10/ECUADOR\\_Folleto\\_Patrimonio\\_Natural\\_compressed.pdf](https://proamazonia.org/wp-content/uploads/2019/10/ECUADOR_Folleto_Patrimonio_Natural_compressed.pdf)
- [30] C. Salas, K. Montes, G. Sanchez, W. Alcívar, A. Murillo, F. Vera, D. Bolcato, S. Iglesias, “Influencia del gradiente altitudinal sobre la estimación del carbono almacenado en biomasa aérea viva y en suelos del ‘Bosque y vegetación protector El Artesan – EcuadorianHands’. Joa, Jipijapa” *Ecosistemas*, vol. 29, no. 2, 2020. <https://doi.org/10.7818/ECOS.1973>

# Distributed Congestion Control Based on Utility Function

Edison Segarra-Guzman<sup>1</sup>, Patricia Ludeña-González<sup>2</sup>

**Abstract**—This paper introduces the Distributed Utility Function Algorithm (D-AFU) as a notable progression in managing and optimizing network traffic within distributed settings. Based on the utility function principle, D-AFU dynamically adjusts data rate in response to ever-changing network demands, with optimal performance and a higher user experience. Contrary to the centralized model, D-AFU employs a distributed, scalable and resilient against failures and system overloads mechanism. Its efficiency was validated using the NS-3 simulator. Three main metrics were used: the data rate allocation, utility per session, and fairness (quantified by the Gini coefficient). D-AFU displays exceptional performance and low latency, particularly vital for real-time applications with high Quality of Service (QoS) requirements.

**Keywords** - Congestion Control, Utility Function, Real-Time applications, Elastic Applications, Distributed Optimization, Proactive Algorithm.

**Resumen**—El artículo presenta el Algoritmo de Función de Utilidad Distribuida (D-AFU) como una notable evolución en la gestión y optimización del tráfico de red en entornos distribuidos. Basado en el principio de función de utilidad, D-AFU ajusta dinámicamente la velocidad de datos en respuesta a las demandas cambiantes de la red, con un rendimiento óptimo y una mejor experiencia para el usuario. A diferencia del modelo centralizado, D-AFU emplea un mecanismo distribuido escalable y con mayor resistencia contra fallos y sobrecargas del sistema. Su eficiencia fue validada utilizando el simulador NS-3. Se utilizaron tres métricas principales: la tasa de asignación de transmisión, la utilidad por sesión y la equidad (cuantificada por el coeficiente de Gini). D-AFU mostró un rendimiento excepcional, especialmente vital para aplicaciones en tiempo real que exigen alta Calidad de Servicio (QoS) y baja latencia.

**Palabras Clave** - Control de congestión, Función de Utilidad, Aplicaciones en Tiempo Real, Aplicaciones Elásticas, Optimización Distribuida, Algoritmo Proactivo.

## I. INTRODUCTION

**I**N recent years, data networks users have increased considerably. It causes big information quantity be transferred in and between networks, demanding more links capacity in them. Nowadays, everyone wants to be always connected by shortening distances, thus telecommunications are a critical factor and optimization of available resources is required to

guarantee QoS. This mission comes with great challenges. Table I shows the number of devices currently connected to the Internet [1].

Problems such as limited memory resources in routers and bandwidth in links, generate network congestion, according to Kurose [2]. It causes packet loss and delay, therefore, in the literature the occurrence of these phenomena is considered a clear sign of congestion. Congestion causes packets to be retransmitted, affecting network performance. For this reason, throughout the networks evolution, several methods have been developed to control congestion and thus provide an efficient and reliable way to transmit data. Traditional congestion control protocols work by using a window to limit the amount of data a source can transmit to the network. The congestion window is a measure of the amount of data the remitter can send without receiving an acknowledgment from the destination. These protocols implement a flow control mechanism that prevents a source from sending more data than a receiver can process [3]. To reach the optimal congestion window, start with a low transmission rate and slowly increase it until fill the capacity of the network. Although these algorithms are widely used, their application in modern networks is inefficient, since they take a long time to reach full network capacity, so they are being replaced by more sophisticated protocols that avoid congestion without affecting network capacity utilization [4]. This paper provides a detailed and critical analysis of existing congestion control algorithms and presents an innovative approach that improves the efficiency of data transmission in networks. It uses utility function to assign data rate, following Max–Min fairness criterion. Thus, it contributes to the academic debate on congestion control in data networks, and provides a practical and feasible solution. It can serve as a starting point for future research and development in this knowledge area.

## II. STATE OF THE ART

Congestion control is one of the most crucial issues in the field of networks, due to its direct impact on performance and quality of service. This aspect becomes even more relevant in the face of increasing network traffic demand.

Based on their behavior in response to congestion, the algorithms can be classified into two main categories [5]: - Proactive: They prevent congestion even before it occurs. These algorithms evaluate the state of the network taking measures periodically and determine the optimal transmission rates or window sizes before starting data transmission, anticipate congestion problems.

<sup>1</sup>Edison Segarra-Guzmán. Of Universidad Técnica Particular de Loja, (e-mail: eesegarra@utpl.edu.ec). ORCID number 0009-0006-9784-434X.

<sup>2</sup>Patricia Ludeña-González. Of the Departamento de Ciencias de la Computación y Electrónica, Universidad Técnica Particular de Loja, (e-mail: pjludeña@utpl.edu.ec). ORCID number 0000-0002-8909-4837.

TABLE I  
COMPARISON OF INTERNET USE BETWEEN 2017 AND 2022.

Year	Internet users (billions)	Devices and connections (billions)	Bandwidth	Video applications
2017	3.4	18.0	39.0 Mbps	75%
2022	4.8	28.5	75.4 Mbps	82%

- Reactive: After the congestion occurs these algorithms take necessary measures to counteract it. In large networks, a large number of packets may even be discarded, causing packet retransmission and generating communication delays, before the congestion is detected. It combines the pro-activity in the sense that it dynamically calculates the available bandwidth and adjusts the congestion window and the reactive part. For example, it is like Transmission Control Protocol (TCP) (Tahoe, Reno, NewReno, among other) works. It reacts to variations in the packet loss rate, RTT and throughput to calculate the congestion control factor and adjust the CWND [3].

According to Alizadeh [6], the search for new methods for congestion control for data centers is because they react to congestion after it has already occurred, this can lead to performance degradation and packet loss, on the one hand, small windows of the key features of the two protocols: Slow start when first establishing a TCP connection, the sender starts with a small window size and gradually increases the window as packets are acknowledged. These two mechanisms work together to adjust TCP's transmission rate to network conditions. 'Slow start' allows TCP to quickly 'bootstrap' to a reasonable congestion window size, while Additive Increment, Multiplicative Decrement (AIMD) allows TCP to adjust the sending rate in response to congestion once the connection is up and running. It mitigates congestion by incrementally scaling the volume of traffic transmitted over the network. Upon reaching a predefined threshold, the sender transitions into congestion prevention mode. In this mode, the sender incrementally expands the window size for each acknowledgment received, thereby proactively averting network congestion.

Both are effective in preventing congestion and guaranteeing reliable delivery of data [7] but are not optimal for datacenter deployments because they are designed for long-lived connections with slow startup phases and congestion avoidance.

Modern congestion control algorithms are proactive. However, they are more complex than traditional congestion control algorithms and may not be suitable for all networks. Constant monitoring may generate additional overhead on network resources, which could negatively affect overall performance. Then, proactive algorithms have a higher processing load than reactive algorithms.

According to Ludeña-González, López-Presa and Muñoz [8] proactive congestion control through explicit rate control (ERC) mechanisms has been proposed as a viable alternative to improve efficiency and fairness in communication networks. These algorithms calculate explicit rates to improve convergence time and ensure a fair distribution of resources among competing sessions.

Shiyong Li [9] considers the problem of bandwidth allocation in peer-to-peer (P2P) networks which are a type of decentralized network where users can share resources with

each other, a new approach for bandwidth allocation based on utility optimization is proposed. The paper considers two types of services: elastic services and inelastic services. Elastic services are services that can adapt to the available bandwidth and inelastic services are services that must have a constant bandwidth. The bandwidth allocation scheme is based on a gradient-based algorithm. It works by finding the direction of greatest increase (or decrease, depending on the context) in a function, and then updating the parameters (in this case, the bandwidth allocation for different data flows) in that direction [10].

In Bahnasy work [11], a distributed congestion avoidance algorithm that functions at both the Ethernet layer and the TCP layer, is proposed and named Ethernet Congestion Control Zero-tailed Congestion Control Protocol (ECCP). It controls data traffic according to the estimated available bandwidth over a network path and attempts to keep link occupancy below the maximum capacity by a percentage called the Availability Threshold. Each node in the network maintains a link capacity table, when a node receives a packet, it updates its fields for the link on which the packet was received, then the node uses that link data (capacity) to estimate the available network bandwidth. To control the transmission rates of the sessions each node maintains a flow table. When a node receives a packet, it updates the rate table for the flow that sent the packet. Then, the node, once its session table is updated, calculates the maximum transmission rate for each flow.

Adams indicates in his research conclusions that working with active queue management (AQM) is an important technique for congestion control in data networks. [12] AQM algorithms can be used to improve network performance by reducing packet loss, queuing delay, and throughput reduction. Random Early Detection (RED) algorithm is part of the AQM family. It is used to avoid congestion by randomly discarding packets when the queue length exceeds a certain threshold. When congestion occurs, the queue length of a router interface increases which can cause delays for packets entering in a queue order and can even cause packets to be lost. However, it is inefficient in cases where, according to Varma [13], the number of connections passing through the link becomes too small, or the latency and capacity for the connection becomes too great.

Shuihai Hu, et. al., [14] also notes that proactive congestion control algorithms have been proposed to improve the performance of data center networks by explicitly scheduling data transmissions based on network bandwidth availability. However, these algorithms can perform poorly for small flows, which typically have short durations and low bandwidth requirements, so they propose as a solution a new algorithm called Aeolus. It addresses the problem of poor performance for small flows, in turn allows new flows to start at line

rate or the full available link capacity and then selectively discard excess unscheduled packets once congestion occurs, the protocol is evaluated through simulations with realistic workloads, provides support for simulation of a variety of network protocols at various levels, allowed researchers to model and analyze the performance of networks under different conditions [15]. Showing that the algorithm can significantly speed up small flows, for example, offering 55.9 % less 99th percentile completion time, while retaining all the good properties of proactive solutions. It functions by maintaining two separate queues for each flow: a scheduled queue and an unscheduled queue. When a new flow arrives, adds its packets to the scheduled queue and starts sending them at line rate. If congestion occurs, starts discarding packets from the unscheduled queue. When congestion is low, increases the size of the scheduled queue, allowing more packets to be sent at line speed [14]. The paper ‘Accurate Congestion Control for RDMA Transfers’ by Dimitris Giannopoulos et al. [16] proposes a new congestion control protocol for Remote Direct Memory Access (RDMA) transfers technology that allows two computers to exchange data directly from their memory without involving the operating system or CPU. ACCurate is crafted to embody efficiency and fairness in congestion control. Its precision is achieved through an algorithm dedicated to estimating available bandwidth. The efficiency is notable as it doesn’t necessitate the maintenance of per-flow state within the network. Moreover, its commitment to fairness is evident in its assignment of accurate Max–Min fair rates to all flows. The novelty of ACCurate lies in its hardware-based design and implementation for congestion control. Through comprehensive performance evaluations conducted under diverse loads, the results demonstrate that it surpasses TCP-derived protocols and RDMA PAUSA-only in terms of flow completion times and fairness.

In addition, for data centers, Mahmoud Bahnasy and Halima Elbiaze [17] indicates how data centers have evolved from a common Ethernet network to a new era of data-intensive applications such as remote direct memory access, high performance computing and cloud computing, which pose new challenges for researchers, requiring minimal network latency, no packet loss and fairness between flows. Faced with the problem posed the authors propose the congestion control protocol for converged data access (DCB) networks (called HetFlow) is designed to achieve fairness between flows of different packet sizes and different RTTs by using a per-flow delay-based congestion control algorithm to adjust the sending rate using feedback messages in each flow based on the measured delay.

It is important to clarify that this protocol is within the congestion control group at the Ethernet layer, unlike protocols such as the Data-Center TCP (DCTCP) which are within the congestion control protocols of the transport layer and its Functionality leverages explicit congestion notification (ECN) in the network to provide multi-bit feedback to end hosts, when a switch detects congestion, marks packets with the Congestion Experienced (CE) code point. DCTCP hosts observe these markings and reduce their sending rate accordingly, this helps to keep queue occupancy low, which influences low latency

and high throughput, it is more resilient to bursts of traffic and is currently one of the most widely used protocols in datacenters. It uses a multiplicative decrementing algorithm of additive increase to recover from congestion [6].

Congestion control in data centers presents challenges due to RTTs expressed in microseconds, the arrival of bursty flows, and a large number of concurrent flows [18]. These factors can force a flow to send at most one packet per RTT or induce a large backlog in the queue. The widespread use of switches with short buffers further exacerbates the problem, as hosts generate multiple flows in bursts. As link speeds increase, algorithms that gradually seek bandwidth take considerable time to reach their fair share. This is why Cho, Jang, and Han [18] propose ExpressPass, a credit-scheduled, end-to-end, delay-scheduled congestion control algorithm for data centers. It uses credit packets to manage congestion, even before sending data packets, leading to bounded delay and fast convergence. This approach handles bursty flow arrivals, for implementation, the results ExpressPass converges up to 80 times faster than DCTCP on 10 Gbps links and the gap increases as link speeds increase. It significantly improves performance under heavy incast workloads and significantly reduces flow completion times [18]. Into wireless networks the authors M. Singh S, et. al, [19] propose the Dynamic TCP (D-TCP) algorithm. It learns the available bandwidth and adjusts the congestion window. It first estimates the available bandwidth using a combination of methods, such as packet loss rate, RTT, and throughput. Once the available bandwidth is estimated, it uses this information to calculate a congestion control factor. Then, this factor is used to adjust the congestion window, which is the amount of data a sender can send before receiving an acknowledgment, D-TCP attempts to adaptively bring the CWND to the previous state with the help of the calculated bandwidth (based on learning). This helps to efficiently control CWND for better network utilization, especially under conditions of high packet loss and high delay bandwidth product.

Machine Learning (ML) is a branch of artificial intelligence that focuses on the development of algorithms and statistical models that allow computer systems to learn and improve their performance based on data and past experience, rather than being explicitly programmed [20]. Within trend analysis in congestion control there are works that use ML for congestion control, the work of Ning Li, et. al., [9], presents AdaBoost-TCP in a satellite network, where congestion control in highly dynamic networks represents a significant challenge due to the frequent switching of satellite links. In the context of this paper ‘boost’ refers to the process of converting a set of weak learners into a strong learner, and ‘adaptive’ refers to how AdaBoost adjusts the misclassification weights to guide the learning of weak learners [21]. Switching in satellite networks can result in connection instability and increase packet loss, thus reducing network efficiency. TCP fails to effectively distinguish packet loss types, leading to network underutilization [22]. The sender adopts adaptive congestion control measures based on the type of packet lost, which allows for greater efficiency in congestion management. The results, when the packet loss rate is between  $10^{-5}$  and  $10^{-4}$ ,

the AdaBoost-TCP strategy can increase throughput by 10 % compared to other congestion control algorithms, such as Hybla [23] which was designed to improve TCP throughput over links with long RTT. In addition, AdaBoost-TCP shows good fairness in comparison to NewReno.

Mozo, López-Presa and Fernandez Anta [24] presents an algorithm based on Max–Min fairness, named B-Neck. It is a distributed, quiescent and proactive protocol. It calculates the optimal data rates for each session without any information about routers flows. B-Neck converges to the optimal solution very fast and keeps the queues short. It is quiescent because stop to transmit packets if reach the optimal data rate, thus it saved energy and bandwidth.

The work of Ludeña-González, López-Presa, and Muñoz [8] proposes a solution to achieve maximum-to-minimum fairness (UMMF) in high-speed multipath networks. A centralized algorithm called c-SLEN (Saturation Level Explicit Notification) is presented and is based on the saturation level of the links to compute the fair rates of flows without affecting the throughput due to link capacity. In addition, a distributed version called d-SLEN is developed, which is the first of its kind and is characterized by its convergence speed independent of network capacity. Simulation results show that c-SLEN achieves session rates similar to other UMMF algorithms, but without saturating links, which improves network utilization. In addition, d-SLEN exhibits faster and more stable convergence than other distributed approaches.

Finally, as part of the study in the field of network congestion control, a novel approach has been observed through the Utility Function Algorithm (UFA). This algorithm, a variant of the B-Neck method, has incorporated Utility Functions with the objective of calculating the performance of the application as a function of the type of traffic generated by the sessions [25]. The Max–Min fairness criterion has been applied by the AFU for bandwidth allocation, demonstrating significant effectiveness in network congestion control management. The AFU algorithm has been evaluated in three different scenarios through Matlab, providing a series of performance metrics including the allocated transmission rate, the utility achieved per session and the fairness measured through the Gini coefficient. The results obtained indicate that real-time applications, particularly those transmitting voice and video, experience better performance when using the AFU algorithm compared to other congestion control strategies. This finding suggests that the AFU could be particularly useful in network environments where real-time traffic is predominant.

Importantly, this work offers promising insights for congestion control in networks and marks a way forward in the investigation of control mechanisms that can efficiently handle the demands of different types of traffic. However, today real-time applications demand increases, so more work is needed to explore and refine strategies such as AFU and to investigate how these techniques can be adapted and optimized for different network conditions.

Research in the area of congestion control in networks has provided a number of innovative algorithms that have informed and enriched this evolving field. In particular, works such as B-Neck and the Algorithm Utility Function (AFU) have proven

to be influential, providing novel and valuable insights for the efficient management of network traffic. It is necessary to emphasize the relevance of these fundamental works. B-Neck and AFU have established novel criteria, compiling resource allocation with fairness, but also based on a utility function, in this area of research, setting a benchmark for future research and algorithm development.

### III. METHODOLOGY: CONGESTION CONTROL AND OPTIMIZATION STRATEGY

#### A. Fair Max–Min Allocation Strategy

Congestion control algorithms and performance metrics are tailored to the needs of the applications. There is no ideal state in delay- and loss-based algorithms. It is complicated to guarantee an equitable distribution of network capacity, especially with different algorithms and routes, to measure the fairness of resource allocation in networks [26].

Equation 1

$$Fairness = \frac{(\sum_{i=1}^n x_i)^2}{n \sum_{i=1}^n x_i^2} \quad (1)$$

This is the formula for the Jain equity index. In this equation,  $x_i$  represents the throughput of the  $i$ -th flow, and  $n$  is the total number of flows.

Max–Min fairness principle seeks a fair bandwidth distribution for all applications, regardless of their criticality. Initially, it assumes that all rates are 0 and increase at the same rate until capacity limits are reached. This process is repeated until the rate cannot be increased any further in one session [27]. However, despite its apparent fairness, Max–Min fairness may not lead to optimal network utilization.

In proportional allocation, resources are distributed according to a metric, such as user demand. This could result in better resource utilization, but may be less fair if some users have a high demand for resources.

It is emphasized that fairness in congestion control seeks a fair distribution of network resources among different data flows. This aspect is critical in the design of congestion control mechanisms, as it contributes to the quality and perception of a better service for users.

#### B. Utility functions

Customer satisfaction in the consumption of goods and services is measured through a utility function. In the network context, it reflects a combination of objectives, such as efficiency, fairness, and quality of experience, and may incorporate factors such as the relative importance of different flows or sessions, so it is a measure of Quality of Service (QoS). Two types of traffic are distinguished in this work: best-effort traffic, which has no QoS requirements, and traffic with QoS requirements that needs specific resources [28], [29].

Figure 1 shows utility functions used in this work. Elastic applications are a subcategory of best-effort traffic. They vary the transmission rate according to the congestion signal and benefit from higher bandwidth. These applications

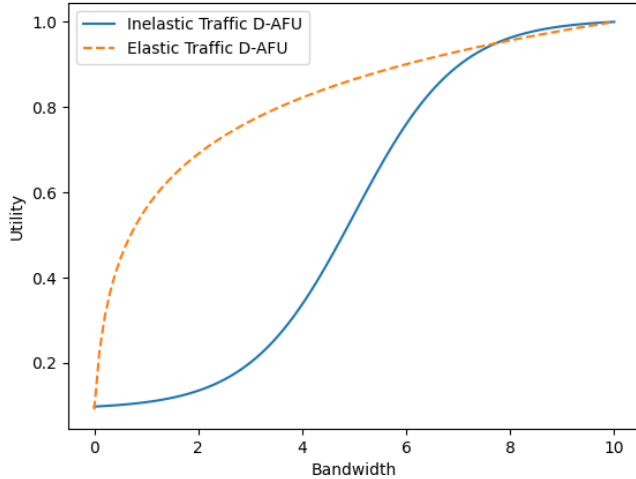


Fig. 1. Utility function used by D-AFU.

or services can adjust to different bandwidth levels. Their utility function is a logarithmic function, showing that utility increases as bandwidth increases, but at a decreasing rate [30]. The visual representation provided in aligns with the theoretical framework outlined by Equations 2 and 3, offering a graphical insight into the key principles presented in this study. Logarithmic form of this function suggests that there is a decreasing benefit to increasing bandwidth. Examples of this function are web browsing, where increasing bandwidth improves the experience up to a certain point, but then further increases have a minor impact.

Equation 2

$$U^s(y) = w(\log(ay + b) + d) \quad (2)$$

$U(y)$ : Represents the utility, or user's perceived satisfaction, associated with the bandwidth  $y$ ,  $w$ : A constant that scales the entire utility function, reflecting the importance or weight assigned to the utility,  $a$ : A parameter that influences the rate at which utility increases with bandwidth.  $b$ : An offset parameter that affects the baseline utility, possibly representing a minimum utility even at low bandwidth.  $d$ : An additional constant that could introduce an offset or baseline utility.

In this utility function the natural logarithm ( $\log$ ) is commonly used to represent diminishing marginal returns, implying that the utility increases at a decreasing rate as bandwidth increases. The parameter  $a$  affects how quickly the utility increases as bandwidth improves. The constant  $b$  could represent a baseline utility even with low bandwidth. The constant  $d$  might introduce an overall offset or baseline utility. The increasing nature of the utility function aligns with the description that as bandwidth increases, the user's perceived satisfaction or utility also increases. This type of utility function is consistent with the idea that additional bandwidth contributes positively to the user experience, and the rate of increase may be subject to diminishing returns.

Consider an application such as file transfer via File Transfer Protocol (FTP). FTP is an elastic application that is it can vary its transmission rate depending on the amount of available bandwidth. If bandwidth is limited, FTP can adapt by reducing its transfer rate. However, if more bandwidth is available, FTP can increase its transfer rate, resulting in faster file transfer.

The utility function for FTP is an increasing function, meaning that as bandwidth increases, so does the user's perceived utility [27]. However, this function is typically logarithmic or concave, meaning that there are diminishing returns: perceived utility increases with bandwidth, but at a decreasing rate [31].

In contrast, inelastic traffic, which includes applications such as audio streaming and VoIP, does not easily adapt to changes in delay and throughput. If the allocated bandwidth is insufficient, throughput is significantly affected [31] because these applications or services has rigid bandwidth requirements. Its utility function is a sigmoidal function, showing a rapid initial increase in utility followed by a deceleration [27]. Specifically, during the very initial phase, the rate of increase is slower compared to an inelastic response. In other words, the utility experiences a gradual ascent during its early stages before entering a phase of accelerated growth. This sigmoidal behavior is indicative of the system's sensitivity to changes, with a more measured initial response that transitions into a steeper incline as the input or conditions vary. There is a point at which additional bandwidth increases no longer add much value (saturation). This could represent, for example, a live video stream where, beyond a certain point, increasing bandwidth does not significantly improve video quality.

Equation 3

$$U^r(y) = w \left( \frac{1}{1 + e^{-a(y-b)}} + d \right) \quad (3)$$

In the context of congestion control and network resource allocation, utility functions play a crucial role in evaluating the performance and fairness of resource distribution. The utility functions are typically used to model the satisfaction or benefit that users derive from the allocated resources, represents the utility associated with a particular resource allocation. The parameters  $a$ ,  $b$ ,  $w$  and  $d$  are essential in shaping the characteristics of the utility function.  $y$ : represents a variable associated with the resource allocation, which could be, for example, network bandwidth or throughput. *Logistic Function Models* the non-linear relationship between the resource allocation and user satisfaction. The parameters  $a$  and  $b$  control the shape of the curve, determining how quickly user satisfaction increases with resource allocation.  $w$ : represents a weight or importance factor, scaling the entire utility function. It could reflect the relative importance of user satisfaction in the overall network management objectives.  $d$ : Represents an additional constant that could introduce an offset or baseline utility.

### C. Algorithms

Distributed control algorithms are important for architecture design and performance engineering of the communication

network. This allow the network to scale more easily because the work is divided among many nodes [32]. This is particularly useful in large networks where a centralized approach can be difficult to manage and could cause bottlenecks: if one node fails, the overall system operation does not stop. The other nodes can continue to function independently, which improves the resilience of the network.

Max–Min fairness principle focuses on fair resource allocation. Under this approach, all data flows start with the same transfer rate. As demand increases, the transfer rate increases proportionally for all flows until one of them reaches its maximum capacity [24]. At this point, the transfer rate of that particular flow remains constant, while the other flows that still have additional capacity can continue to increase their transfer rate. This process is repeated until all transfer rates have been maximized, ensuring that no flow receives less than what would be given to any other.

The utility function describes the relationship between resource allocation and user satisfaction. For example, for elastic applications, which can adjust their transfer rate as a function of bandwidth availability, user utility or satisfaction increases as more bandwidth is allocated to the application, but at a decreasing rate [25].

In practice, these two concepts can be combined to develop resource allocation algorithms that balance fairness and maximization of user satisfaction. One possible approach would be to use the Max–Min fairness principle to determine an initial resource allocation and then adjust it based on the Utility Functions of different applications.

In one scenario, it could start by allocating bandwidth equally among all applications. Then, it could examine the Utility Functions and reallocate bandwidth from applications with decreasing marginal utilities (those that derive less benefit from additional increases in bandwidth) to applications with increasing marginal utilities (those that derive more benefit from additional increases in bandwidth).

By distributing decision making, each node can make adjustments and decisions based on local information, which can lead to more efficient and effective resource management. In the context of congestion control, distributed algorithms can respond to local traffic conditions, which helps to avoid congestion before it becomes a network-level problem [24].

Defining the part of the distributed algorithm has been taken as a source designed by Mozo, Lopez and Fernandez [24], where they define the following tasks according to the network segment in question, which the authors call them tasks, each of them is described below, the router tasks and the source node 1 are responsible for processing the majority of messages referring to the algorithm, while the destination node III-C tasks are limited to receiving messages to know when a session has joined, a test has started, or there is a message.

Router Link: Receives packets from source nodes and forwards them to other routers. Maintains a table of the current forwarding rates of all sessions traversing the router. Periodically updates the forwarding rates of all sessions based on the B-Neck algorithm. Measures the current bandwidth available on the link. Provides this information to the routers connecting to the link.

---

### Algorithm 1

Task SourceNode( $s, e$ ).

---

```

procedure STARTPROBECYCLE  $F_e \leftarrow \emptyset$ ;  $R_e \leftarrow \{s\}$ 
pending_probe_s  $\leftarrow$  FALSE bneck_rcv_s  $\leftarrow$  FALSE  $\mu_s^e \leftarrow$ 
WAITING_RESPONSE Send downstream Probe( $s, D_s, e$ )
end procedure
while received API.Join( $s, r$ ) do  $F_e \leftarrow \emptyset$ ;  $R_e \leftarrow$ 
 $\{s\}$   $D_s \leftarrow \min(r, C_e)$  pending_probe_s  $\leftarrow$  FALSE
pending_leave_s  $\leftarrow$  FALSE bneck_rcv_s  $\leftarrow$  FALSE  $\mu_s^e \leftarrow$ 
WAITING_RESPONSE Send downstream Join( $s, D_s, e$ )
  while received API.Leave( $s$ ) do
    if  $\mu_s^e =$  IDLE then  $F_e \leftarrow \emptyset$ ;  $R_e \leftarrow \emptyset$  send downstream
    Leave( $s$ )
    else pending_leave_s  $\leftarrow$  TRUE

  while received Update( $s$ ) do
    if  $\mu_s^e =$  IDLE then StartProbeCycle()

  while received Bottleneck( $s$ ) do
    if  $\mu_s^e =$  IDLE  $\wedge$  bneck_rcv_s then bneck_rcv_s  $\leftarrow$ 
    TRUE API.Rate( $s, \lambda_s^e$ )
    if  $D_s > \lambda_s^e$  then  $F_e \leftarrow \{s\}$ ;  $R_e \leftarrow \emptyset$  send
    downstream SetBottleneck( $s, D_s = \lambda_s^e$ )

    while received Response( $s, \tau, \lambda, \eta$ ) do
      if pending_leave_s then  $F_e \leftarrow \emptyset$ ;  $R_e \leftarrow \emptyset$  send
      downstream Leave( $s$ )
      else if  $\tau =$  UPDATE  $\vee$  pending_probe_s then
      StartProbeCycle()
      else if  $\tau =$  BOTTLENECK then  $\lambda_s^e \leftarrow \lambda$   $\mu_s^e \leftarrow$ 
      IDLE bneck_rcv_s  $\leftarrow$  TRUE API.Rate( $s, \lambda_s^e$ )
      if  $D_s = \lambda_s^e$  then bneck_rcv_s  $\leftarrow$  TRUE
      API.Rate( $s, \lambda_s^e$ ) send downstream SetBottleneck( $s, TRUE$ )
      else send downstream
      SetBottleneck( $s, FALSE$ )

```

---

Source node: Sends packets to the router. Receives updates from the router on the current sending rates of all sessions. Adjusts its own sending rate based on updates from the router.

Destination Node: Receives packets from router. Delivers packets to application. Provides feedback to router.

---

### Algorithm 2

Task DestinationNode( $s$ ).

---

```

while received SetBottleneck( $s, \beta$ ) do
  if  $\neg\beta$  then Send upstream Update( $s$ )
  end if
end while
while received Join( $s, \lambda, \eta$ ) do Send upstream Response( $s,$ 
RESPONSE,  $\lambda, \eta$ )
end while
while received Probe( $s, \lambda, \eta$ ) do Send upstream Response( $s,$ 
RESPONSE,  $\lambda, \eta$ )
end while

```

---

It should be noted that, once stable, the algorithm remains idle until a new session occurs or resources are released.

The Algorithm Utility Function (AFU) is a sophisticated method designed for the optimal allocation of bandwidth in a network, with the objective of controlling network congestion efficiently. AFU incorporates the Max–Min fairness criterion, which means that it seeks to maximize the minimum bandwidth allocation to any node in the network. The key to AFU’s efficiency is its use of Utility Functions. These functions quantify the ‘value’ or ‘utility’ of a given bandwidth allocation for a particular application or type of traffic. Different applications and traffic types may have different Utility Functions or depending on their bandwidth requirements, their sensitivity to latency [26]. As can be seen the pseudocode of the 3 algorithm proposes bandwidth allocation according to the utility function.

---

**Algorithm 3**

Centralized AFU

---

$e \in E$

**if**  $e \neq E$  **then**

$R_e \leftarrow S_e^*$

**end if**

$L \leftarrow \{e \in E \mid R_e \neq 0\}$

**while**  $L \neq \emptyset$  **do**  $e \in E$

**if**  $e \neq E$  **then**  $s \in e$

$U_s^*(y) \leftarrow U[1, 0]$

$B_s \leftarrow \frac{1}{U_s^*(y)} \cdot (C_e - \sum_{s' \in F_e} \lambda_{s'}^*)$

$B_e \leftarrow \{B_s\}$

**end if**

$B \leftarrow \min_{e \in L} \{B_e\}$

$L' \leftarrow \{e \in L \mid B_e = B\}$

$X \leftarrow \cup_{e \in L'} R_e \quad s \in X$

**if**  $s \neq 0$  **then**

$\lambda_s^* \leftarrow B$

**end if**

$e \in L \setminus L'$

**if**  $e \neq 0$  **then**

$F_e \leftarrow F_e \cup (R_e \cap X)$

$R_e \leftarrow R_e \setminus F_e$

**end if**

$L \leftarrow \{e \in (L \setminus L') \mid R_e \neq 0\}$

**end while=0**

---

**Initialization:** Resources are initially allocated equitably among all users, each user is associated with a utility function representing their satisfaction with the resource allocation. **Max–Min:** Users with lower utility (or less allocation) have the opportunity to obtain additional resources until their utility matches that of others. **Utility Function Evaluation:** The utility function for each user is evaluated based on their current resource allocation. The shape and parameters of the utility function determine the user’s satisfaction in relation to the allocated resources. **Iterative adjustments:** The algorithm iterates to dynamically adjust resource allocations, users with lower utility are given priority for resource increments, promoting

fairness. **Dynamic Adaptation:** The algorithm dynamically adapts to changes in network conditions, such as fluctuations in available bandwidth or the introduction of new users.

#### D. Simulation settings

In the simulation, the proposed protocol is tested on various network configurations to explore how different conditions may affect the performance of the strategies. This includes variations in the number of nodes, the amount of available resources, the demand for resources. The simulated network for this study considers two main types of traffic: Voice over Internet Protocol (VoIP) and File Transfer Protocol (FTP). These two types of traffic have been selected because of their divergent characteristics and common usage in today’s networks. VoIP traffic is real-time and latency sensitive. It requires constant and relatively small bandwidth, and prioritizes low latency over absolute data integrity. Dropped or delayed packets can result in a noticeable degradation of call quality. On the other hand, FTP traffic is not real-time and is less sensitive to latency. It requires high volumes of bandwidth and prioritizes absolute data integrity over low latency. FTP transfers can occupy much of the available bandwidth, but can tolerate higher latencies.

#### E. Metrics

The network topology in simulations can vary depending on the number of routers to be incorporated, with several hops for a packet to reach its destination or within a single domain. Each router is configured to handle both VoIP and FTP traffic, and allocates bandwidth between these services using the Utility Function Algorithm (UFA), which applies the Max–Min fairness criterion to control network congestion. The topology depicted in Figure III-D is constructed using routers and hosts connected by links with fixed bandwidth. Hosts in this network play specific roles, serving as both traffic senders and receivers. The fixed bandwidth of the links establishes the capacity for data transfer between network elements. This configuration allows for the simulation and evaluation of network traffic scenarios, facilitating the assessment of the performance and adaptability of congestion control algorithms under controlled conditions. The role distinction of hosts as traffic sources and destinations contributes to a comprehensive evaluation of the algorithm’s efficiency in handling bidirectional communication.

It has measured a number of metrics to evaluate the performance of the proposed strategies and algorithms. These include resource allocation fairness, resource usage efficiency, delay and packet loss. These metrics allow to quantify and compare the results in an objective manner.

In our experiment within a consistent network topology, we aimed to validate the effectiveness of a congestion control algorithm by diversifying traffic types and routing. Deploying distinct traffic categories, including voice, video, data, and routing them through various paths allowed us to assess the algorithm’s adaptability and performance under diverse conditions. By measuring key parameters such as latency, packet loss, and bandwidth utilization, we gained insights into the

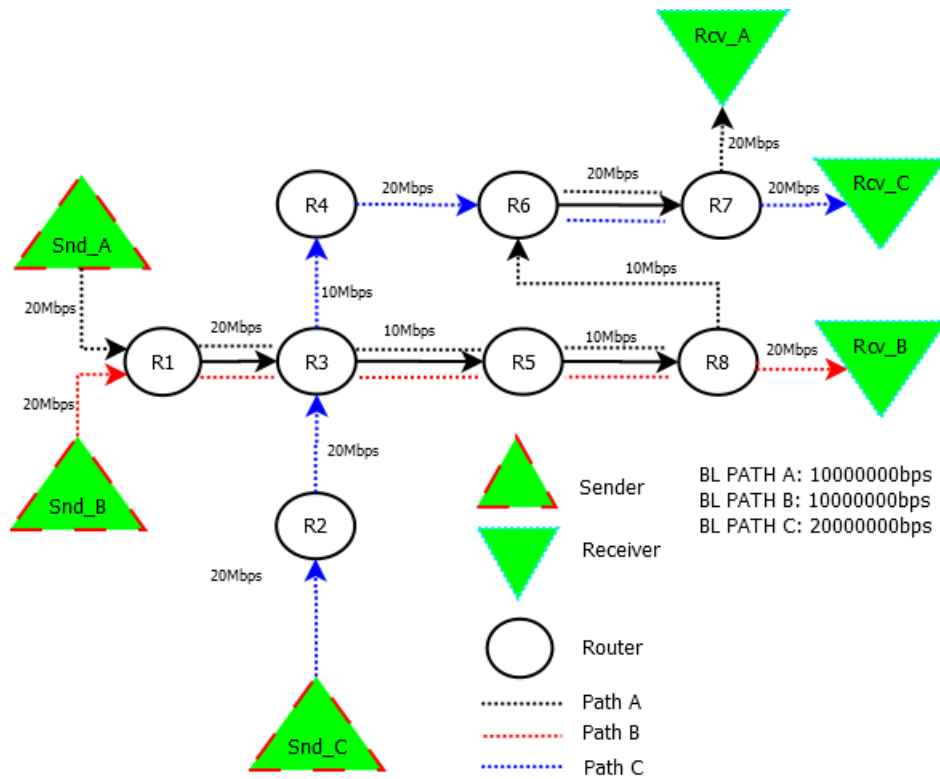


Fig. 2. Network topology used in simulations.

algorithm's responsiveness and efficiency. The experiment's findings provide valuable confirmation of the algorithm's validity, demonstrating its ability to handle varied network scenarios and optimize resource allocation based on the nature of the transmitted data.

#### F. Lost packages and queues

Packet loss refers to the number or percentage of packets that are sent from a source but do not reach their intended destination. This loss can be due to errors in network devices, congestion and collisions. Packet loss can have a significant impact on real-time applications, such as VoIP or online gaming, while network queuing refers to the temporary accumulation of packets at a network point, such as a router or switch, before they are processed or forwarded. Metrics related to queues can include queue length (number of packets in queue), queue delay (time a packet waits in queue) and discard due to full queues [33].

#### G. End-to-end packet delay

End-to-end packet delay, commonly referred to as latency, refers to the time it takes for a data packet to travel from a source to a destination over a network [34]. This delay can be caused by a variety of factors, including propagation time, transmission time, processing speed of intermediate devices, and queuing time on network devices. It is important to note that on larger or more congested networks latency can vary considerably. Latency variability is known as 'jitter' and can be problematic for time-sensitive applications.

The RTT is a crucial metric in networking that quantifies the time required for a data packet to traverse from the sender to the receiver and then return to the sender. RTT is a fundamental parameter in assessing the responsiveness and efficiency of network communication. It directly influences the perceived delay in data transmission, making it a significant consideration for real-time applications, such as video conferencing and online gaming

#### H. Fairness in resource distribution

Gini coefficient in the context of congestion control is a measure that quantifies the unequal allocation of resources in a network. Its value varies between 0 and 1, where 0 represents a completely equal distribution of resources and a completely unequal allocation [35]. The Lorenz curve, which plots the distribution of resources in the network, shows the cumulative proportion of bandwidth allocated in relation to the cumulative proportion of sessions or flows in the network [36].

## IV. RESULTS

All experiments have been performed in the NS3 network simulator. It is a discrete event simulator that is widely used in network research to model the behavior of computer networks [37]. This simulator has allowed to accurately and controlled recreate the required network conditions, and has provided a platform for D-AFU implementing and testing.

In this work, we proposed a novel congestion control algorithm with the aim of enhancing network performance in specific scenarios. To assess the effectiveness and efficiency

of our algorithm, we conducted a comprehensive comparison with TCP Reno, a widely recognized and utilized congestion control algorithm in networking environments.

TCP Reno has stood out as one of the most commonly implemented and studied congestion control algorithms in the networking community. Its approach of slow start, congestion avoidance, and fast recovery has served as a foundational framework for numerous developments in this field.

Throughout our testing and comparative analyses, we assessed the performance of our algorithm across diverse scenarios, taking into account factors such as bandwidth utilization efficiency, adaptability to network changes, and tolerance to packet loss. The comparison with TCP Reno provides a robust benchmark for understanding how our algorithm fares in relation to a well-established standard within the congestion control domain.

- 1) Lost packages and queues: From the results of a simulation of the network topology, where it plots the packets in the queue on the interface according to the flows sent, a larger queue is an indicator of congestion and packet loss occurs due to the timers in the applications. Figure 3 shows D-AFU keeps short queue all-time. It can be concluded by applying D-AFU, the queue decreases substantially, there is no packet loss and no packet retransmissions.

The absence of lost packets implies that all packets sent by the sources reach their intended destinations, which in turn may indicate that the network congestion control system is effectively functioning to prevent network saturation.

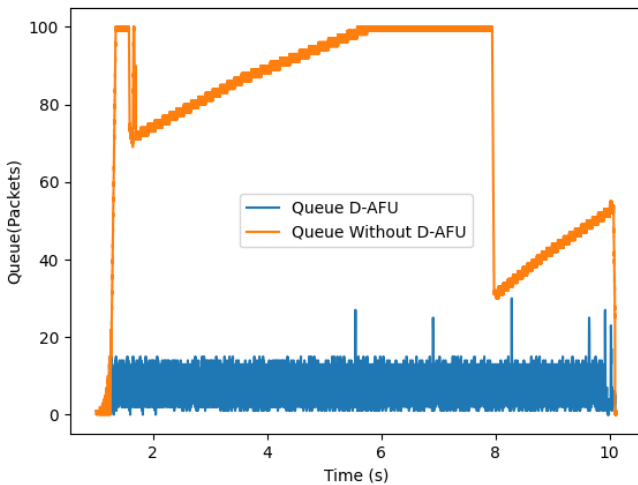


Fig. 3. Queues in intermediate nodes.

- 2) Data rates for each session: The results of the simulation applying elastic and inelastic traffic (real time) can be seen in the Figure 4. It shows that when applying D-AFU the values that the application needs are reached in a shorter time than the same resources obtained without applying the algorithm. In the elastic traffic instead it adapts to the available resources, which is directly

TABLE II  
COMPARATIVE METRICS FOR THE NETWORK.

Strategy	Pkt. Send	Pkt. Recv	Avg. RTT (ms)	Freq. (sec)
D-AFU	300	300	61.5	0.3
Without D-AFU	300	250	718.6	0.3

related to the size of the queue. Vertical lines have been traced where alert a change made in the traffic. The application in real time obtains the bandwidth requirement in a shorter time than without the algorithm strategy. For the elastic traffic instead when sharing resources on a link this adjusts its bandwidth requirement based on the availability of: first the type of application with which it shares and second with the total bandwidth available, which can be noted from time six in the graph and at time 8 they manage to adjust a fair distribution of resources.

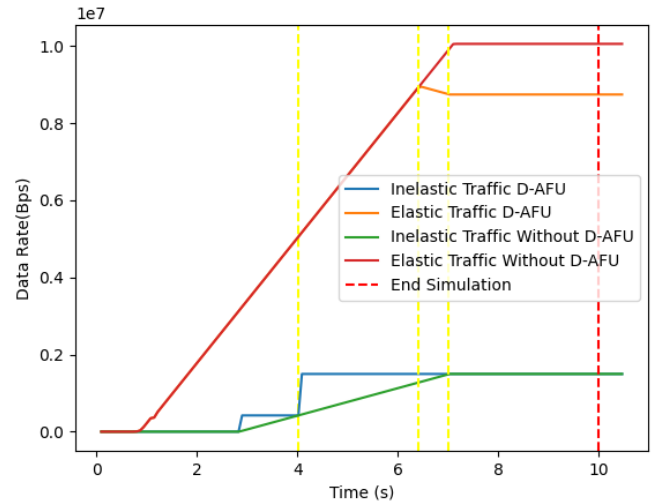


Fig. 4. Data rates for different traffic.

In addition, to analyze the effectiveness of congestion control, performance parameters were obtained using the D-AFU approach and a traditional method without D-AFU. The results presented in the Table II indicate a clear superiority of the D-AFU approach in terms of packets received. Both methods sent the same number of packets (300 packets in 10 seconds). The D-AFU method managed to deliver all packets successfully, while the non-D-AFU method delivered only 250 of the 300 packets. That noted, while the results of this particular simulation are positive, it is important to remember that simulations are simplifications of the real world and their results are dependent on user-specified conditions. In addition, having zero dropped and lost packets does not necessarily mean that the network is perfect. Other factors, such as latency or jitter, could still affect network quality. In Table II it can see the average RTT values. With D-AFU the latency is slower that without D-AFU because, it proves to be almost ten times faster than the non-D-AFU method.

These results suggest that D-AFU congestion control is more efficient in saturated environments, providing better quality of service and faster response times. It improves the network performance.

### 3) Fair distribution of resources

Figure 5 plots Gini coefficient and Lorenz curve for the allocation data rate in the network. For D-AFU algorithm Gini coefficient is 0.52 while without applying the proposed algorithm is 0.81. This means that D-AFU, considering the utility function, makes a more fair distribution of network resources.

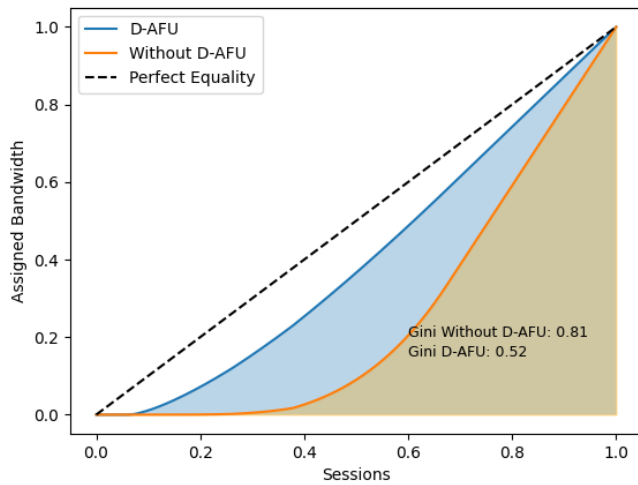


Fig. 5. Fairness measure.

## V. CONCLUSIONS

Distributed Utility Function Algorithm (D-UFA) is an algorithm that achieves Max–Min fairness. This implies that it ensures that all sessions receive a fair share of the network bandwidth, a factor especially relevant in contexts with significant variations in traffic types, for example VoIP and FTP applications. It is a distributed algorithm, meaning that it does not require any central coordination. This allows D-AFU to efficiently adapt to network variations and respond locally to congestion. It is efficient and scalable, which means that it can be used in large networks. It is a quiescent algorithm because it stops generating traffic once it has converged to optimal sending rates. This is an important feature to avoid adding additional congestion to the network once the optimal state is reached. The results show D-AFU is a promising approach for network congestion control.

## VI. REFERENCES

### REFERENCES

- [1] Cisco, "Cisco Annual Internet Report (2018–2023)," 2020. [Online]. Available: [https://www.cisco.com/c/dam/en/us/solutions/collateral/executive-perspectives/annual-internet-report/white-paper-c11-741490.docx/\\_jcr\\_content/renditions/white-paper-c11-741490\\_0.png](https://www.cisco.com/c/dam/en/us/solutions/collateral/executive-perspectives/annual-internet-report/white-paper-c11-741490.docx/_jcr_content/renditions/white-paper-c11-741490_0.png)
- [2] J. F. Kurose and K. W. Ross, *Computer Networking: A Top-down Approach*. Pearson, 2017. [Online]. Available: <https://books.google.com.ec/books?id=OljpOAAACAAJ>
- [3] W. R. Stevens and G. R. Wright, *TCP/IP Illustrated: The Protocols*, ser. Addison-Wesley professional computing series. Addison-Wesley, 1994. [Online]. Available: <https://books.google.com.ec/books?id=btNds68w84C>
- [4] R. Buyya, C. S. Yeo, and S. Venugopal, "Market-Oriented Cloud Computing: Vision, Hype, and Reality for Delivering IT Services as Computing Utilities," in *Proceedings - 10th IEEE International Conference on High Performance Computing and Communications, HPCC 2008*. IEEE, 2008, pp. 5–13.
- [5] P. Ludeña, "Fairness and Proactive Congestion Control in Multipath Networks," Ph.D. dissertation, Universidad Politécnica de Madrid, 2021.
- [6] M. Alizadeh, A. Greenberg, D. A. Maltz, J. Padhye, P. Patel, B. Prabhakar, S. Sengupta, and M. Sridharan, "Data Center TCP (DCTCP)," *SIGCOMM Comput. Commun. Rev.*, vol. 40, no. 4, pp. 63–74, 2010. [Online]. Available: <https://doi.org/10.1145/1851275.1851192>
- [7] K. R. Fall and S. Floyd, "Simulation-Based Comparisons of Tahoe, Reno and SACK TCP," *Comput. Commun. Rev.*, vol. 26, pp. 5–21, 1996. [Online]. Available: <https://api.semanticscholar.org/CorpusID:7459148>
- [8] P. Ludeña-González, J. L. López-Presa, and F. D. Muñoz, "Upward Max-Min Fairness in Multipath High-Speed Networks," *IEEE Access*, 2021.
- [9] N. Li, Z. Deng, Q. Zhu, and Q. Du, "AdaBoost-TCP: A Machine Learning-Based Congestion Control Method for Satellite Networks," in *2019 IEEE 19th International Conference on Communication Technology (ICCT)*, 2019, pp. 1126–1129.
- [10] S. Boyd and L. Vandenberghe, *Convex Optimization*. Cambridge University Press, 2004. [Online]. Available: [https://books.google.com.ec/books?id=IUZdAAAAQBAJ&printsec=frontcover&hl=es&source=gbs\\_ge\\_summary\\_r&cad=0#v=onepage&q&f=false](https://books.google.com.ec/books?id=IUZdAAAAQBAJ&printsec=frontcover&hl=es&source=gbs_ge_summary_r&cad=0#v=onepage&q&f=false)
- [11] M. Bahnasy, H. Elbiaze, and B. Boughzala, "Zero-Queue Ethernet Congestion Control Protocol Based on Available Bandwidth Estimation," *Journal of Network and Computer Applications*, vol. 105, pp. 1–20, 2018.
- [12] R. Adams, "Active Queue Management: A Survey," *IEEE Communications Surveys and Tutorials*, vol. 15, no. 3, pp. 1425–1476, 2013.
- [13] S. Varma, *Internet Congestion Control*. Elsevier Science, 2015. [Online]. Available: [https://books.google.com.ec/books?id=gbPobGAAQBAJ&printsec=frontcover&hl=es&source=gbs\\_ge\\_summary\\_r&cad=0#v=onepage&q&f=false](https://books.google.com.ec/books?id=gbPobGAAQBAJ&printsec=frontcover&hl=es&source=gbs_ge_summary_r&cad=0#v=onepage&q&f=false)
- [14] S. Hu, W. Bai, B. Qiao, K. Chen, and K. Tan, "Augmenting Proactive Congestion Control with AEOLUs," in *ACM International Conference Proceeding Series*, 2018, pp. 22–28.
- [15] T. Issariyakul and E. Hossain, *Introduction to Network Simulator NS2*. Springer US, 2009.
- [16] D. Giannopoulos, N. Chrysos, E. Mageiropoulos, G. Vardas, L. Tzanakis, and M. Katevenis, "Accurate Congestion Control for RDMA Transfers," *2018 Twelfth IEEE/ACM International Symposium on Networks-on-Chip (NOCS)*, pp. 1–8, 2018.
- [17] M. Bahnasy and H. Elbiaze, "Fair Congestion Control Protocol for Data Center Bridging," *IEEE Systems Journal*, vol. 13, no. 4, pp. 4134–4145, 2019.
- [18] I. Cho, K. Jang, and D. Han, "Credit-Scheduled Delay-bounded Congestion Control for Datacenters," in *SIGCOMM 2017 - Proceedings of the 2017 Conference of the ACM Special Interest Group on Data Communication*, 2017, pp. 239–252.
- [19] M. R. Kanagarathinam, S. Singh, I. Sandeep, A. Roy, and N. Saxena, "D-TCP: Dynamic TCP Congestion Control Algorithm for Next Generation Mobile Networks," in *2018 15th IEEE Annual Consumer Communications & Networking Conference (CCNC)*, 2018, pp. 1–6.
- [20] T. M. Mitchell, *Machine Learning*, ser. McGraw-Hill International Editions. McGraw-Hill, 1997.
- [21] Y. Freund and R. E. Schapire, "A Decision-Theoretic Generalization of On-Line Learning and an Application to Boosting," *Journal of Computer and System Sciences*, vol. 55, no. 1, pp. 119–139, 1997. [Online]. Available: <https://www.sciencedirect.com/science/article/pii/S002200009791504X>
- [22] C. D. Maciel and C. M. Ritter, "TCP/IP Networking in Process Control Plants," *Computers & Industrial Engineering*, vol. 35, no. 3, pp. 611–614, 1998. [Online]. Available: [https://doi.org/10.1016/S0360-8352\(98\)00171-5](https://doi.org/10.1016/S0360-8352(98)00171-5)
- [23] C. Caini and R. Firrincieli, "TCP Hybla: A TCP Enhancement for Heterogeneous Networks," *International Journal of Satellite Communications and Networking*, vol. 22, no. 5, pp. 547–566, 2004.
- [24] A. Mozo, J. L. López-Presa, and A. Fernández Anta, "A distributed and Quiescent Max-Min Fair Algorithm for Network Congestion Control," *Expert Systems with Applications*, vol. 91, pp. 492–512, 2018.

- [25] J. R. Carrion Torres, "Aplicabilidad de Funciones de Utilidad Para el Control de Congestión en Redes de Computadores," Master's thesis, Universidad Técnica Particular de Loja, Loja, 2020.
- [26] R. Al-Saadi, G. Armitage, J. But, and P. Branch, "A Survey of Delay-Based and Hybrid TCP Congestion Control Algorithms," *IEEE Communications Surveys and Tutorials*, vol. 21, no. 4, pp. 3609–3638, 2019.
- [27] M. Welzl, *Network Congestion Control: Managing Internet Traffic*. J. Wiley, 2005.
- [28] J. Jin, W.-H. Wang, and M. Palaniswami, "Utility Max–Min Fair Resource Allocation for Communication Networks with Multipath Routing," *Computer Communications*, vol. 32, no. 17, pp. 1802–1809, 2009. [Online]. Available: <https://doi.org/10.1016/j.comcom.2009.06.014>
- [29] L. Chen, B. Wang, X. Chen, X. Zhang, and D. Yang, *Utility-Based Resource Allocation for Mixed Traffic in Wireless Networks*. Institute of Electrical and Electronics Engineers, 2011.
- [30] S. Li, Y. Zhang, Y. Wang, and W. Sun, "Utility Optimization-Based Bandwidth Allocation for Elastic and Inelastic Services in Peer-to-Peer Networks," *International Journal of Applied Mathematics and Computer Science*, vol. 29, no. 1, pp. 111–123, 2019.
- [31] Q. V. Pham and W. J. Hwang, "Network Utility Maximization-Based Congestion Control over Wireless Networks: A Survey and Potential Directives," *IEEE Communications Surveys and Tutorials*, vol. 19, no. 2, pp. 1173–1200, 2017.
- [32] M. Chiang, "Distributed Network Control Through Sum Product Algorithm on Graphs," in *Global Telecommunications Conference, 2002. GLOBECOM '02. IEEE*, vol. 3, 2002, pp. 2395–2399 vol.3.
- [33] A. S. Tanenbaum and D. J. Wetherall, *Computer Networks*, 5th ed. Prentice Hall, 2011.
- [34] C. Demichelis and P. Chimento. (2002) IP Packet Delay Variation Metric for IP Performance Metrics (IPPM). Network Working Group, RFC 3393.
- [35] C. Gini, *Variabilità e mutabilità*, 1912, vol. 5, no. 20.
- [36] M. O. Lorenz, "Methods of Measuring the Concentration of Wealth," *Publications of the American Statistical Association*, vol. 9, no. 70, pp. 209–219, 1905.
- [37] G. F. Riley and T. R. Henderson, "The NS-3 Network Simulator." in *Modeling and Tools for Network Simulation*, K. Wehrle, M. Günes, and J. Gross, Eds. Springer, 2010, pp. 15–34. [Online]. Available: <http://dblp.uni-trier.de/db/books/collections/Wehrle2010.html#RileyH10>

# Current Status and Challenges of IoT Research in the Ecuadorian Healthcare Sector: A Systematic Literature Review

Cristina Vaca Orellana<sup>1</sup>, and María Valle Dávila<sup>2</sup>

**Abstract** — The Internet of Things (IoT) has the potential to revolutionize healthcare by enabling remote patient monitoring, personalized care and disease prevention. In Ecuador, research on IoT in the healthcare field is rapidly expanding. However, there's a need for a clearer understanding of the current state of this research. This study examines the contributions of Ecuadorian authors in this field through their publications in two globally impactful bibliographic databases. The methodology employed is a systematic review using the PRISMA statement, resulting in a final stage comprising 23 articles. These publications encompass system proposals, prototypes, and reviews with applications in areas such as epidemiology, cardiology and nursing. The recurrent mention of patient information privacy is a challenge in implementing IoT-based healthcare systems. The conclusions emphasize that future work perspectives should address the challenges identified, considering the growing trend of publications from Ecuadorian authors.

**Keywords** — Internet of Medical Things; Emerging Technologies; Remote Patient Monitoring; Privacy and Information Security; Systematic Reviews.

**Resumen** — El Internet de las Cosas (IoT) tiene el potencial de revolucionar la atención médica al permitir la monitorización remota de pacientes, atención personalizada y prevención de enfermedades. En Ecuador, la investigación sobre IoT en el campo de la salud está expandiéndose rápidamente. Sin embargo, es necesario tener una comprensión más clara del estado actual de esta investigación. Es así como el presente trabajo analiza las contribuciones de los autores ecuatorianos en este campo, a través de sus publicaciones en dos bases de datos bibliográficas de impacto global. La metodología empleada es una revisión sistemática utilizando la declaración PRISMA, lo que resulta en una etapa final con 23 artículos. Las publicaciones abarcan propuestas de sistemas, prototipos y revisiones con aplicaciones en áreas como epidemiología, cardiología y enfermería. Se destaca la mención recurrente de la privacidad de la información del paciente como un desafío en la implementación de sistemas de atención médica basados en IoT. En las conclusiones se enfatiza que las perspectivas de trabajo futuro deben abordar los desafíos expuestos, teniendo en cuenta la creciente tendencia de publicaciones de autores ecuatorianos.

**Palabras Clave** – Internet de las Cosas Médicas; Tecnologías Emergentes; Monitorización Remota de Pacientes; Privacidad y Seguridad de la Información; Revisión Sistemática.

## I. INTRODUCTION

THE digital revolution has transformed all aspects of everyday life and industries worldwide. One of the fields that has experienced a significant impact and has been propelled to a higher position in society is the healthcare sector [1], [2]. The convergence of Information and Communication Technologies (ICT), connectivity, and smart devices have aided in this field to improve healthcare, diagnosis, patient monitoring, and overall quality of life, especially for vulnerable populations [3], [5].

One of the emerging technologies, such as the Internet of Things (IoT), considered a part of the future internet and envisioned to comprise billions of intelligently connected ‘things’ [6] has transformed healthcare, giving rise to what is known as the Internet of Medical Things (IoMT). This has paved the way for different healthcare delivery models, such as telemedicine, seen as an evolution of providing healthcare services remotely through telecommunications [7], [8], benefiting patients in rural or remote regions where healthcare is insufficient.

Furthermore, with interconnected medical devices healthcare professionals can diagnose, monitor and provide healthcare effectively [9], [10]. Smartwatches and activity trackers, among the most common, track health metrics such as heart rate, activity level and sleep quality [11], benefiting patients with chronic diseases by providing early alerts in case of emergencies [12]. Thus, the future of healthcare is shaped by increased connectivity. Just in Latin America, the interconnection of IoMT devices is projected to increase from 2 billion in 2019 to 9 billion in 2025 [13].

However, amidst the numerous opportunities IoT presents in healthcare, it also encounters significant challenges. One of the main challenges is the privacy and security of health data. Data protection is essential to build trust with patients [10]. Another challenge, as noted by Yacchirema et al. [14], is the interoperability between IoT devices and systems, considering that the lack of common standards has hindered effective communication among devices and systems [15].

The problem within this entire context is that there needs to be a clearer understanding of the current state of IoT research in Ecuador's healthcare field. This lack of awareness can hinder the development of public policies and decision-making in this area. Additionally, it may limit healthcare professional's access

<sup>1</sup> Cristina Vaca Orellana MSc. of the Faculty of Health Sciences, GIVE research group, Universidad Técnica del Norte, Ibarra 100103, Ecuador, (e-mail: cvaca@utn.edu.ec). ORCID <https://orcid.org/0000-0002-2684-4696>.

<sup>2</sup> María Valle Dávila Ph.D. of the Faculty of Health Sciences, GIVE research group, Universidad Técnica del Norte, Ibarra 100105, Ecuador (e-mail: mfvalle@utn.edu.ec). ORCID <https://orcid.org/0000-0001-9078-9620>.

Manuscript Received: 15/01/2024

Revised: 18/02/2024

Accepted: 26/02/2024

DOI: <https://doi.org/10.29019/enfoqueute.1023>

to the latest research and technologies and their connection with the specific healthcare field under investigation. The hypothesis is that IoT research in the healthcare field in Ecuador is growing rapidly, but faces significant challenges. For example, patient information privacy and medical device interoperability being among the most crucial.

To test this hypothesis, the research objective is to conduct a systematic literature review analyzing contributions from publications with Ecuadorian authors in globally impactful bibliographic databases. This aims to provide an overview of the current state of IoT research in the healthcare field in Ecuador, including trends, challenges, and opportunities that can guide and foster future developments in the Ecuadorian context.

## II. MATERIALS AND METHODS

This study employed a systematic review, as proposed by Arksey & O'Malley [16], using the PRISMA statement. The study adopts a mixed and inferential approach. For data analysis were utilized R Core Team software [17] and the bibliographic manager Zotero [18].

### A. Phase 1: Identification of the research question

In the context of technological evolution and the demand for IoT in the biomedical and healthcare domains, and for the scope of the systematic review, were identified four research questions using the Population, Intervention, Comparison, and Out-comes (PICO) approach.

RQ1: What are the characteristics of manuscripts, bibliographic databases, and the predominant language in publications by researchers focused on the application of IoT in healthcare?

RQ2: What are the contributions of publications with Ecuadorian authors in globally impactful bibliographic databases regarding IoT?

RQ3: In which health fields have the Internet of Things (IoT) application been investigated?

RQ4: What are the obstacles and challenges in implementing IoT in the healthcare domain?

### B. Phase 2: Establishment of inclusion and exclusion criteria

Several inclusion criteria have been considered for this study. The timeframe will be from the year 2016 to August 2023, with publications in high-impact bibliographic databases written with the collaboration of Ecuadorian authors. This includes articles related to applications, solutions, smart devices, and wearables. Additionally, publications in spanish and english will be included, categorized as conference outcomes, original works, reviews, and systematic reviews.

Regarding exclusion criteria, duplicate publications and those categorized as books will be discarded.

#### B.1. DESCRIPTION OF INFORMATION SOURCES

Bibliographic databases have a global scope, are multilingual and have a high scientific impact. According to Abad-García et al. [19] and Vuotto et al. [20], these databases include Scopus and Web of Science (WoS). Additionally, LILACS, PubMed,

and EMBASE were considered to expand the number of manuscripts. However, no publications related to the topic were found.

#### B.2. Selecting keywords and search terms

The terms were defined using Health Science Descriptors (DeCS) / Medical Subject Headings (MeSH) and technology-related keywords. These strings have been designed to align with the research questions and encompass information related to 'IoT', 'IoMT', 'Big Data', 'Biomedical Technologies', 'Healthcare', 'Ecuador', 'Quality of Technology in Health', 'Health Technology', 'Wireless Technologies', 'New Technologies', and 'Wearable Technology'.

#### B.3. Developing a search strategy

The search terms were combined using boolean operators 'AND' and 'OR' as a database search strategy to compile a set of manuscripts that met the inclusion and exclusion criteria and addressed the research questions. Additionally, the specific search requirements of each bibliographic database were considered.

The search was conducted in both spanish and english across all platforms of the bibliographic databases to ensure the inclusion of relevant studies, guaranteeing a comprehensive review of the available literature.

Initially, the publication period was set as 2020, based on Saadoughi et al. study [21], suggesting that around 40 % of all IoT devices in medicine and healthcare would be involved by 2020. However, due to a limited number of contributions from Ecuadorian authors, the period was expanded to include studies from 2016.

Table 1 presents a breakdown of some of the search strings used during the search.

TABLE I  
SEARCH STRINGS IN BIBLIOGRAPHIC DATABASES

Research database	Search strategy
Scopus	ALL ('internet of things') AND ALL ('biomedical technologies') OR ALL (Ecuador) OR ALL ('quality of health technology') OR ALL ('health technology') OR ALL ('wireless technologies') OR ALL ('new technologies') OR ALL ('wearable technology')
Web of Science	internet of things* (Topic) and biomedical technologies* (Topic) or Ecuador* (Topic) or quality of health technology* (Topic) or health technology (Topic) or new technologies (Topic) or wearable technology (Topic) or Preprint Citation Index (Exclude-Database)

### C. Phase 3: Review and selection of studies

The literature search was limited to Scopus and Web of Science. Additional, were applied filters to restrict results to articles aligned with the study objective and inclusion/exclusion criteria.

The search results are presented in Figure 1. The literature search identified a representative sample of relevant literature. These results will be used in subsequent study phases for comparative analysis of the findings.

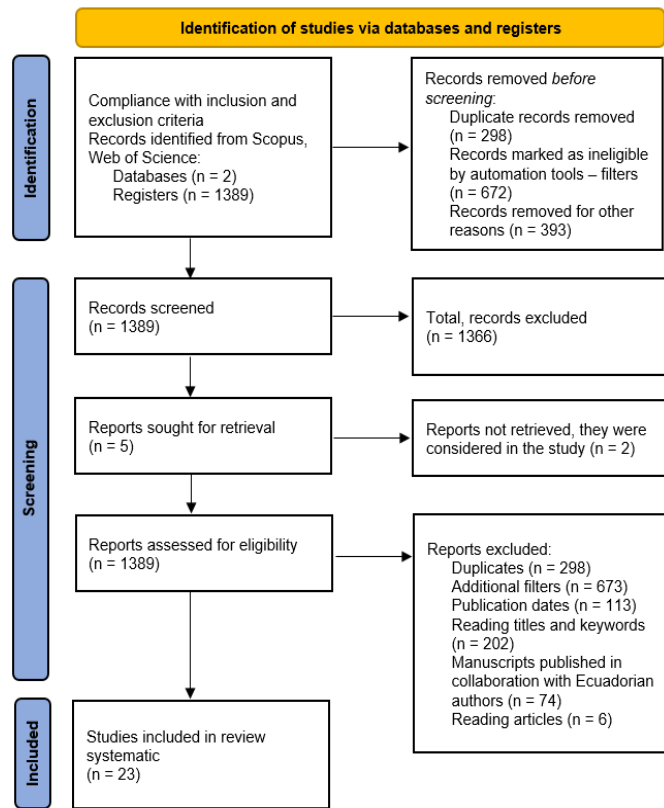


Fig. 1. PRISMA statement, flow diagram for new systematic reviews that included searches of databases and registers only.

D. Phase 4: Data extraction

With all the data was created a database in which were recorded the bibliographic database name, publication title in spanish and english, journal name, publication type, year of publication, objective, keywords, author affiliations, and participating countries. Additionally, the database included the abstract, methodology used, key results, publication characteristics, leading countries and focus.

It was ensured that the data were complete in the database, avoiding errors in data transcription. This process was carried out in collaboration with the research team. Using these variables or criteria of interest was identified how to address each research question. The details are shown in Table 2.

TABLE II  
VARIABLES OF INTEREST THAT WILL ADDRESS THE RESEARCH QUESTIONS

Research question	Criteria of interest
RQ1: What are the characteristics of manuscripts, bibliographic databases and the predominant language in publications by researchers focused on the application of IoT in healthcare?	Reference Manuscript type Bibliographic databases Language Title Authors Countries that collaborate Universities that publish Year of publication Keywords

RQ2: What are the contributions of publications with Ecuadorian authors in globally impactful bibliographic databases regarding IoT?	Main contributions Title Authors Key results
RQ3: In which health fields have the Internet of Things (IoT) application been investigated?	Health fields (UNESCO classification) Article title Summary Conclusions
RQ4: What are the obstacles and challenges in implementing IoT in the healthcare domain?	Classes and subclasses Title Summary Conclusions Key results

After completing the data extraction process, were identified a total of 23 articles authored of Ecuadorian researchers. These articles were selected from the 111 globally identified publications addressing IoT in healthcare. Despite the relatively small number of articles written by Ecuadorian authors in high-impact journals, this quantity is representative and relevant for addressing the research questions.

E. Phase 5: Analysis and reporting of results

The data processing was conducted using qualitative research techniques such as group discussion, observation, and thematic analysis [22], [23]. The data were also quantitatively analyzed, through a correlational analysis of keywords and international collaboration.

III. RESULTS AND DISCUSSION

The results will be presented per research question, aiming to provide organization to the publication and address the study's objective and methodology.

RQ1: What are the characteristics of manuscripts, bibliographic databases and the predominant language in publications by researchers focused on the application of IoT in healthcare?

According to the bibliographic database, Scopus represents 65.21 % (n=15) of the manuscripts and WoS 34.78 % (n=8). Of the 23 identified manuscripts, 21.73 % (n=5) are literature reviews or theoretical studies, and 78.26% (n=18) are original articles. Regarding the source, 39.13 % (n=9) are conference papers, and 60.86 % (n=14) are journal articles. Journal articles are frequent in 2020, 2022 and 2023, while conference articles are notable in 2016, 2017, 2018 and 2021. The year with the highest number of articles published was 2018, with seven manuscripts, followed by 2020 and 2022, with four publications each one.

The 23 articles were written by 92 authors from various countries, 53.26 % (n=49) of which were Ecuadorian. Considering the Covid-19 pandemic as a turning point in the study period, between 2016 and 2018, 10 publications were made with the participation of 58.82 % Ecuadorian authors. After the pandemic, between 2019 and 2023, this number increased to 13 publications, and the participation of Ecuadorian authors was 50 %.

Martínez & Galmés [10] mention a peak of 11 articles in one year related to the topic of information security in IoMT. Furthermore, González-Zamar [24] argues that IoT is an emerging research area in Latin America, with a somewhat modest increase in the publication of scientific articles in recent years. However, is mention a rapid evolution of these technologies, giving rise to a prolific scientific literature in the rest of the world [25]. It is claimed that after 20 years of research, this has been expanded to include smart healthcare [26] and healthcare [27] content.

Furthermore, Herrera-Franco et al. [28] mentions that in the period 2011-2020 the field of engineering was increased in publications by Ecuadorian authors, mainly conference articles at 58 % and magazine articles at 37 %.

The journals cover computer science and communications, engineering, mechanics and health, including Neural Computing and Applications and Computers in Biology and Medicine. The 86.95 % (n=20) of the manuscripts were published in english, suggesting an orientation towards the international audience [24] and active participation in the global conversation on IoT and health. The 13.04 % (n=3) were in spanish, emphasizing the importance of making research accessible to the local audience and promoting communication at the national level. Herrera-Franco et al. [28] found a similar result

in relation to the languages in which research is published in Ecuador.

Of the articles mentioned, 39.13 % are authored exclusively by Ecuadorian writers, while 34.78 % involve collaboration with Spanish authors. Furthermore, with a correlation coefficient of 0.22, Ecuador demonstrates a significant relationship with Spain regarding international collaboration. The remaining articles include contributions from authors from Pakistan, Chile, Dubai, Algeria, India, Finland and Italy, all exhibiting null correlation coefficients. According to Herrera-Franco [28], Spain is the leading scientific collaborator of Ecuador, and these publications involve international solid collaboration, being indexed in high-impact bibliographic databases such as Scopus and resulting in a significant contribution to the country and to the academic world.

As for the author’s affiliations, various Ecuadorian universities are represented, most notably the Universidad Politécnica Nacional and the Universidad Politécnica del Litoral. According to Herrera-Franco et al. [28] these universities are mentioned among the institutions with the most significant scientific production in the country. In Table 3 is presented detailed information about the characteristics of the manuscripts. Note that in the quartiles field, those articles without quartiles are denoted with *N/Q*.

TABLE III  
CHARACTERISTICS OF THE PUBLICATIONS

Year	Ref.	Authors	Journal / Proceeding	Type	Countries	Ecuadorian university	Bibliographical base	Quartile	Journal name
2016	[1]	J. Gómez, B. Oviedo, & E. Zhuma.	Proceeding paper	Original	Colombia, Ecuador	Universidad Técnica Estatal de Quevedo	Scopus	N/Q	Procedia Computer Science
	[29]	S.G. Yoo, & F. Castro-De La Gruz.	Proceeding paper	Original	Ecuador	Escuela Politécnica Superior del Ejército	Scopus	N/Q	IEEE Xplore (IRIS)
2017	[30]	J.M. Parra, W. Valdez, A. Guevara, P. Cedillo, & J. Ortíz-Segarra.	Proceeding paper	Original	Ecuador	Universidad de Cuenca	Scopus	N/Q	IEEE Xplore (BIOMEDIC)
	[31]	A.M. Plaza, J. Díaz, & J. Pérez.	Journal	Review	Spain, Ecuador	Universidad Politécnica Salesiana	Scopus	Q2	Special Issue: SECH
	[32]	D.C. Yachirema, C.E. Sarabia-Jácome, C.E. Palau, & M. Esteve.	Journal	Original	Ecuador, Spain	Escuela Politécnica Nacional	WoS	Q2	IEEE Access
	[11]	D. Yachirema, J.S. De Puga, C. Palau, & M. Esteve.	Proceeding paper	Original	Spain, Ecuador	Escuela Politécnica Nacional Ecuador	Scopus	N/Q	Procedia Computer Science
	[4]	D. Yachirema, C.E. Sarabia-Jácome, C.E. Palau, & M. Esteve.	Journal	Original	Ecuador, Spain	Escuela Politécnica Nacional Ecuador	WoS	Q2	Pervasive and Mobile Computing
2018	[33]	M.G. Molina, P.E. Garzón, C.J. Molina, & J.X. Nicola.	Proceeding paper	Original	Ecuador	Escuela Superior Politécnica del Litoral	Scopus	N/Q	Computers communications - (CSCC 2018)
	[34]	W. Velásquez, A. Muñoz-Arcantales, & J. Salvachúa.	Proceeding paper	Original	Spain, Ecuador	Escuela Superior Politécnica Del Litoral	Scopus	N/Q	IEEE Xplore (CCWC 2018)
	[9]	L. Enciso-Quispe, S. Sarmiento, & E. Zelaya-Policarpo.	Proceeding paper	Original	Ecuador	Universidad Técnica Particular de Loja	Scopus	N/Q	IEEE Xplore (CISTI 2018)
	[35]	W. Velasquez, J. Muñoz, & J. Salvachua.	Journal	Original	Ecuador, Spain	Escuela Superior Politécnica del Litoral	WoS	Q3	Engineering Letters
2019	[2]	J. Bedón-Molina, M. J. López, & I.S. Derpich.	Journal	Original	Chile, Ecuador	Universidad Central del Ecuador, Escuela Politécnica Superior del Ejército	WoS	Q3	Advances in Mechanical Engineering
	[37]	M.A. Quiroz-Martínez, R.A. Arguello-Ruiz, M.D. Gómez-Ríos, M.Y. Leyva- Vázquez.	Journal	Original	Ecuador	Universidad Politécnica Salesiana	WoS	Q4	Conrado
2020	[38]	M.Y.L. Vazquez, B.S.M. Arteaga, J.A.M. López, & M.A.Q. Martínez.	Journal	Original	Ecuador	Universidad Politécnica Salesiana	Scopus	Q4	RISTI



regarding challenges related to data privacy and interoperability standards [10].

RQ2: What are the contributions of publications with Ecuadorian authors in globally impactful bibliographic databases regarding IoT?

Among the contributions are implementing real-time patient monitoring systems, designing IoT-based medical devices for patients with chronic and geriatric conditions, as well as developing innovative solutions for telemedicine and patient care in remote areas.

As for the contributions of Ecuadorian authors in the global field of IoT in health, the research covers various areas. In the ‘real-time health monitoring and medical device design’ category, contributions integrating IoT into healthcare services have been identified, such as the obstructive sleep apnea (OSA) monitoring system [4] and fall detection for the elderly [11]. These contributions are developed in the specific fields of medicine and nursing. Zeadally’s study [46] also emphasizes the importance of a patient monitoring application for transmitting blood pressure readings and detecting health issues.

In ‘specific IoT technologies’ contributions incorporate advancements such as 3D accelerometers and wearables for real-time monitoring [11]. IoT interoperability facilitates the integration of devices in a connected environment, while low-power networks focus on sustainable efficiency [4]. The development of devices, like heart rate monitors with Arduino microcontrollers, highlights the practical applicability of IoT in healthcare [33]. The home-based approach is reflected in telemedicine systems and care modules, promoting remote healthcare and health monitoring [39]. These innovative applications enhance the quality of life and the comprehensive management of healthcare services [47].

In this same field of medicine and nursing, contributions have been made to data analysis and efficient healthcare management [1], [29]. For instance, in Herrera-Franco et al. [28], under the management category it has led to the generation of studies related to big data, which is becoming an increasingly challenging area. Other studies have addressed specific areas of health, such as epidemiology and cardiology, highlighting the diversity of approaches and solutions proposed in specialized healthcare fields [12], [33].

Another contribution lies in telemedicine and remote patient care, emphasizing the importance of remote connectivity and efficiency in medical communication, such as developing a home telemedicine system with a positive assessment by healthcare professionals [39]. This potential of IoT is applied in the specific field of social assistance and counseling [36], [40]. According to Banerjee et al. [47] and Herrera-Franco et al. [28], there is a discussion about the advancement of this technology designed specifically for this purpose. Additionally, computational sciences have strengthened the field of telemedicine.

Table 4 presents the information detailing the contributions from the 23 articles.

TABLE IV  
CONTRIBUTIONS OF THE PUBLICATIONS

Reference / Title	Contributions
[1] Patient Monitoring System Based on Internet of Things	Use of mobile technologies and smart devices in the field of health. MHealth and E-Health. Health monitoring.
[29] Enhanced BSN-Care: Cryptanalysis of BSN-Care and Proposal of Improved Authentication System	Integration of IoT in health services. Implementation of OpenMRS and DHIS2. Evaluation through a case study.
[30] Intelligent Pillbox: Automatic and Programmable Assistive Technology Device	Development of an assisted technology (AT) device. Use of open source technologies with a low cost and without limitations of licenses and functions. Management of medication-taking programs. Focus on supporting older people and vulnerable groups.
[31] Software architectures for health care cyber-physical systems: A systematic literature review	Literature on Cyber-Physical Systems in Health (Healthcare CPS). Identification of successful solutions. Identification of research gaps.
[32] A Smart System for Sleep Monitoring by Integrating IoT with Big Data Analytics	Obstructive sleep apnea (OSA) monitoring system. Two-processing system architecture. Batch data processing (Batch).
[11] Fall Detection System for Elderly People Using IoT and Big Data	Fall detection system for seniors. Use of emerging technologies. Use of 3D accelerometer and wearable. Data processing and Big Data modeling.
[4] System for Monitoring and Supporting the Treatment of Sleep Apnea Using IoT and Big Data	Monitoring and management of sleep apnea in older people. IoT interoperability. Reduce latency for sending notifications. Low energy networks and smart devices. Large-scale data analysis (Big Data).
[33] Heart Rate Monitor Based on IP Networking	Development of a device to measure heart rate. Use of IoT technology. Use of Arduino microcontrollers.
[34] Fast-Data Architecture Proposal to Alert People in Emergency	Summary of technologies related to smart cities and big data. Architecture proposal for fast data. Focus on the resilience of smart cities.
[9] Personalized Medical Alert System Based on Internet of Things with DHIS2	Implementation of an IoT Solution in Health. Use of OpenMRS and DHIS2. Smart Medical Alerts. Study of cases in continuous monitoring, based on MHealth for detecting diseases.
[35] E-Health Services Role in a Smart City. A View After a Natural Hazard	Exploration of concepts and techniques in smart cities (Smart Cities). Preparation for unexpected events such as earthquakes. Development of rules and priorities. Prioritized services such as E-Health.
[2] A Home-Based Smart Health Model	Creation of a hardware-software architectural model. Focus on smart home health. Analysis of the potential of IoT and IoMT. Model evaluation.

[38] Design of an IoT Architecture in Medical Environments for the Treatment of Hypertensive Patients	Design of an IoT architecture in medical environments, patients with Arterial Hypertension pathology. Use the TOPSIS method (Technique for Ordering Preferences by Similarity to the Ideal Solution). Greater control and monitoring of patients. It provides scalability, fluidity and security, where its main characteristic is adaptability to growth without losing quality.
[39] Low-Cost Iot Framework for Tele-Medicine Applications	Development of home telemedicine system. Data analysis by health professionals. Medical prescriptions. Positive assessment from health professionals.
[40] Systematic Literature Review of Internet of Things Solutions Oriented to People with Physical and Intellectual Disabilities	A systematic review of IoT solutions for people with disabilities. Identification of research gaps. Description of the main characteristics of IoT solutions for this group of people.
[10] Analysis of the Primary Attacks on IoMT Internet of Medical Things Communications Protocols	Analysis of security in IoMT communication protocols. Exploring vulnerabilities and threats in IoMT. Proposal for future research directions.
[41] A Systematic Review of Internet of Things in Clinical Laboratories: Opportunities, Advantages and Challenges	A systematic review of IoT in clinical laboratory processes. Identification of challenges and open problems. Relevance for the development of IoT in clinical laboratories.
[42] A Deep Learning System for Health Care IoT and Smartphone Malware Detection	Efficient malware detection. Application on connected devices. Evaluation of precision and effectiveness.
[43] A Computational Framework for Cyber Threats in Medical IoT Systems	Development of a secure and efficient medical IoT communication framework. Preventing cyber threats in intelligent social systems. Use of Artificial Intelligence techniques.
[44] Smart Healthcare Applications Over 5G Networks: A Systematic Review	Impact of 5G technology on the provision of health services. A systematic review of the literature. Promising prospects.
[12] An Intelligent Health Monitoring and Diagnosis System Based on the Internet of Things and Fuzzy Logic for Cardiac Arrhythmia Covid-19 Patients	Smart health monitoring and diagnosis system. Use of Artificial Intelligence (AI). IoT-based health monitoring. Intelligent Electrocardiogram (ECG) signal processing algorithm. Benefit for isolated patients with critical cardiac arrhythmia Covid-19.
[45] Assistance Module to Measure a Person's Vital Signs Using the Internet of Things	Development of a care module to measure vital signs. Use of IoT technology. Contribution to the development of health technology in Ecuador.

RQ3: In which health fields have the Internet of Things (IoT) application been investigated?

Have been found proposals, models and systems, starting in internal medicine and gerontology [32] and moving on to medical services and clinical laboratories [41]. Other publications have presented prototypes and experimental proposals [11], while others have conducted comprehensive reviews and original studies in fields such as epidemiology, cardiology and nursing [12], [33].

Although several of the works do not explicitly address the area and sub-area of knowledge in which they apply IoT, the diversity of approaches and proposed solutions highlight the application of this technology in the broad field of Health and Wellness. Table 5 shows the UNESCO sub-area of knowledge in which each publication falls, considering that the knowledge area is Health and Wellness. Note that some references are cited in several areas.

TABLE V  
CLASSIFICATION OF PUBLICATIONS  
BY UNESCO AREAS AND SUBAREAS

Area/Subarea	Specific subarea	References
Health	Medicine	[1], [2], [10], [31], [41], [12], [33], [38]
	Medicine/nursing and midwifery	[29], [8]
Wellness	Care of the elderly and adults with disabilities	[32], [11], [4], [30]
	Social assistance and advice	[40]
Health & Wellness	Medicine / care of the elderly and adults with disabilities	[9], [10], [42], [34], [35], [37], [39], [44], [43], [45]

The devices for assistance and technology for vulnerable groups demonstrate concern for developing assistive technology devices and managing medication-taking programs for these population groups [30]. These efforts highlight the practical application of IoT to improve the quality of life. In this regard, the field of elderly care and adults with disabilities has been taken into account for the development of approaches and models that will enhance healthcare and public health services [3], [4], [10], [42], [44]. Even in Banerjee et al. [47] and Zeadally et al. [46] is mentioned that these devices collect data to be analyzed through artificial intelligence for possible predictions of health-related issues, contributing to the evolution towards intelligent health where are used conventional mobile devices in conjunction with portable medical devices.

RQ4: What are the obstacles and challenges in implementing IoT in the healthcare domain?

Implementing the Internet of Things (IoT) in the health field faces various obstacles and challenges that require attention. It is important to note that, since the publications are contributions from Ecuadorian authors, they do not necessarily focus on specific challenges and limitations of Ecuador, but address general aspects in this field. Also, it is essential to note that not all articles in their full publications explicitly mention these challenges or limitations. The details are shown in Table 6 where is noteworthy that certain manuscripts delineate various challenges.

TABLE VI  
CHALLENGES AND LIMITATIONS REFERENCED  
BY THE MANUSCRIPTS

Challenges and limitations	References
Data privacy and security	[3], [10], [11], [12], [29], [35], [36], [41], [44]
Device interoperability	[41]
Regulatory compliance	[12], [35]
Implementation costs	[9], [41]
Management of large volumes of data	[12], [35]
Technical faults and reliability	[3], [9], [11], [29], [32], [41], [43], [45]
Scalability	[35], [38], [41]
Ethics in data collection and use	[29], [35]

Regarding the challenges in implementing IoT-based health systems, most of them generally mention that privacy and data security emerge as crucial challenges. They focus on protecting the confidential patient information and highlight limitations in the security protocols, emphasizing the need for robust approaches to safeguard information [3], [10], [11], [12], [29], [35], [36], [41], [44]. Additionally, Banerjee et al. [47] and Wang et al. [26] emphasize the issue of data privacy as a top challenge, demonstrating that critical studies in this field primarily concentrate on IoT security, wireless sensor networks, IoT management, IoT challenges and privacy.

Another challenge is the interoperability of medical devices, emphasizing the need for standardization to facilitate effective communication between systems [41]. According to Hendriks [15], open standards can enhance interoperability. However, which strategies should be implemented to create standards that enable a certain degree of functional openness still needs to be better understood.

Compliance with regulations, particularly with acts like the Health Insurance Portability and Accountability Act (HIPAA), adds complexity to the implementation. This challenge underscores the importance of aligning solutions with established standards and regulations to ensure legality and ethics [12], [35]. In Kante & Ndayizigamiye [48], Senegal is mentioned as the only country with regulations addressing this issue. Their analysis of Medical Internet of Things (IoMT) policies suggests that academics should provide more evidence on IoMT so that policymakers can act accordingly to enhance healthcare.

Managing large volumes of data is another challenge, emphasizing the importance of efficient solutions for data collection, storage, and analysis using artificial intelligence techniques [12], [35]. Reliability and technical failures are also highlighted, underscoring the need for robust and dependable systems to ensure consistent and secure performance in critical healthcare environments [3], [9], [11], [29], [32], [41], [43], [45].

Regarding scalability, technical failures and reliability are challenges that require solutions to ensure the adaptability and reliability of systems for their continuous growth and to meet the changing demands of the healthcare system [35], [38],

[41]. Ethical considerations in data collection and use are also highlighted as critical challenges [29], [35]. These aspects underscore the complexity faced in effectively integrating IoT in the healthcare domain.

#### IV. CONCLUSION

In recent years, there has been an increase in the publication of scientific articles by Ecuadorian authors in the field of IoT applied to health, especially in collaboration with Spain. Furthermore, the active participation of authors affiliated with Ecuadorian universities indicates a prominent role of the academic community in this area. Areas of contribution were identified, including real-time health monitoring, medical devices, security and vulnerabilities, data management and big data and medical applications. These categories cover the contributions of publications in bibliographic databases of global impact.

Future research should address the identified challenges, particularly protecting patient data privacy and security. It is essential to establish standards to ensure the interoperability of medical devices and develop mechanisms to comply with regulations through ethical policies and regulations on data use.

In addition, regional bibliographic databases such as Scielo and Latindex should be considered to verify and expand the status of publications on the topic and obtain a complete view of the scientific literature by Ecuadorian authors. While this systematic review provides an overview, some limitations were identified, such as the number of manuscripts included. The final number of articles may have been affected by the availability of specific studies in high-impact bibliographic databases, also, during the comprehensive review were excluded many titles that did not meet the inclusion criteria.

#### APPENDIX

##### A. Author contributions

For research articles with several authors must be provided a short paragraph specifying their individual contributions. C.V.O refers to Cristina Vaca Orellana and M.V.D refers to María Valle Dávila. The following statements should be used: Conceptualization, C.V.O. and M.V.D.; methodology, C.V.O.; software, C.V.O.; validation, C.V.O., M.V.D.; formal analysis, M.V.D.; investigation, C.V.O.; resources, C.V.O.; data curation, C.V.O.; writing—original draft preparation, M.V.D.; writing—review and editing, C.V.O. and M.V.D.; visualization, M.V.D.; supervision, M.V.D.; project administration, C.V.O. and M.V.D.; funding acquisition, C.V.O. and M.V.D. All authors have read and agreed to the published version of the manuscript.

##### B. Funding

This research received no external funding.

##### C. Conflicts of interest

The authors declare no conflict of interest. The funders had no role in the design of the study or in the collection, analyses,

or interpretation of data; even in the writing of the manuscript or in the decision to publish the results.

## REFERENCES

- [1] J. Gómez, B. Oviedo, and E. Zhuma, "Patient Monitoring System Based on Internet of Things," *Procedia Computer Science*, vol. 83, no. 1, pp. 90–97, 2016, doi: 10.1016/j.procs.2016.04.103.
- [2] J. Bedón-Molina, M.J. López, and I.S. Derpich, "A Home-Based Smart Health Model," *Advances in Mechanical Engineering*, vol. 12, no. 6, pp. 1–16, 2020, doi: 10.1177/1687814020935282.
- [3] G. Guerrero-Ulloa, C. Rodríguez-Domínguez, and M.J. Hornos, "IoT-Based System to Help Care for Dependent Elderly," in *Communications in Computer and Information Science*, M. Botto-Tobar, G. Pizarro, M. Zúñiga-Prieto, Eds. Cham, Switzerland, Springer International Publishing, 2019, pp. 41–55.
- [4] D. Yacchirema, C.E. Sarabia-Jácome, C.E. Palau, and M. Esteve, "System for Monitoring and Supporting the Treatment of Sleep Apnea Using IoT and Big Data," *Pervasive and Mobile Computing*, vol. 50, pp. 25–40, 2018, doi: 10.1016/j.pmcj.2018.07.007.
- [5] W.G.C. Sailema, T. Olivares, and F. Delicato, "Topologías en el Internet de las Cosas Médicas (IoMT)," *Revista Tecnológica – ESPOL*, vol. 34, no. 4, pp. 120–136, 2022, doi: 10.37815/rte.v34n4.960.
- [6] S. Li, L.D. Xu, and S. Zhao, "The Internet of Things: A Survey". *Information Systems Frontiers*, vol. 17, no. 2, pp. 243–259, 2015, doi: <https://doi.org/10.1007/s10796-014-9492-7>.
- [7] J.C.V. Ferreira, M.F.C. Higuera, and J.A.V. Barrera, "Nuevos desafíos en el desarrollo de soluciones para E-Health en Colombia, soportados en Internet de las Cosas (IoT)," *Revista EIA*, vol. 18, no. 36, pp. 1–19, 2021, doi: 10.24050/reia.v18i36.1508.
- [8] L. Pozo-Guzman, J. Berrezueta-Guzman, "IoT as an Alternative Way to Improve the Telemedicine Methods Against Covid-19 in Vulnerable Zones," in *Computer and Information Science*, G. Rodríguez Morales, E.R. Fonseca, J.P. Salgado, M. Pérez-Gosende, M. Orellana Cordero, S. Berrezueta, Eds. Cham, Switzerland: Springer International Publishing, 2020, pp. 64–76.
- [9] L. Enciso-Quispe, S. Sarmiento, and E. Zelaya-Policarpo, "Personalized Medical Alert System Based on Internet of Things with DHIS2," in *Proceeding of the 13th Iberian Conference on Information Systems and Technologies (CISTI)*, Cáceres, Spain, 2018, pp. 1–6.
- [10] C.J. Martínez, S. Galmés, "Analysis of the Primary Attacks on IoMT Internet of Medical Things Communications Protocols," in *Proceedings of the IEEE World AI IoT Congress (AIoT)*, Seattle, WA, USA, June 2022.
- [11] D. Yacchirema, J.S. De Puga, C. Palau, and M. Esteve, "Fall Detection System for Elderly People Using IoT and Big Data," *Procedia Computer Science*, vol. 130, pp. 603–610, 2018, doi: 10.1016/j.procs.2018.04.110.
- [12] M.Z. Rahman, M.A. Akbar, V. Leiva, A. Tahir, M.T. Riaz, and C. Martín-Barreiro, "An Intelligent Health Monitoring and Diagnosis System Based on the Internet of Things and Fuzzy Logic for Cardiac Arrhythmia Covid-19 patients," *Computers in Biology and Medicine*, vol. 154, pp. 106583, Mar. 2023, doi: 10.1016/j.combiomed.2023.106583.
- [13] K. Kakhi, R. Alizadehsani, H.M.D. Kabir, A. Khosravi, S. Nahavandi, and R. Acharya, "The Internet of Medical Things and Artificial Intelligence: Trends, Challenges, and Opportunities," *Biocybernetics and Biomedical Engineering*, vol. 42, no. 3, pp. 749–771, 2022, doi: 10.1016/j.bbe.2022.05.008.
- [14] C. Yacchirema-Vargas, "Arquitectura de interoperabilidad de dispositivos físicos para el Internet de las Cosas (IoT)". Ph.D. dissertation, Universidad Politécnica de Valencia, Valencia, España, 2019, [Online]. Available: <https://dialnet.unirioja.es/servlet/tesis?codigo=250219>
- [15] S. Hendriks, "Internet of Things: How the World Will be Connected in 2025". Master thesis, Utrecht University, Netherlands. 2016, [Online]. Available: <https://studenttheses.uu.nl/handle/20.500.12932/23719>
- [16] H. Arksey, L. O'Malley, "Scoping Studies: Towards a Methodological Framework," *International Journal of Social Research Methodology*, vol. 8, no. 1, pp. 19–32, 2005, doi: 10.1080/1364557032000119616.
- [17] R, The R Project for Statistical Computing. [Online]. Available: <https://www.r-project.org/>.
- [18] Zotero, Your Personal Research Assistant. [Online]. Available: <https://www.zotero.org/>.
- [19] M.F. Abad-García, A. González-Teruel, J. Argento, and J.M. Rodríguez-Gairín, "Características y visibilidad de las revistas españolas de ciencias de la salud en bases de datos", *Profesional de la información*, vol. 24, no. 5, pp. 537–550, 2015, doi: 10.3145/epi.2015.sep.04.
- [20] A. Vuotto, V. Di Césare, and N. Pallota, "Fortalezas y debilidades de las principales bases de datos de información científica desde una perspectiva bibliométrica," *Palabra clave*, vol. 10, no. 1, pp. 101, 2020.
- [21] F. Sadoughi, A. Behmanesh, and N. Sayfori, "Internet of Things in Medicine: A Systematic Mapping Study," *Journal of Biomedical Informatics*, vol. 103, no., pp. 103383, 2020, doi: 10.1016/j.jbi.2020.103383.
- [22] M.A.G. Bejarano, "La investigación cualitativa," *INNOVA Research Journal*, vol. 1, no. 2, pp. 1–9, 2016, doi: 10.33890/innova.v1.n2.2016.7.
- [23] H. Fernández-Sánchez, K. King, and C.B. Enríquez-Hernández, "Revisión sistemática exploratoria como metodología para la síntesis del conocimiento científico," *Enfermería universitaria*, vol. 17, no. 1, pp. 87–94, 2020, doi: 10.22201/eneo.23958421e.2020.1.697.
- [24] M.D. González-Zamar, E. Abad-Segura, E. Vásquez-Cano, and E. López-Meneses, "IoT Technology Applications-Based Smart Cities: Research Analysis," *Electronics*, vol. 9, no. 8, pp. 1246, 2008, doi: 10.3390/electronics9081246
- [25] B. Mazon-Olivo, A. Pan, "Internet of Things: State-of-the-art, Computing Paradigms and Reference Architectures," *IEEE Latin America Transactions*, vol. 20, no. 1, pp. 49–63, 2022, doi: 10.1109/TLA.2022.9662173.
- [26] J. Wang, M.K. Lim, C. Wang, and M.L. Tseng, "The Evolution of the Internet of Things (IoT) Over the Past 20 Years," *Computers & Industrial Engineering*, vol. 155, pp. 107174, 2021, doi: 10.1016/j.cie.2021.107174.
- [27] J. Ruiz-Rosero, G. Ramirez-Gonzalez, J.M. Williams, R. Khanna, and R. Pisharody, "Internet of Things: A Scientometric Review," *Symmetry*, vol. 9, no. 12, pp. 301, 2017, doi: 10.3390/sym9120301.
- [28] G. Herrera-Franco, N. Montalván-Burbano, C. Mora-Frank, and L. Bravo-Montero, "Scientific Research in Ecuador: A Bibliometric Analysis," *Publications*, vol. 9, no. 4, pp. 55, 2021, doi: 10.3390/publications9040055.
- [29] S.G. Yoo, F. Castro De la Cruz, "Enhanced BSN-Care: Cryptanalysis of BSN-Care and Proposal of Improved Authentication System," in *Proceeding of the IEEE International Symposium on Robotics and Intelligent Sensors (IRIS)*, Tokyo, Japan, 2016, pp. 17–20.
- [30] J.M. Parra, W. Valdez, A. Guevara, P. Cedillo, and J. Ortiz-Segarra, "Intelligent Pillbox: Automatic and Programmable Assistive Technology Device," in *Proceeding of the 13th IASTED International Conference on Biomedical Engineering (BioMed)*, Innsbruck, Austria, 2017, pp. 20–21.
- [31] A.M. Plaza, J. Díaz, and J. Pérez, "Software Architectures for Health Care Cyber-Physical Systems: A Systematic Literature Review," *Journal of Software: Evolution and Process*, vol. 30, no. 7, pp. 1–23, 2018, doi: 10.1002/smr.1930.
- [32] D.C. Yacchirema, C.E. Sarabia-Jácome, C.E. Palau, and M. Esteve, "A Smart System for Sleep Monitoring by Integrating IoT with Big Data Analytics," *IEEE Access*, vol. 6, pp. 35988–36001, 2022, doi: 10.1109/ACCESS.2018.2849822.
- [33] M.G. Molina, P.E. Garzón, C.J. Molina, and J.X. Nicola, "Heart Rate Monitor Based on IP Networking," in *Proceeding of the 22nd International Conference on Circuits, Systems, Communications and Computers (CSCC 2018)*, 2018, pp. 1006.
- [34] W. Velásquez, A. Muñoz-Arcenales, and J. Salvachúa, "Fast-Data Architecture Proposal to Alert People in Emergency," in *Proceeding of the IEEE 8th Annual Computing and Communication Workshop and Conference (CCWC)*, Las Vegas, USA, 2018, pp. 188–200.
- [35] W. Velásquez, J. Muñoz, and J. Salvachúa, "E-Health Services Role in a Smart City-A View after a Natural Hazard," *Engineering Letters*, vol. 27, no. 4, pp. 686–695, 2019.
- [36] G. Guerrero-Ulloa, M.J. Hornos, C. Rodríguez-Domínguez, and M. Fernández-Coello, in "IoT-Based Smart Medicine Dispenser to Control and Supervise Medication Intake," C.A. Iglesias, J.I. Moreno Novella, A. Ricci, D. Rivera, D. Roman, Eds. *Intelligent Environments 2020*, 2020, vol. 28, pp. 39–48.
- [37] M.A. Quiroz-Martínez, R.A. Arguello-Ruiz, M.D. Gómez-Ríos, and M.Y. Leyva-Vázquez, "Evaluación de potencial del Internet de las Co-

- sas en la salud mediante mapas cognitivos difusos,” *Conrado*, vol. 16, no. 35, pp. 131-136, 2020.
- [38] M.Y.L. Vázquez, B.S.M. Arteaga, J.A.M. López, and M.A.Q. Martínez, “Design of an IoT Architecture in Medical Environments for the Treatment of Hypertensive Patients,” *Revista Ibérica de Sistemas e Tecnologías de Informação*, vol. E33, pp. 188-200, 2020.
- [39] A. Garcés-Salazar, S. Manzano, C. Nuñez, J.P. Pallo, M. Jurado, and M.V. García, in “Low-cost IoT framework for tele-medicine applications,” *Revista Ibérica de Sistemas e Tecnologías de Informação*, vol. E43, pp. 153-166, 2021.
- [40] U. Ulloa, D. Prado, and P. Cedillo, “Systematic Literature Review of Internet of Things Solutions Oriented to People with Physical and Intellectual Disabilities,” in *Proceedings of the 7th International Conference on Information and Communication Technologies for Ageing Well and e-Health (ICT4AWE 2021)*, 2021, pp. 228-235.
- [41] T. Munir, M. Akbar, S. Ahmed, A. Sarfraz, Z. Sarfraz, M. Sarfraz, M. Feliz, and I. Cherrez-Ojeda, “A Systematic Review of Internet of Things in Clinical Laboratories: Opportunities, Advantages, and Challenges,” *Sensors*, vol. 22, no. 20, pp. 8051, 2022, doi: 10.3390/s22208051.
- [42] M. Amin, D. Shehwar, A. Ullah, T. Guarda, T.A. Tanveer, and S. Anwar, “A Deep Learning System for Health Care IoT and Smartphone Malware Detection,” *Neural Computing & Applications*, vol. 34, no. 14, pp. 11283-11294, 2022, doi: 10.1007/s00521-020-05429-x.
- [43] G. Rathee, H. Saini, C.A. Kerrache, and J. Herrera-Tapia, “A Computational Framework for Cyber Threats in Medical IoT Systems,” *Electronics*, vol. 11, no. 11, pp. 1705, 2022, doi: 10.3390/electronics11111705.
- [44] A.M. Peralta-Ochoa, P.A. Chaca-Asmal, L.F. Guerrero-Vásquez, J.O. Ordoñez-Ordoñez, and E.J. Coronel-González, “Smart Healthcare Applications over 5G Networks: A Systematic Review,” *Applied Sciences*, vol. 13, no. 3, pp. 1469, 2023, doi: 10.3390/app13031469.
- [45] J. Villacís, F. Morales, E. González, and R. Coral, “Módulo asistencial para medir signos vitales de una persona mediante Internet de las Cosas,” *Revista Ibérica de Sistemas e Tecnologías de Informação*, vol. E55, pp. 52-66. Jan. 2023.
- [46] S. Zeadally, F. Siddiqui, Z. Baig, and A. Ibrahim, “Smart Healthcare: Challenges and Potential Solutions Using Internet of Things (IoT) and Big Data Analytics,” *PSU Research Review*, vol. 4, no. 2, pp. 149-168, 2019, doi: 10.1108/PRR-08-2019-0027.
- [47] A. Banerjee, C. Chakraborty, A. Kumar, and D. Biswas, “Emerging Trends in IoT and Big Data Analytics for Biomedical and Health Care Technologies,” V.E. Balas, V.K. Solanki, R. Kumar, M. Khari, Eds. *Handbook of Data Science Approaches for Biomedical Engineering*, Academic Press, 2020, pp.121-152.
- [48] M. Kante, P. Ndayizigamiye, “An Analysis of the Current Status of Internet of Medical Things Policies in Developing Countries,” *NPG Neurologie - Psychiatrie – Gériatrie*, vol. 20, no. 119, pp. 259-265, 2020, doi: 10.1016/j.npg.2020.03.002.

# Nutritional Physiology of *Spodoptera frugiperda* (J. E. Smith) (Lepidoptera: Noctuidae) Fed on Different Wheat Varieties

Aqsa Amjad<sup>1</sup>, Muhammad I. Ullah<sup>2</sup>, Muhammad Arshad<sup>3</sup>,  
Muhammad Z. Majeed<sup>4</sup>, Rafia Umar<sup>5</sup>, Nahdia Perveen<sup>6</sup>, Muqadas Qadeer<sup>7</sup>, Haroon Gul<sup>8</sup>

**Abstract** — Within the context of agricultural ecosystems, understanding the nutritional physiology of insects and their host plant preferences is essential for optimizing pest management strategies and improving crop production. In this study, we conducted an in-depth examination of the nutritional physiology of the fall armyworm, *Spodoptera frugiperda* (J. E. Smith) (Lepidoptera: Noctuidae) in the context of different host plants, specifically wheat varieties, in comparison to maize. Our investigation focused on key parameters, including the Relative Consumption Rate (RCR), Relative Growth Rate (RGR), and Efficiency of Conversion of Ingested Food (ECI) of *S. frugiperda* fed on different wheat varieties including: Dilkash-20, Fakhar-E-Bhakar-17, Subhani-21, Faisalabad-08, and Akbar-19 in comparison to maize (NK-6654). The results revealed that *S. frugiperda* displayed a significantly ( $P < 0.05$ ) higher RCR (8.08 g/g/day), RGR (1.50 g/g/day), and ECI (25.1 %) when feeding on maize, followed by Fakhar-E-Bhakar-17 (RCR = 7.00 g/g/day, RGR = 1.24 g/g/day and ECI = 21.4 %) and Akbar-19 (RCR = 6.06 g/g/day, RGR = 1.04 g/g/day and ECI = 19.7 %) wheat varieties after 1 week of feeding. The lowest values of all these nutritional parameters were recorded on the Dilkash-20 variety (RCR = 2.98 g/g/day, RGR = 0.38 g/g/day, and ECI = 7.94 %). These findings offer valuable insights into the nutritional interactions between *S. frugiperda* and the host plants, shedding light on potential implications for pest management strategies and crop patterns.

**Keywords** — Feeding Indices Parameters; *Spodoptera frugiperda*; Wheat Varieties; Insect-plant Interaction.

**Resumen** — En el contexto de los ecosistemas agrícolas, comprender la fisiología nutricional de los insectos y sus preferencias de plantas hospedantes es fundamental para optimizar las estrategias de manejo de plagas y mejorar la producción de cultivos. En este estudio, llevamos a cabo un examen en profundidad de la fisiología nutricional del gusano cogollero, *Spodoptera frugiperda* (J. E. Smith) (Lepidoptera: Noctuidae) en el contexto de diferentes plantas hospedantes, específicamente variedades de trigo, en comparación con el maíz. Nuestra investigación se centró en parámetros clave, incluida la Tasa de consumo relativo (RCR), la Tasa de crecimiento relativo (RGR) y la Eficiencia de conversión de los alimentos ingeridos (ECI) de *S. frugiperda* alimentada con diferentes variedades de trigo, incluidas: Dilkash-20, Fakhar-E-Bhakar-17, Subhani-21, Faisalabad-08 y Akbar-19 en comparación con el maíz (NK-6654). Los resultados revelaron que *S. frugiperda* mostró un RCR (8.08 g/g/día), un RGR (1.50 g/g/día) y un ECI (25.1 %) significativamente mayores ( $P < 0.05$ ) cuando se alimentaba de maíz, seguido por Fakhar-E-Bhakar-17 (RCR = 7.00 g/g/día, RGR = 1.24 g/g/día y ECI = 21.4 %) y Akbar-19 (RCR = 6.06 g/g/día, RGR = 1.04 g/g/día y ECI = 19.7 %) variedades de trigo después de 1 semana de alimentación. Los valores más bajos de todos estos parámetros nutricionales se registraron en la variedad Dilkash-20 (RCR = 2.98 g/g/día, RGR = 0.38 g/g/día y ECI = 7.94 %). Estos hallazgos ofrecen información valiosa sobre las interacciones nutricionales entre *S. frugiperda* y las plantas hospedantes, arrojando luz sobre las posibles implicaciones para las estrategias de manejo de plagas y los patrones de cultivo.

**Palabras Clave** — Parámetros de índices de alimentación; *Spodoptera frugiperda*; Variedades de trigo; Interacción insecto-planta.

No funding was available for this research work. The authors are thankful to the Department of Plant Pathology, University of Sargodha, for providing research facilities. All the authors contributed equally.

1. Aqsa Amjad is with the Department of Entomology, University of Sargodha, Sargodha 40100, Pakistan, (e-mail: [aqsaaqsi836@gmail.com](mailto:aqsaaqsi836@gmail.com)). ORCID number <https://orcid.org/0009-0009-5135-438X>

2. Muhammad Irfan Ullah is with the Department of Entomology, University of Sargodha, Sargodha 40100, Pakistan, (e-mail: [muhammad.irfanullah@uos.edu.pk](mailto:muhammad.irfanullah@uos.edu.pk)). ORCID number <https://orcid.org/0000-0002-2463-2665>

3. Muhammad Arshad is with the Department of Entomology, University of Sargodha, Sargodha 40100, Pakistan, (e-mail: [makuaf@gmail.com](mailto:makuaf@gmail.com)). ORCID number <https://orcid.org/0000-0002-5442-0380>

4. Muhammad Zeeshan Majeed is with the Department of Entomology, University of Sargodha, Sargodha 40100, Pakistan, (e-mail: [zeeshan.majeed@uos.edu.pk](mailto:zeeshan.majeed@uos.edu.pk)). ORCID number <https://orcid.org/0000-0002-3786-8589>

5. Rafia Umar is with the Department of Entomology, University of Sargodha, Sargodha 40100, Pakistan, (e-mail: [rrafiaumar@gmail.com](mailto:rrafiaumar@gmail.com)). ORCID number <https://orcid.org/0009-0002-9215-3268>

6. Nahdia Perveen is with the Department of Entomology, University of Sargodha, Sargodha, 40100, Pakistan, (e-mail: [nasirnhdi@gmail.com](mailto:nasirnhdi@gmail.com)). ORCID number <https://orcid.org/0009-0002-8429-7683>

7. Muqadas Qadeer is with the Department of Entomology, University of Sargodha, Sargodha 40100, Pakistan, (e-mail: [muqadasqadeer5455@gmail.com](mailto:muqadasqadeer5455@gmail.com)). ORCID number <https://orcid.org/0009-0003-8026-7740>

8. Haroon Gul is with the Department of Entomology, University of Sargodha, Sargodha 40100, Pakistan, (e-mail: [haroongulquraishi3811@gmail.com](mailto:haroongulquraishi3811@gmail.com)). ORCID number <https://orcid.org/0009-0003-6317-3283>

Manuscript Received: 13/12/2023

Revised: 18/02/2024

Accepted: 26/02/2024

DOI: <https://doi.org/10.29019/enfoqueute.1016>

## I. INTRODUCTION

THE fall armyworm, *Spodoptera frugiperda*, is a significant insect pest of various important agricultural crops [1]. It is native to subtropical and tropical areas of America [2]. *S. frugiperda* was discovered in western Africa in January 2016 [3], [4] and in India in May 2018 [5]. In Pakistan, the presence of *S. frugiperda* on maize crop was reported in 2019 [6].

More than 350 species of plants have been identified which are the hosts of *S. frugiperda* [7]. Other than maize, this pest has a wide host range, particularly soybeans, rice, cotton, and sorghum [7], [8]. The larvae of *S. frugiperda* have the potential to damage more plant species, leading to significant reductions in yields of economically important crops [8]. Several studies

have confirmed the susceptibility of this pest to various economic crops [7], [10]. Without any control measures, the annual maize losses in Africa have been reported to be 8.3 million to 20.6 million tons. These losses might reach 2531 million to 6312 million USD annually [11].

The nutritional value of the host plant affects the population growth of any insects [12]. The nutrition that insects consume from their host plants significantly impacts their growth, reproduction, and survival [13]. In order to investigate how different insect pests impact various plants through their feeding behavior, it is imperative to conduct fundamental biological research on the feeding habits and consumption patterns across different host plants. *S. frugiperda*, while having a preference for maize as its primary crop, can also target alternative crops in the absence of maize availability [14]. There is a need to investigate how *S. frugiperda* affects economically important crops such as rice, sorghum and wheat, given the continued spread of pests in Pakistan.

Wheat (*Triticum aestivum*) holds paramount global importance as a widely cultivated crop. It stands as a staple food crop in Pakistan and plays an important role in the economy of our country. Wheat contributes 9.6 % of the agricultural sectors output and 1.9 % of the nations GDP, which highlights the significance of improving wheat production [15]. According to earlier research done in Brazil, female *S. frugiperda* preferably lays eggs on the upper part of the wheat crop rather than on other parts of the plant [16]. The *S. frugiperda* can harm wheat crops at any phase of growth, from the booting to the milking period. A large population of *S. frugiperda* larvae may accelerate the maturation of wheat in areas where the pest migrates throughout the year [17], [18].

The pest status of *S. frugiperda* is predominantly determined by the growth stages of the host plant infested [19]. Consequently, to effectively evaluate the potential harm inflicted by *S. frugiperda* is essential to examine the influence of different wheat varieties on the pests growth. Understanding this relationship is crucial to accurately assess the risk of damage that *S. frugiperda* poses to wheat crops, as well as to develop an overall understanding of its potential impact. There is limited research available on the influence of wheat compared to maize on the consumption and rate of development of *S. frugiperda*. Also, is becoming a significant pest to other crops such as cotton and soybeans in different countries [19]. We hypothesize that *S. frugiperda* will inflict damage on wheat varieties. In addition, we expect to observe significant differences in the nutritional physiology of the insects when feeding on different wheat varieties compared to maize, indicating potential impacts on their development and survival rates.

## II. MATERIALS AND METHODS

### A. Collection and rearing of *Spodoptera frugiperda*

*Spodoptera frugiperda* egg batches and larvae were collected from a maize field near University of Sargodha. The eggs were placed in petri dishes, and the neonate larvae were provided

with a natural diet (maize leaves). Fresh maize leaves were used as the primary food source and the larval diet was replaced every 24 hours until they reached the pupal stage. Upon pupation, the pupae were separated and placed in plastic cages until the emergence of adults. The adult moths were paired and kept in rearing cages to facilitate oviposition. The larvae from F3 generations were used for further study.

### B. Host plants

The seeds of five varieties of wheat (Dilkash-20, Fakhar-E-Bhakar-17, Subhani-21, Faisalabad-08, and Akbar-19), and one variety of maize (NK-6654) were purchased from the local market of Sargodha. The wheat varieties were selected based on their extensive cultivation by farmers in the selected region. The seeds were set in plastic pots measuring 11x12 cm. Throughout the study, the proper agronomic practices were followed including irrigation and removal of weeds.

### C. Nutritional physiology of *Spodoptera frugiperda* on different hosts

The second instar larvae were obtained from a reared culture. Prior to their release into the experimental arena (petri plates), the larvae were subjected to 24 24-hour period of starvation. Each petri plate contained one larva and was considered as one replication. Almost the same size and weight of leaves from each tested hosts were provided to each larva on a daily basis. The treatments were replicated three times and 10 larvae were tested in each replication. The weighted amount of leaves from each host was provided to larvae and replaced after 24 hours. The experiment was conducted under controlled laboratory conditions ( $25 \pm 2$  °C temperature,  $70 \pm 10$  % RH, and a photoperiod of 14h10 from Monday to Sunday). The data of the developmental period of each larval instar, pupal stage, and adult stage was recorded on a daily basis. The length of the larvae was measured before and after a 24 hour feeding period using a measuring scale. Furthermore, the weight of each larva and its feces was measured on a daily basis using a digital weight balance. Similarly, the weight of the diet provided to the larvae was measured before and after the 24 hour feeding period to determine the consumption rate. Larval mortality data was also recorded daily throughout the duration of the experiment. The parameters of the feeding rates that were calculated from the recorded data (shown in Table 1) were based on Waldbauer's formulas [20].

### D. Statistical analysis

Data were analyzed by one-way ANOVA to assess the importance of host plants on the parameters of *S. frugiperda* feeding rates. The means were compared using Tukey HSD all pairwise comparison test and all the analyses were performed using Mintab 17.0 software.

TABLE 1  
FEEDING INDICES PARAMETERS CALCULATED  
USING FORMULAS SUGGESTED BY WALDBAUER ET AL. [20]

Term	Parameters	Formula	Detail
RCR	relative consumption rate	$RCR = I / B \times T$	I = dry weight of food (g) consumed. T = duration of feeding period (d). and B = insect dry weight gain (g).
RGR	relative growth rate	$RGR = [\Delta B / BI] \times T$	$\Delta B$ = change in body weight of the insect (g). BI = initial larval weight
ECI	efficiency of conversion of ingested food	$ECI = B / I \times 100$	

### III. RESULTS

A significant difference was recorded in the relative consumption rate (RCR) of *S. frugiperda* among different host plants at 1 day ( $F = 1381.0$ ,  $P < 0.001$ ), 3 days ( $F = 1374.0$ ,  $P < 0.001$ ), 5 days ( $F = 814.0$ ,  $P < 0.001$ ) and 7 days ( $F = 1205.0$ ,  $P < 0.001$ ) of feeding. Results revealed that the RCR value of *S. frugiperda* was higher when the larvae fed on maize (5.16-8.08 g/g/day), followed by Fakhar-E-Bhakar-17 (3.99- 7.00 g/g/day), and Akbar-19 (3.13 to 6.06 g/g/day). The lowest RCR value of *S. frugiperda* was recorded on Dilkash-20 (0.98-2.98 g/g/day) and Subhani-21 (1.47-4.05 g/g/day) by 1 week of feeding (Table 2).

A significant difference was recorded in the relative growth rate (RGR) of *S. frugiperda* among different host plants at 1 day ( $F = 1167$ ,  $P < 0.001$ ), 3 days ( $F = 746.0$ ,  $P < 0.001$ ), 5 days ( $F = 679.0$ ,  $P < 0.001$ ) and 7 days ( $F = 229.0$ ,  $P < 0.001$ ) of feeding. The RGR of *S. frugiperda* larvae was higher on maize (1.20 to 1.50 g/g/day), followed by Fakhar-E-Bhakar-17 (0.89 to 1.24g/g/day) in 1 week of feeding. When larvae fed on Akbar-19, the relative growth rate was 0.62-1.04 g/g/day. The lowest RGR value of *S. frugiperda* larvae was recorded on Dilkash-20 ranging from 0.10-0.38 g/g/day in 7 days (Table 3).

A significant difference was recorded in the relative efficiency of conversion of ingested food (ECI) of *S. frugiperda* among different host plants at 1 day ( $F = 5322.0$ ,  $P < 0.001$ ), 3 days ( $F = 2460.0$ ,  $P < 0.001$ ), 5 days ( $F = 2822.0$ ,  $P < 0.001$ ) and 7 days ( $F = 1924.0$ ,  $P < 0.001$ ) of feeding. Results showed that the ECI percentage of *S. frugiperda* was significantly higher on maize (17.92 to 25.09 %) for 1 week of larvae feeding as compared to other wheat varieties. However, the ECI percentage was 15.6-21.4% on Fakhar-e-Bhakar-17 and 13.7-19.7% on the Akbar-19 variety of wheat. The lowest percentage of ECI was 4.05 to 7.937 % on Dilkash-20 (Table 4).

### IV. DISCUSSION

*Spodoptera frugiperda* is a polyphagous pest that feeds on a wide range of crops [9]. Damage caused by this pest can lead to significant yield losses in wheat production, so one aspect of the research focuses on the evaluation of nutritional indices of *S. frugiperda* in various wheat varieties, with the objective of designing

pest management strategies. Although maize is the preferred host for *Spodoptera frugiperda*, the feeding parameters of this pest on Fakhr-e-Bhakar-17 and Akbar-19 wheat varieties were almost similar to those observed on maize. The relative consumption and growth rate of the pests, as well as the conversion efficiency of the ingested feed, were satisfactory in these two wheat varieties. These findings regarding *S. frugiperda* feeding on wheat plants are in agreement with the results of Zhang et al. [17].

According to Gebretsadik et al [21], the development of *S. frugiperda*, including the duration of larval and pupal stages, adult longevity and survival, was significantly influenced by maize compared to other crops. Our results showed that the feeding indices parameters, including relative consumption and growth rate and ingested feed conversion efficiency, were satisfactory when the larvae fed on wheat varieties Fakhr-e-Bhakar-17 and Akbar-19, compared to maize. These results suggested that these varieties may be susceptible to *S. frugiperda* infestation. It should also be mentioned that other factors, such as plant age and abiotic stress, may also affect the nutritional quality of wheat and consequently influence *S. frugiperda* feeding and growth. Feed conversion efficiencies of *S. frugiperda* larvae show significant variations in different host plants. This phenomenon is not unique to this pest, but is a general characteristic observed in almost all insects. A potential factor contributing to this variability could be the ability of insects to make homeostatic adjustments in their consumption rates and efficiency parameters.

These adjustments allow insects to achieve their 'ideal' growth rate, even when consuming foods of varying quality [22].

Even though the main host of fall armyworm remains corn, the results of the study suggest that it can also feed on wheat. Therefore, it is necessary to monitor fall armyworm infestation in wheat crops and employ integrated pest management techniques to effectively control the pest population. The nutritive quality of a host plant can significantly impact on feeding and growth of herbivorous insects including *Spodoptera* sp [23]. Several researchers have examined the effect of host plants on the nutritional indices of insect pests [22], [24]. Awmack & Leather [13] reported that the nutritional value and quality of host plants are crucial

TABLE 2  
RELATIVE CONSUMPTION RATE (MEANS±SE)  
OF *SPODOPTERA FRUGIPERDA* FEEDING ON DIFFERENT  
WHEAT VARIETIES IN COMPARISON TO MAIZE

Host plants	RCR (Relative Consumption Rate, g/g/day)			
	1 DAF	3 DAF	5 DAF	7 DAF
Dilkash-20	0.98±0.013f	1.47±0.012f	2.10±0.132f	2.98±0.132f
Subhani-21	1.47±0.213e	2.00±0.121e	2.94±0.143e	4.05±0.231e
Fasilabad-08	2.01±0.312d	3.03±0.141 d	4.07±0.213d	5.10±0.313d
Akbar-19	3.13±0.345c	4.02±0.213 c	5.03±0.345c	6.06±0.454c
Fakhar-E-Bhakar-17	3.99±0.424b	4.93±0.231b	5.83±0.321b	7.00±0.456b
Maize	5.16±0.432a	6.08±0.442a	6.99±0.453a	8.08±0.463a

DAF = days after feeding, Means sharing similar letters within a column are not significantly different at  $p=0.05$ .

TABLE 3  
RELATIVE GROWTH RATE (MEANS±SE) OF *SPODOPTERA FRUGIPERDA*  
FEEDING ON DIFFERENT WHEAT VARIETIES IN COMPARISON TO MAIZE

Host plants	RGR (Relative Growth Rate, g/g/day)			
	1 DAF	3 DAF	5 DAF	7 DAF
Dilkash-20	0.10±0.001f	0.14±0.012f	0.27±0.001f	0.38±0.021f
Subhani-21	0.28±0.012e	0.37±0.031e	0.45±0.032e	0.56±0.032e
Fasilabad-08	0.48±0.023d	0.56±0.034d	0.69±0.034d	0.79±0.042d
Akbar-19	0.62±0.043c	0.69±0.042c	0.86±0.042c	1.04±0.053c
Fakhar-E-Bhakkar-17	0.89±0.042b	1.06±0.121b	1.16±0.102b	1.24±0.101b
Maize	1.20±0.130a	1.28±0.102a	1.38±0.121a	1.50±0.132a

DAF = days after feeding. Means sharing similar letters within a column are not significantly different at p=0.05.

TABLE 4  
RELATIVE EFFICIENCY OF CONVERSION OF INGESTED FOOD (MEANS±SE)  
OF *SPODOPTERA FRUGIPERDA* FEEDING ON DIFFERENT WHEAT VARIETIES IN COMPARISON TO MAIZE

Host plants	ECI (Efficiency of Conversion of Ingested food %)			
	1 DAF	3 DAF	5 DAF	7 DAF
Dilkash-20	4.05±0.324f	5.12±0.423f	6.20±0.312f	7.94±0.431f
Subhani-21	5.87±0.342e	7.94±0.453e	9.50±0.452e	11.7±0.621e
Fasilabad-08	10.0±0.543d	11.7±0.643d	12.9±0.634d	15.4±0.732d
Akbar-19	13.8±0.532c	15.6±0.743c	17.8±0.843c	19.7±0.934c
Fakhar-E-Bhakkar-17	15.6±0.743b	17.5±0.734b	19.6±0.874b	21.4±0.845b
Maize	17.9±0.745a	19.5±0.845a	21.8±0.943a	25.1±0.823a

DAF = days after feeding. Means sharing similar letters within a column are not significantly different at p=0.05.

Factors within the plant characteristics that impact insect survival and fitness. Insects are highly dependent on their diet for development [25], and the utilization of various plant food sources introduces variation in insect vita variables [8], [26]. Our study demonstrated that *S. frugiperda* had higher relative growth rates, consumption rates, and conversion efficiency of ingested food in maize and two wheat varieties Fakhar-E-Bhakkar-17 and Akbar-19. These results suggest that the nutritional quality of a host plant can have a significant impact on the feeding and growth of insect herbivores. This preference could be attributed to the nutrition of these plants, which could be preferable for the insect [19].

Insects are known to improve their ability under optimal larval feeding conditions, as shown by studies such as those of Barros et al. [19] and Xu et al. [27]. Evaluating the adequacy of particular food sources for insect development may involve consideration of several indicators of suitability. Each plant species possesses a number of secondary metabolic and nutritional compounds, each with distinct defensive attributes, encompassing tolerance, antibiosis, antixenosis, and various combinations of these three mechanisms [28].

The results of this study will contribute to the understanding of the biology of *S. frugiperda*, which could help in its mana-

gement and control. Consequently, future research is needed on the examination of a wider range of host plant species conducive to the development of *S. frugiperda*. In addition, evaluation of the chemical constituents of these host plant species would improve understanding the mechanisms underlying host suitability.

The cropping system, particularly the practice of intercropping, is explored as an alternative approach to the management arthropod pests affecting crops, as discussed by Smith and McSorley [29]. However, in our country, farmers grow maize and wheat crops at the same time. Some crops are known to exert a deterrent influence on herbivores.

This is attributed to the potential alteration of the ability of pests to locate their host plants through visual and smell interference caused by cultivated vegetation [30]. Conversely, certain crops can create a favorable microenvironment for insects [31], [32]. Our study was conducted under controlled conditions and the results showed that *S. frugiperda* can successfully feed on two wheat varieties.

However, the potential of wheat crops with a maize cropping system warrants further investigation to test the incidence of *S. frugiperda* on wheat crops under field conditions. In addition, this study did not evaluate the nutritional composition of different wheat varieties. Therefore, future research could attempt

to quantify the precise nutritional content and assess quality variations among host plant conditions. This would facilitate a more complete understanding of the influence of nutrition on ecological and physiological traits.

## V. CONCLUSION

Our study revealed that the nutritional physiology of *S. frugiperda* was satisfactory on maize and some wheat varieties as well. The findings of the study have important implications for pest management strategies and crop breeding programs in wheat cultivation. Moreover, the presence of various crops within the agro-ecosystem, notably wheat and maize, can induce altered feeding preferences when the primary host is not available. The results of this research indicate that *S. frugiperda* could become a pest on other agricultural plants in the future, especially wheat. Future studies should prioritize the examination of a broader spectrum of host plants to assess nutritional indices relevant to *S. frugiperda*. Additionally, evaluating the chemical components of the tested cultivars would provide valuable insights into the mechanisms underlying host suitability.

## REFERENCES

- [1] R. N. Nagoshi, D. Koffi, K. Agboka, K. A. Tounou, R. Banerjee, J. L. Jurat-Fuentes, R. L. Meagher, "Comparative Molecular Analyses of Invasive Fall Armyworm in Togo Reveal Strong Similarities to Populations from the Eastern United States and the Greater Antilles," *Plos One*, vol. 12, 2017, <https://doi.org/10.1371/journal.pone.0181982>
- [2] A. N. Sparks, "Fall Armyworm Symposium: A Review of the Biology of the Fall Armyworm," *Annual Review of Entomology*, vol. 47, pp. 82-87, 1979, <https://doi.org/10.2307/3494083>
- [3] G. Goergen, P. L. Kumar, S. B. Sankung, A. Togola, M. Tamo, "First Report of Outbreaks of the Fall Armyworm *Spodoptera Frugiperda* (J.E. Smith) (Lepidoptera, Noctuidae), A New Alien Invasive Pest in West and Central Africa," *Plos One*, vol. 11, 2016, <https://doi.org/10.1371/journal.pone.0165632>
- [4] R. N. Nagoshi, G. Goergen, K. A. Tounou, K. Agboka, D. Koffi, R. L. Meagher, "Analysis of Strain Distribution, Migratory Potential, and Invasion History of Fall Armyworm Populations in Northern Sub-Saharan Africa," *Scientific Reports*, vol. 8, pp. 1-10, 2018.
- [5] D. Sharanabasappa, C. M. Kalleshwaraswamy, R. Asokan, H. M. Swamy, M. S. Martuthi, H.B. Pavithra, G. Goergen, "First Report of the Fall Armyworm, *Spodoptera Frugiperda* (J.E. Smith) (Lepidoptera: Noctuidae). An Alien Invasive Pest on Maize in India," *Pest Management in Horticultural Ecosystems*, vol. 24, pp. 23-29, 2018.
- [6] U. Naeem-Ullah, M.A. Ansari, N. Iqbal, S. Saeed, "First Authentic Report of *Spodoptera Frugiperda* (J.E. Smith) (Noctuidae: Lepidoptera) An Alien Invasive Species From Pakistan," *Applied Sciences and Business Economics*, vol. 6, pp. 13, 2019.
- [7] D. G. Montezano, A. Specht, D. R. Sosa-Gómez, V. F. Roque-Specht, J. C. Sousa-Silva, S. V. Paula-Moraes, J. A. Peterson, T. E. Hunt, "Host Plants of *Spodoptera Frugiperda* (Lepidoptera: Noctuidae) in the Americas," *African Entomology*, vol. 26, pp. 286-300, 2018, <https://doi.org/10.4001/003.026.0286>
- [8] J. F. Guo, M. D. Zhang, Z. P. Gao, D. J. Wang, K. L. He, Z. Y. Wang, "Comparison of Larval Performance and Oviposition Preference of *Spodoptera Frugiperda* Among Three Host Plants: Potential Risks to Potato and Tobacco Crops," *Insect Science*, vol. 28, pp. 602-610, 2021, <https://doi.org/10.1111/1744-7917.12830>
- [9] R. N. Nagoshi, "Can the Amount of Corn Acreage Predict Fall Armyworm (Lepidoptera: Noctuidae) Infestation Levels in Nearby Cotton?" *Journal of Economic Entomology*, vol. 102, pp. 210-218, 2009, <https://doi.org/10.1603/029.102.0130>
- [10] R. C. Bueno, F. Moscardi, J. R. Parra, C. B. Hoffmann-Campo, "Lepidopteran Larva Consumption of Soybean Foliage: Basis for Devel-

- ping Multiple-Species Economic Thresholds for Pest Management decisions," *Pest Management Science*, vol. 67, pp. 170-174, 2011, <https://doi.org/10.1002/ps.2047>
- [11] R. Day, P. Abrahams, M. Bateman, T. Beale, V. Clotney, M. Cock, Y. Colmenarez, N. Corniani, R. Early, J. Godwin, J. Gomez, P. G. Moreno, S. T. Murphy, B. Oppong-Mensah, N. Phiri, C. Pratt, S. Silvestri, A. Witt, "Fall Armyworm: Impacts and Implications for Africa," *Outlooks on Pest Management*, vol. 28, pp. 196-201, 2017, [https://doi.org/10.1564/v28\\_oct\\_02](https://doi.org/10.1564/v28_oct_02)
- [12] S. Shafqat, A. H. Sayyed, A. Ijaz, "Effect of Host Plants on Life-History Traits of *Spodoptera Exigua* (Lepidoptera: Noctuidae)," *Journal of Pest Science*, vol. 83, pp. 165-172, 2010.
- [13] C. S. Awmack, S. R. Leather, "Host Plant Quality and Fecundity in Herbivorous Insects," *Annual Review of Entomology*, vol. 47, pp. 817-844, 2002, <https://doi.org/10.1146/annurev.ento.47.091201.145300>
- [14] A. Idrees, Z. A. Qadir, K. S. Akutse, A. Afzal, M. Hussain, W. Islam, M. S. Waqas, B. S. Bamisile, J. Li, "Effectiveness of Entomopathogenic Fungi on Immature Stages and Feeding Performance of Fall Armyworm, *Spodoptera Frugiperda* (Lepidoptera: Noctuidae) Larvae," *Insects*, vol. 12, pp. 1-1044, 2021, <https://doi.org/10.3390/insects12111044>
- [15] S. Mahpara, M. S. Bashir, R. Ullah, M. Bilal, S. Kausar, M. I. Latif, A. Alfagham, "Field Screening of Diverse Wheat Germplasm for Determining their Adaptability to Semi-arid Climatic Conditions," *Plos one*, vol. 17, 2022, e0265344. <https://doi.org/10.1371/journal.pone.0265344>
- [16] D. M. D. Silva, A. D. F. Bueno, K. Andrade, C. D. S. Stecca, P. M. O. J. Neves, M. C. N. D. Oliveira, "Biology and Nutrition of *Spodoptera Frugiperda* (Lepidoptera: Noctuidae) Fed on Different Food Sources," *Scientia Agricola*, vol. 74, pp. 18-31, 2017, <https://doi.org/10.1590/1678-992X-2015-0160>
- [17] Z. Zhang, Y. Jiang, X. Li, A. Zhang, X. Zhu, Y. Zhang, "Effects of Different Wheat Tissues on the Population Parameters of the Fall Armyworm (*Spodoptera Frugiperda*)," *Agronomy*, vol. 11, pp. 2044, 2021, <https://doi.org/10.3390/agronomy11102044>
- [18] X. M. Yang, Y. F. Song, X. X. Sun, X. J. Shen, Q. L. Wu, H. W. Zhang, K. M. Wu, "Population Occurrence of the Fall Armyworm, *Spodoptera Frugiperda* (Lepidoptera: Noctuidae) in the Winter Season of China," *Journal of Integrative Agriculture*, vol. 20, pp. 772-782, 2021, [https://doi.org/10.1016/S2095-3119\(20\)63292-0](https://doi.org/10.1016/S2095-3119(20)63292-0)
- [19] E. M. Barros, J. B. Torres, J. R. Ruberson, M. D. Oliveira, "Development of *Spodoptera Frugiperda* on Different Hosts and Damage to Reproductive Structures in Cotton," *Entomologia Experimentalis et Applicata*, vol. 137, pp. 237-245, 2010, <https://doi.org/10.1111/j.1570-7458.2010.01058.x>
- [20] G. P. Waldbauer, "The Consumption and Utilization of Food by Insects," *Advances in Insect Physiology*, vol. 5, pp. 229-288, 1968, [https://doi.org/10.1016/S0065-2806\(08\)60230-1](https://doi.org/10.1016/S0065-2806(08)60230-1)
- [21] K. G. Gebretsadik, Y. Liu, Y. Yin, X. Zhao, X. Li, F. Chen, A. Chen, "Population Growth of Fall Armyworm, *Spodoptera Frugiperda* Fed on Cereal and Pulse Host Plants Cultivated in Yunnan Province, China," *Plants*, vol. 12, p. 950, 2023, <https://doi.org/10.3390/plants12040950>
- [22] J. H. Zhu, F. P. Zhang, H. G. Ren, "Development and Nutrition of *Prodenia Litura* on Four Food Plants," *Chinese Journal of Entomology*, vol. 42, pp. 643-646, 2005.
- [23] M. Xue, Y. Pang, H. Wang, Q. Li, T. Liu, "Effects of Four Host Plants on Biology and Food Utilization of the Cutworm, *Spodoptera Litura*," *Journal of Insect Science*, vol. 10, 2010, <https://doi.org/10.1673/031.010.2201>
- [24] M. Ahmad, M. I. Arif, M. Ahmad, "Occurrence of Insecticide Resistance in Field Populations of *Spodoptera Litura* (Lepidoptera: Noctuidae) in Pakistan," *Crop Protection*, vol. 26, pp. 809-817, 2007, <https://doi.org/10.1016/j.cropro.2006.07.006>
- [25] S. J. Tuan, Y. H. Lin, C. M. Yang, R. Atlihan, P. Saska, H. Chi, "Survival and Reproductive Strategies in Two-Spotted Spider Mites: Demographic Analysis of Arrhenotokous Parthenogenesis of *Tetranychus Urticae* (Acari: Tetranychidae)," *Journal of Economic Entomology*, vol. 109, pp. 502-509, 2016, <https://doi.org/10.1093/jee/tov386>
- [26] F. Hong, H. L. Han, P. Pu, D. Wei, J. Wang, Y. Liu, "Effects of Five Host Plant Species on the Life History and Population Growth Parameters of *Myzus Persicae* (Hemiptera: Aphididae)," *Journal of Insect Science*, vol. 19, pp. 15, 2019, <https://doi.org/10.1093/jisesa/iez094>
- [27] P. J. Xu, D. D. Zhang, J. Wang, K. M. Wu, X. W. Wang, X. F. Wang, G. W. Ren, "The Host Preference of *Spodoptera Frugiperda* on Mai-

- ze and Tobacco,” *Journal of Plant Protection Research*, vol. 45, pp. 61-64, 2019.
- [28] E. L. Baldin, M. D. Stamm, J. P. Bentivenha, K. G. Koch, T. M. Heng-Moss, T. E. Hunt, “Feeding Behavior of *Aphis Glycines* (Hemiptera: Aphididae) on Soybeans Exhibiting Antibiosis, Antixenosis, and Tolerance Resistance,” *Florida Entomologist*, vol. 101, pp. 223-228, 2018, <https://doi.org/10.1653/024.101.0211>
- [29] H. A. Smith, R. McSorley, “Intercropping and Pest Management: A Review of Major Concepts,” *American Entomologist*, vol. 46, pp. 154-161, 2000, <https://doi.org/10.1093/ae/46.3.154>
- [30] O. O. R. Pitan, C. O. Filani, “Effect of Intercropping Cucumber *Cucumis Sativus* (Cucurbitaceae) at Different Times with Maize *Zea Mays* (Poaceae) on the Density of Cucumber Insect Pests,” *International Journal of Tropical Insect Science*, vol. 34, pp. 269-276, 2014, <https://doi.org/10.1017/S1742758414000435>
- [31] J. Liu, Y. Yan, A. Ali, N. Wang, Z. Zhao, M. Yu, “Effects of Wheat Maize Intercropping on Population Dynamics of Wheat Aphids and Their Natural Enemies,” *Sustainability*, vol. 9, pp. 1390, 2017, <https://doi.org/10.3390/su9081390>
- [32] U. Amala, T. M. Shivalingaswamy, “Effect of Intercrops and Border Crops on the Diversity of Parasitoids and Predators in Agroecosystem,” *Egyptian Journal of Biological Pest Control*, vol. 28, 2018.





# Investigation of Wind Effects on UAV Adaptive PID Based MPC Control System

Andrés Santiago Martínez-León<sup>1</sup>, Sergey Jatsun<sup>2</sup>, Oksana Emelyanova<sup>3</sup>

**Abstract** — In this paper, an assessment of the state of coastal territories of Ecuador monitoring issue is conducted. The use of an autonomous robotic aerial platform is proposed as a technical solution to enhance the efficiency of remote surveillance missions performed by national security services along coastline. Considering the UAV nonlinear flight dynamics, as well as the missing information of the environment, is designed a UAV hierarchical control structure composed of an adaptive PID based MPC control strategy. The implementation of an adaptive PID based MPC controller leads to significantly improve the UAV optimal trajectory tracking task, as well as satisfy properties such as adaptiveness, self-learning, and capability of handling uncertainties caused by the unpredictable behavior of sea currents and wind loads retaining robust performance features. In this work, the investigation of external disturbances on UAV stabilization and positioning accuracy considers swirling wind flows and short-term wind gusts. These correspond to deterministic and random processes, are mathematically represented as trigonometric functions with random amplitudes determined by the gust coefficients and the wind loading periods of the pulses. The established range is given by a set of several observations of wind loads in the coastal territories of Ecuador. The analyzed data is collected from the database of national meteorological stations. Finally, the simulation process of the perturbed controlled motion of the UAV along a segmented linear trajectory, as well as the data analysis and graphics are carried out in the MATLAB environment.

**Keywords** — Unmanned Aerial Vehicle (UAV); Coastal Monitoring; Remote Surveillance Missions; Adaptive PID; Model Predictive Control (MPC); External Disturbances Analysis.

**Resumen** — En este trabajo se realiza una evaluación del estado de los territorios costeros del Ecuador en términos de monitoreo. El uso de una plataforma aérea robótica autónoma se propone como una solución técnica para mejorar la eficiencia de las misiones de vigilancia remota realizadas por los servicios de seguridad nacional a lo largo de la zona costanera. Considerando la no linealidad de la dinámica de un UAV, así como la inexistencia de información sobre el entorno, se ha diseñado una estructura

jerárquica de control compuesta por una estrategia adaptativa de PID basada en un controlador MPC. La implementación del controlador adaptativo PID basado en MPC conduce a mejorar significativamente la tarea de seguimiento de trayectoria óptima del UAV, así como a satisfacer propiedades tales como la adaptabilidad, el autoaprendizaje y la capacidad de manejar incertidumbres causadas por el comportamiento impredecible de las corrientes marinas y las cargas de viento, manteniendo características robustas de rendimiento. En este trabajo, la investigación de los efectos de las perturbaciones externas sobre la estabilización y precisión de posicionamiento del UAV considera flujos arremolinados y ráfagas de corta duración. Estos corresponden a procesos deterministas y aleatorios, son representados matemáticamente como funciones trigonométricas con amplitudes aleatorias determinadas por los coeficientes de perturbaciones y los períodos de carga de viento de las pulsaciones. El rango establecido se da mediante un conjunto de varias observaciones de cargas de viento en los territorios costeros de Ecuador. Los datos analizados son recogidos de la base de datos de las estaciones meteorológicas nacionales. Finalmente, el proceso de simulación del movimiento controlado perturbado del UAV a lo largo de una trayectoria lineal segmentada, así como el análisis de datos y gráficos, se llevan a cabo en el entorno de MATLAB.

**Palabras clave** — Vehículo Aéreo no Tripulado (UAV); Monitoreo Costero; Misiones de Monitoreo Remoto; PID Adaptativo; Control Predictivo (MPC); Análisis de Perturbaciones Externas.

## I. INTRODUCTION

IN recent decades, the dynamic evolution of information technologies and microelectronics has led to the improvement of modern aviation. This, contributed to rethinking the concepts of unmanned aerial vehicles (UAV's) use, spheres of their further development, improvement of payload and flight characteristics, hardware-software implementation of promising algorithms of control, among others, all this give to UAV's a multipurpose character in civil and military fields [1], [3]. Nowadays, fully autonomous small-sized multirotor UAV's represent a demanded field of research and provide cost-effective solutions for a wide range of applications. This is because their features and ability to carry out operational and high-precision work in hard-to-reach or dangerous areas when performing missions such as search and inspection of remote areas, aerial photography and mapping, agricultural crop monitoring, hazardous material recovery, disaster prevention and relief support or surveillance of sensitive areas (borders, ports, oil pipelines), just to name a few. [1], [2], [4].

Coastal territories constitute a strategic area of interest for any country in terms of trade and responsible natural resource exploitation, also in terms of economic, industrial, political

<sup>1</sup> Associate professor, Faculty of Earth Sciences, Universidad Estatal Amazónica, Puyo 160150, Ecuador, and Researcher, Department of Mechanics, Mechatronics and Robotics, Southwest State University, Kursk 305040, Russia. (e-mail: [amartinez@uea.edu.ec](mailto:amartinez@uea.edu.ec)). ORCID number <https://orcid.org/0000-0002-8598-7304>.

<sup>2</sup> Head of the Department of Mechanics, Mechatronics and Robotics, Southwest State University, Kursk 305040, Russia (email: [teormeh@inbox.ru](mailto:teormeh@inbox.ru)). ORCID number <https://orcid.org/0000-0002-7420-0772>.

<sup>3</sup> Associate professor, Department of Mechanics, Mechatronics and Robotics, Southwest State University, Kursk 305040, Russia (email: [oks-emelyanova@yandex.ru](mailto:oks-emelyanova@yandex.ru)). ORCID number <https://orcid.org/0000-0002-6067-3114>.

Manuscript Received: 22/02/2024

Revised: 08/03/2024

Accepted: 13/03/2024

DOI: <https://doi.org/10.29019/enfoqueute.1032>

and defense activities in general [4], [5]. However, the presence of coastal territories represents a high responsibility for governmental authorities and implies an accurate control over before mentioned activities by national security services. The coastal territory of Ecuador is no exception, the coastline of the country is characterized by a complex terrain, the presence of hard-to-reach and relatively extended uninhabited territories. This situation is used by some organizations to carry out various types of activities not responding to compliance with law, namely: illegal extraction and trade of natural resources (minerals, petroleum products, wood, poaching, among others.), causing large economic losses [2], [4], [6]. In this regard, maritime security services are constantly in need of expanding and modernizing the technologies used to improve the efficiency of the work carried out to ensure control and safety in these areas. Thus, it becomes necessary to perform remote activities to lead successful interventions along the coastline aimed to identification and detention of members of several illegal organizations, preserving the integrity of the staff of security services [2], [5], [7].

In this paper, the use of a robotic aerial platform is considered to complete remote surveillance missions focused on small sea vessels, as one of the most recurrent means for transporting illegally obtained production. Besides, small sea vessels are difficult to track by standard radar and satellite systems [7]. The proposed aerial platform includes an autonomous small-sized UAV type quadcopter with attachments and a hardware-software system [2], [4], [8], [10].

The peculiarity of monitoring coastal territories belongs to the unpredictability of the air and water environment behavior, as well as the periodic absence of visual contact between the operator and the aerial vehicle when performing remote autonomous missions. Therefore, the robotic aerial platform at least must satisfy conditions such as the use of a lightweight, robust and moisture-resistant UAV frame, based on structural topology optimization principles for better aerodynamics, vibration and payload features [2], [4], [10]. The availability of an energy-efficient system for extended flights, long-range telemetry and video-transmitter modules for real-time flight status management and reception of visual information about ground target identification process respectively. As well as onboard implementation of advanced algorithms of control for an adaptive controlled flight in presence of external uncertainties [4], [7], [8], [9], [13], [19].

The influence of wind loads on the aerial platform can be considered an energy-transfer process, where air and water environment generate additional disturbing forces and momentums of an uncertain nature, which negatively impact on the desired behavior and performance of the aerial platform even at low absolute speeds [2], [9]. Besides, is important taking into account the nonlinearities of the aerial platform, minimal or completely missing information about the environment, external disturbing loads such as swirling wind flows or short-term wind gusts, considered as deterministic or random processes

recurring after a certain time or in a certain area, among others. It becomes necessary to work on the implementation of control strategy, which could satisfy properties, including adaptiveness, self-learning, and capability of handling uncertainties during the flight missions performed by the aerial robotic platform [13], [14], [15], [18].

In this regard, the scope of this research work concerns to the investigation and assessment of model-based wind load effects on stabilization and positioning accuracy of the proposed robotic aerial platform operating by an adaptive PID based MPC control system during aerial surveillance missions along the coastline of Ecuador [2]. Thus, the above presented UAV control strategy focuses on a hierarchical control architecture, where the adaptation of PID controller parameters (lower level) and matches the MPC performance (higher level). In this way, the proposed control architecture combines the strengths of PID and MPC methods, minimizing their limitations [2], [19], [23]. Although the implementation of a PID controller provides a simple and accurate control of the UAV electromechanical drives, the efficiency of a PID controller is greatly reduced in presence of uncertainties. Therefore, the use of an MPC control strategy at higher control level by optimizing the PID controller parameters over a certain horizon of prediction and exploiting the knowledge of the UAV dynamic model. It becomes possible to significantly improve the UAV optimal trajectory tracking task, as well as satisfy input and state constraints retaining robust performance, while completing aerial surveillance missions [19], [24].

The aim of this work is related to the implementation of an UAV model-based virtual simulator for investigating the incidence of external uncertainties on the aerial platform flight dynamics for generating the main criteria of a real behavior of the UAV during surveillance missions in coastal region before its implementation. This paper is based on the approaches from previous works [2], [4], namely UAV mathematical model, control and trajectory strategies.

## II. METHODOLOGY

### A. UAV Generalized Mathematical Model

Small-sized multirotor UAV's incorporate various design configurations. In this paper, it is proposed to use an UAV executed on a quadcopter pattern (cross-shaped scheme). Let's consider the dynamics of the quadcopter flight in accordance with the given calculation scheme (figure 1). Let the quadcopter motion occur in a global cartesian coordinate system  $OX_0Y_0Z_0$ , then  $CX_1Y_1Z_1$ ,  $A_ix_iz_i$  ( $i=1-4$ ) – local coordinate systems passing through the center of mass of the UAV  $C$  body and the center of mass of the  $i$ -th rotor  $A_i$ , respectively. The orientation in space is set by the Euler angles of roll  $j$ , pitch  $q$  and yaw  $y$ .

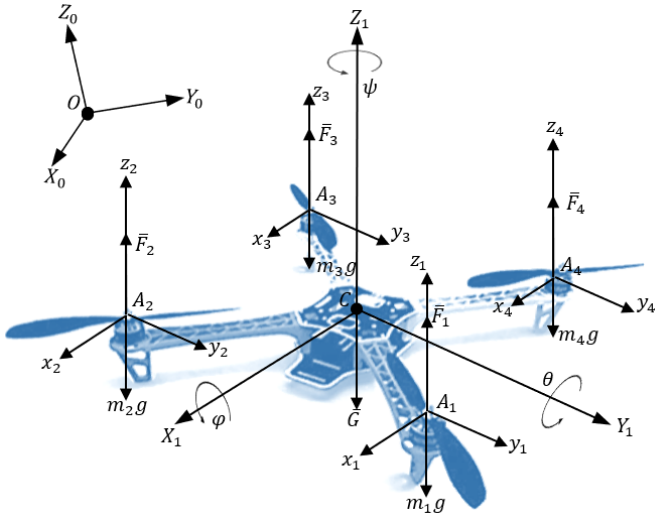


Fig. 1. Calculation scheme of a quadcopter (excluding drag forces).

In general, the motion of a UAV as a solid body involves the motion of the center of mass and rotational motion relative to its center of mass. Consequently, the vector of motion modes (input) of the quadcopter  $\bar{U}$ , which determines the connection between the electric drives and the quadcopter platform, can be written in the following way [11], [12], [17]:

#### Equation 1

$$\bar{U} = \begin{bmatrix} U_1 \\ U_2 \\ U_3 \\ U_4 \end{bmatrix} = \begin{bmatrix} F_1 + F_2 + F_3 + F_4 \\ (F_1 - F_2 - F_3 + F_4) \cdot L \\ (-F_1 - F_2 + F_3 + F_4) \cdot L \\ (M_1 - M_2 + M_3 - M_4) \end{bmatrix} \quad (1)$$

Where:

$F_i$  - lifting force of the  $i$ -th rotor

$M_i$  - momentum created by the electric drives of the system

$L$  - beams length from the quadcopter center of mass to the  $i$ -th rotor platform center of mass

$U_1$  - UAV motion control mode along the vertical axis  $OZ$

$U_2$  - roll angle  $\phi$  control mode along the  $OY$  axis

$U_3$  - pitch angle  $\theta$  control mode along the  $OX$  axis

$U_4$  - yaw angle  $\psi$  control mode providing UAV rotation around the  $OZ$  axis.

Besides, the UAV state vector declaration facilitates the calculation of the next states of the aerial platform based on the decoupled dynamic system by using characteristic time step responses for the four controlled states of the UAV according to the output of a designed control system. Thus, the UAV multi-dimensional state vector  $\bar{\xi}(t) = [\bar{\alpha}, \bar{\gamma}]^T$  includes the vectors of position and orientation of the center of mass  $\bar{\alpha} = [x, y, z]^T$  and  $\bar{\gamma} = [\varphi, \theta, \psi]^T$  respectively. From works [14], [16] the system of differential equations describing the full dynamic model of a UAV type quadcopter (cross-shaped scheme) can be represented as follows:

#### Equation 2

$$\ddot{\bar{\xi}} = \begin{cases} \dot{V}_{x_1} = \frac{U_1(\cos\varphi \cdot \sin\theta \cdot \cos\psi + \sin\varphi \cdot \sin\psi)}{m} - \Phi_x \\ \dot{V}_{y_1} = \frac{U_1(\cos\varphi \cdot \sin\theta \cdot \sin\psi - \sin\varphi \cdot \cos\psi)}{m} - \Phi_y \\ \dot{V}_{z_1} = \frac{U_1(\cos\varphi \cdot \cos\theta)}{m} - g - \Phi_z \\ \dot{\omega}_{x_1} = \frac{U_2}{I_{xx}} + \omega_{y_1}\omega_{z_1} \left( \frac{J_{yy} - J_{zz}}{J_{xx}} \right) - \frac{J_R}{J_{xx}} \omega_{y_1} \Omega_R \\ \dot{\omega}_{y_1} = \frac{U_3}{I_{yy}} + \omega_{x_1}\omega_{z_1} \left( \frac{I_{zz} - I_{xx}}{I_{yy}} \right) - \frac{J_R}{I_{yy}} \omega_{x_1} \Omega_R \\ \dot{\omega}_{z_1} = \frac{U_4}{I_{zz}} + \omega_{x_1}\omega_{y_1} \left( \frac{I_{xx} - I_{yy}}{I_{zz}} \right) \end{cases} \quad (2)$$

Where:

$\dot{V}_{x_1}, \dot{V}_{y_1}, \dot{V}_{z_1}$  and  $\dot{\omega}_{x_1}, \dot{\omega}_{y_1}, \dot{\omega}_{z_1}$  - projections of linear and angular accelerations of the quadcopter center of mass on the axes  $OX_1, OY_1, OZ_1$  respectively,  $\varphi, \theta, \psi$  - Euler angles,  $J_{xx}, J_{yy}, J_{zz}$  - axial momentums of inertia,  $J_R$  - momentum of inertia generated by the electric drives,  $\Omega_R$  - angular velocity of the electric drives,  $\Phi_x, \Phi_y, \Phi_z$  - projections of the wind load disturbing force,  $m = m_c + \sum m_i$  - total weight of the UAV.

The presented UAV generalized mathematical model is based on decomposition methods simplifying the complexity of the UAV and contributing to the design of algorithms and synthesis of the control system. Considering equations 1 and 2, is proposed to transform the UAV mathematical model as noted below:

#### Equation 3

$$\ddot{\bar{\xi}} = \bar{A}(\dot{\bar{\xi}}) + \bar{B}(\bar{\xi}) \quad (3)$$

Where:

$\dot{\bar{\xi}}$  - vector of linear and angular velocities of the center of mass of the UAV,  $\bar{A}(\dot{\bar{\xi}}) = [J^{-1} \frac{d\bar{G}}{dt}]$  - matrix containing the gravitational vector  $\bar{G} = [0 \ 0 \ -g]^T$  and vector of projections of the kinetic momentum on the associated coordinate system,

$\bar{B}(\bar{\xi}) = [\bar{U}_1/m - \bar{\Phi}]$  - matrix including projection vector of resulting lifting force  $\bar{U}_1$ , as well as vectors of the external axial momentums  $\bar{M}_i = [\bar{U}_2 \ \bar{U}_3 \ \bar{U}_4]^T$  and wind load disturbing force  $\bar{\Phi} = [\Phi_x \ \Phi_y \ \Phi_z]^T$ .

In general, the vector of wind load force  $\bar{\Phi}$  describing the effect of external disturbances on the dynamics and stability of the UAV during a flight mission can be represented as follows [14]:

#### Equation 4

$$\bar{\Phi} = \bar{\nu} \mu \bar{\nu}^T = [\Phi_x \ \Phi_y \ \Phi_z]^T \quad (4)$$

Where:

$\mu = \text{diag}(\mu_x, \mu_y, \mu_z)$  - matrix of empirical drag coefficients depending on the aerodynamic characteristics of the fuselage and the angle of attack of the rotors,  $\bar{\nu}$  - vector of the relative velocity of the center of mass of the UAV.

Then, the vector of relative velocity of the UAV center of mass  $\bar{v}$  can be described as the difference between the vectors of absolute velocity  $\bar{V}_C$  and wind load velocity  $\bar{V}_B$  [2], [14]:

### Equation 5

$$\bar{v} = \bar{V}_C - \bar{V}_B \quad (5)$$

However, the rate of change of wind load is a random variable, which can be represented as a trigonometric function with random amplitudes determined by the coefficients of gustiness and the periods of pulsations of the wind load.

### B. Wind Load Disturbance Model

During a surveillance mission along coastal territories, the UAVs is quite sensitive to short-term movements of air masses and sea water currents. Moreover, wind load disturbances represent a source of additional forces and momentums acting on the UAV with a complex and unpredictable distribution in space negatively affecting to the static and dynamic stability of the system. In general, wind load disturbances can be directed counter, orthogonally or along the same direction of the UAV movement. In this work, a particular case of orthogonal (lateral) wind disturbance has been considered (figure 2).

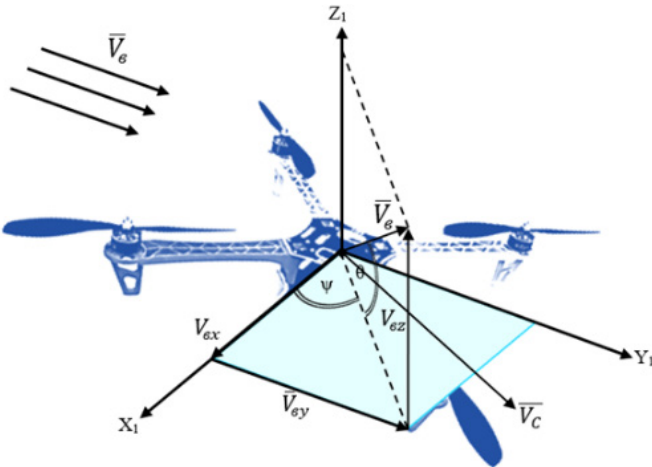


Fig. 2. Scheme of orthogonal wind load disturbance acting on the UAV.

The orthogonal wind disturbance vector  $\bar{V}_g = [V_{gx}^x, V_{gx}^y, V_{gx}^z]^T$  is composed of its projections located in the local coordinate system  $CX_1Y_1Z_1$ . These wind load projections along the axes mostly contribute to significant roll disturbances affecting to the accuracy of the UAV trajectory tracking task, including thrust variation and a higher energy consumption by UAV modules [10], [14], [19].

In addition, wind disturbances can be considered deterministic or random processes that repeat after a certain period (periodic or non-periodic) or occur at a specific time interval (pulse signal). In this work, both mentioned random models are considered.

The modeling process of a random wind load can be described through the next equation [14], [25]:

### Equation 6

$$\bar{V}_B(t) = V_0 + V_B \sin \Omega t \quad (6)$$

Where:

$V_0$  - wind constant disturbance,  $V_B, W$  - arbitrary parameters of orthogonal wind load amplitude and frequency, both resulting from the spectral analysis.

Besides, arbitrary variation of amplitude and frequency parameters is performed by creating time intervals of varying length and generating a continuous random function with a normal (Gaussian) distribution respectively [25].

### Equation 7

$$f(V_B) = \frac{1}{\sigma\sqrt{2\pi}} e^{-\frac{V_B - \langle V_B \rangle}{2\sigma}} \quad (7)$$

Where:

$\langle V_B \rangle$  - average value of the wind speed (mathematical expectation),  $\sigma$  - mean square deviation of the wind (variance).

In contrast, wind loads of a deterministic nature (wind shear) often occurs in a relative short time and represent a strong atmospheric disturbance. In this study, the wind shear model is presented by short equation 8 and jump-like equation 9 pulse signals, including a periodic pulse signal in equation 10 modeled by the Fourier series decomposition method [14], [25].

### Equation 8

$$\bar{V}_B(t) = k_1(t)V_0 \quad (8)$$

Where:

$k_1(t) = \begin{cases} 0, & t_i < t_0^p \\ 1, & t_f^p \geq t_i \geq t_0^p \end{cases}$  - defined function in a certain interval (from the initial time value corresponding to the appearance of the pulse signal  $t_0^p$  to its final value  $t_f^p$  at maximum amplitude value of the signal;  $V_0$  - maximum permissible value of the wind load.

### Equation 9

$$\bar{V}_B(t) = k_2(t)V_0 \quad (9)$$

Where:

$k_2(t) = \begin{cases} 0, & t_i < t_0^p \\ 1, & t_i \geq t_0^p \end{cases}$  - time-dependent switch function;  $V_0$  - maximum permissible value of the wind load.

### Equation 10

$$\bar{V}_B(t) = \frac{V_0}{2} + \sum_{n=0}^N V_n \sin(n\omega_0 t) \quad (10)$$

Where:

$V_0$  - constant of the disturbing effect,  $V_n$  - amplitude of the  $n$ -th oscillation;  $n\omega_0$  - cyclic frequency of the harmonic oscillation.

### C. UAV Control System Design

In general, equation 3 presents a compact representation of the UAV generalized mathematical model including kinematic, dynamic and electromechanical components of the system. In order to simplify the design process of the controller of the UAV, the above noted equation is transformed to [2]:

#### Equation 11

$$\begin{cases} \dot{\vec{v}} = f(\vec{Y}, \vec{v}, \vec{U}), \\ \vec{Y} = \chi(\vec{\xi}) \end{cases} \quad (11)$$

Where:

$\vec{\xi} = [x, y, z, \varphi, \theta, \psi]^T$  - multi-dimensional state vector;  $\dot{\vec{v}} = d\vec{\xi}/dt$  - vector of accelerations of the UAV center of mass;  $\vec{U}$  - control vector of the UAV motion modes,  $\vec{Y}$  - vector of the controlled output signals,  $\chi$  - data filtering matrix.

On the other hand, the UAV control system structurally can be presented as a set of the following modules: Operator, Human-Machine Interface (HMI) and UAV (figure 3). In turn, HMI includes the blocks of trajectory planning, data processing and decision-making.

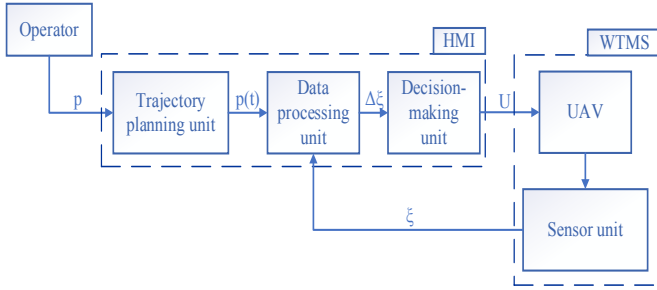


Fig. 3. General diagram of the structure of the UAV control system.

Based on figure 3, the Operator sets an array of GPS coordinates of a specific territory  $p = [p_1, p_2, \dots, p_i]$ . The resulting array data constitutes the input for the trajectory planning unit, where the controlled trajectory law is formed by the vector  $\vec{p}(t) = [x^d, y^d, z^d, \psi^d]^T$ . On the other hand, the UAV sensor unit provides accurate feedback of the current state of the system turning possible to estimate the error vector  $\Delta\vec{\xi}(t) = [\Delta x, \Delta y, \Delta z, \Delta\varphi, \Delta\theta, \Delta\psi]^T$ . In this way, the output vector of the UAV controlled states  $\vec{U}(t) = [U_1, U_2, U_3, U_4]^T$  is generated considering the system current information and algorithms embedded in the decision-making unit. As presented in introduction section, the design of the UAV controller focuses on a hierarchical architecture, where the adaptation of the PID controller parameters in presence of probabilistic uncertainties is performed by the prediction of the plant response at every sample  $k$  to enhance the desired behavior over a prediction horizon  $N$  using a robust MPC controller [2], [14], [23], [24]. Moreover, the adaptation of controller parameters aims to overcome the PID algorithm limitations implementing an online tuning method given by MPC algorithm, which leads to lower complexity and computations. In figure 4, the internal structure of the

decision-making block is presented. According to this diagram, two control loops based on the use of the PID controller are distinguished: an external loop for controlling the  $x, y$  coordinates; an internal loop providing control of height  $z$  and UAV angles  $\varphi, \theta, \psi$ .

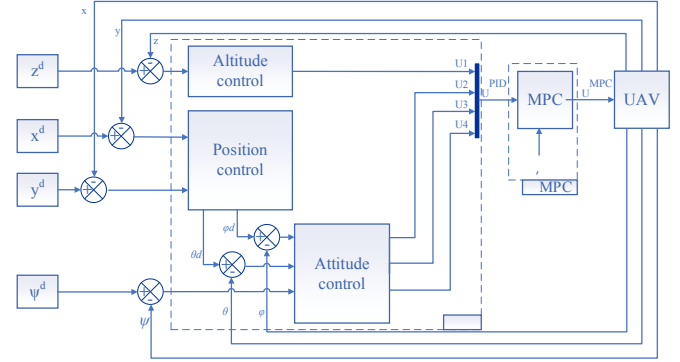


Fig. 4. Internal structure diagram of the UAV making-decision unit.

The implementation of the method for synthesizing the parameters of the UAV control system is performed according to the presented diagram in figure 4. The formation of the output vector of the UAV controlled states  $\vec{U}(t) = [U_1, U_2, U_3, U_4]^T$  is carried out based on available information about the system and embedded algorithms in the decision-making unit. This vector establishes the relation between the electric drives and the UAV current states. On the other hand, the estimation of the vector of required voltages  $\vec{u}(t) = [u_1, u_2, u_3, u_4]^T$  is generated in accordance with the output vector  $\vec{U}$ . In this way, the vector of required voltages  $\vec{u}$  depends on the deviation vector of controlled states  $\Delta\vec{\xi}$ . In this regard, the UAV angular velocity generated by the electric drives is represented as follows [17]:

#### Equation 12

$$\omega_i = f(\vec{U}(\Delta\vec{\xi})), \quad i = 1 - 4 \quad (12)$$

Where:  $\omega_i$  - angular velocity of the  $n$ -th electric drive.

In general, the generation of controlled states of the output vector  $\vec{U}$  can be described in a matrix form:

#### Equation 13

$$\vec{U}(\Delta\vec{\xi}) = \bar{k} \cdot \vec{\sigma} = \begin{bmatrix} k_p^{U1} & k_d^{U1} & k_i^{U1} \\ k_p^{U2} & k_d^{U2} & k_i^{U2} \\ k_p^{U3} & k_d^{U3} & k_i^{U3} \\ k_p^{U4} & k_d^{U4} & k_i^{U4} \end{bmatrix} \cdot \begin{bmatrix} \Delta\vec{\xi}(t) \\ \int_0^t \Delta\vec{\xi} dt \\ \Delta\dot{\vec{\xi}}(t) \end{bmatrix} \quad (13)$$

Where:

$\bar{k}$  - matrix of proportional  $K_p$ , integral  $K_i$  and differential coefficients of each controlled state of the output vector  $\vec{U}$ ;  $\vec{\sigma}$  - matrix containing the estimation of the deviation of the state vector  $\Delta\vec{\xi}(t)$ , its integral  $\int_0^t \Delta\vec{\xi} dt$  and differential  $\Delta\dot{\vec{\xi}}(t)$  components respectively.

In figure 6, the internal structure of the MPC control unit is presented. The prediction of the elements of the output vector  $\bar{U}^{MPC}$  is obtained by solving an optimization task within a certain prediction horizon  $N$  (time interval).

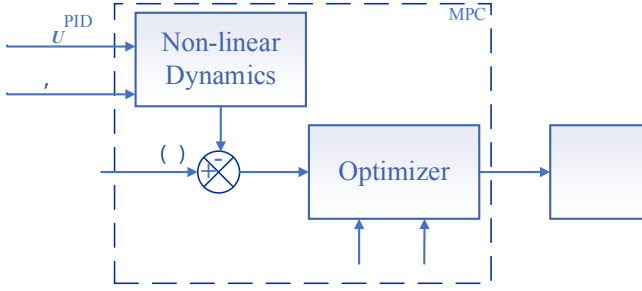


Fig. 5. Internal structure diagram of the UAV making-decision unit.

The nonlinear system describing the dynamics of the UAV is solved by the Euler integration method and can be represented as:

#### Equation 14

$$\ddot{\bar{\xi}} = f[\bar{\xi}, \bar{U}] \quad (14)$$

Where:

$\bar{\xi} = [x, y, z, \varphi, \theta, \psi]^T$  - multi-dimensional state vector,  
 $\bar{U} = [U_1^{PID}, U_2^{PID}, U_3^{PID}, U_4^{PID}]$  - vector of the control signals requiring optimization.

The mathematical significance of the MPC control algorithm synthesis belongs to form a vector of predictive output signals of the UAV for a certain number of iterations ahead within a given prediction horizon based on the ideal dynamic model of the UAV [19], [23].

#### Equation 15

$$\bar{y} = f(\bar{\xi}) \quad (15)$$

Where:  $\bar{y} = [x, y, z, \psi]^T$  - vector of predicted output signals of the control object.

Thus, the deviation vector  $\bar{e}$  between the predicted  $\bar{y}_d$  and specified by the operator  $\bar{y}$  trajectories can be determined as noted below:

#### Equation 16

$$\bar{e} = \bar{y}_d - \bar{y} \quad (16)$$

Besides, the quality functional  $J$  can be considered as a quadratic sum function of accumulated deviations of the predicted output vector  $\bar{y}$ .

#### Equation 17

$$J = \sum_{i=1}^N \|\bar{e}_{k+1}\|^2 \quad (17)$$

Further, the optimization task is carried out by calculating the quality functional  $J$  according to the quadratic programming algorithm (figure 6), based on predictive models considering system constraints  $\tau(\bar{k}) \in R^n$  for the estimation of the optimized output vector  $\bar{U}^{MPC} = [U_1^{MPC}, U_2^{MPC}, U_3^{MPC}, U_4^{MPC}]$ .

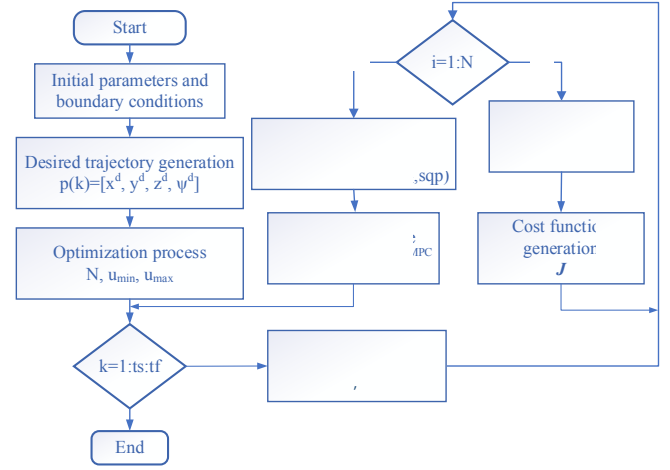


Fig. 6. Internal structure diagram of the UAV making-decision unit.

#### D. UAV Surveillance Trajectory Design

In figure 7 is described a particular case of the surveillance trajectory. The spatial motion of the UAV can be considered as a set of straight-line segments forming a piecewise linear trajectory. The controlled trajectory motion is represented by the displacement of the point P (center of mass of the UAV) along a straight-line segment  $P_{i-1}P_i$ . Besides, it is necessary to consider the possibility to perform an open (along the coastline with a subsequent landing process at an intermediate control point) and a closed (local surveillance of a specific territory with a return to the take-off point) trajectory pattern.

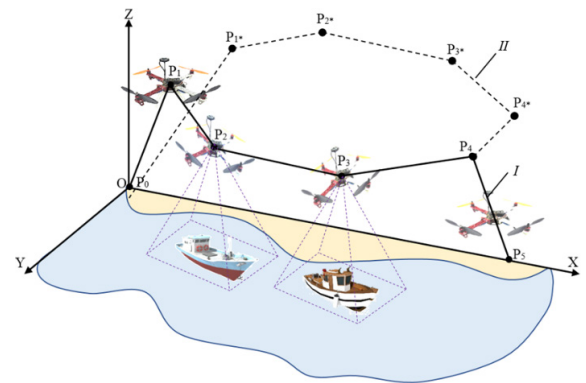


Fig. 7. UAV surveillance trajectory: I, II – open and closed trajectory pattern.

The generation of the  $i$ -th segment of the trajectory is a two-point problem, which depends on the available information about neighboring waypoints  $P_i$  acting as boundary conditions: coordinates, velocity and acceleration values at the initial and final time points on each segment. Thus, the spatial motion law

can be represented by three parametrized time-dependent polynomials of 5-th order [9], [11], [22]:

### Equation 18

$$\vec{p}(t) = \left( \sum_{i=0}^5 cx_i \cdot t^i, \sum_{i=0}^5 cy_i \cdot t^i, \sum_{i=0}^5 cz_i \cdot t^i \right)^T \quad (18)$$

Where:

$cx_i, cy_i, cz_i$  - coefficients calculated from boundary conditions.

In this work, an open trajectory pattern is considered for further calculations and presentation of results. According to [figure 7](#), the open trajectory pattern consists of three main stages: take off, cruise flight and landing. The first stage (takeoff) occurs from the point  $P_0$  to  $P_1$ . The second stage (cruise flight) involves the UAV motion from the point  $P_1$  to  $P_4$ , passing through the intermediate points  $P_2$  and  $P_3$  respectively. The last stage (landing) is carried out from point  $P_4$  to  $P_5$ .

It is known that the start of UAV flight from the ground occurs when the normal reaction generated on the UAV by the support surface  $\vec{N} = 0$ , while the following condition is satisfied:  $U_1 > F_{mg}$ ,  $\varphi = \theta \approx 0$ . In addition, during the flight is necessary to orient the UAV relative to the given trajectory by the heading angle  $c$  (angle between the diametral plane of the aerial vehicle and the direction to the trajectory) turning around the UAV center of mass at the yaw angle  $y$ , and then adjusting the UAV position into an angle  $\beta$ , which is defined as the tangent of the inclination angle between the straight-line  $\vec{p}$  and the  $OY$  axis ([figure 8a](#)). Therefore, the heading angle  $c$  turns equals to the yaw angle  $y$ . This correlation could be determined by the equation:

### Equation 19

$$\chi = \text{atan2} \frac{Y_1}{X_1} \quad (19)$$

Where:

$X_p, Y_p$  - direction of the local coordinate system.

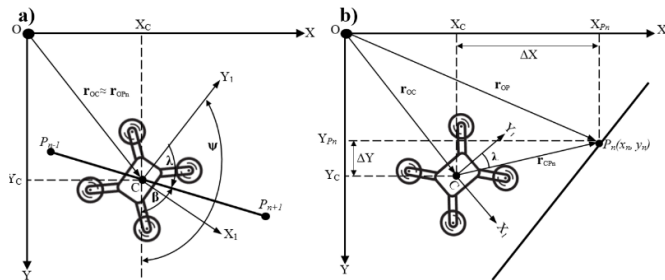


**Fig. 8.** UAV angle orientation scheme: a) heading angle correction  $\lambda$ , b) motion correction along the horizontal plane.

As mentioned before, the presence of external disturbances significantly affects the dynamics of the UAV flight, which leads to motion deviations from the desired trajectory ([figure 8b](#)). In this regard, it is proposed to carry out the return of the aerial vehicle to the desired trajectory by turning the UAV at

heading angle  $c$ , and then calculate the path deviation vector according to the equation [11], [16]:

### Equation 20

$$\Delta = [\Delta_x \quad \Delta_y \quad \Delta_z]^T = T_{10} (\vec{r}_i^{CP_n}) \quad (20)$$

Where:

$\vec{r}_i^{CP_n} = r_{OC} - \vec{r}_i^{OP_n}$  - vector representing the UAV path to the  $i$ -th point of given trajectory,  $T_{10} = \begin{bmatrix} \cos \chi & \sin \chi & 0 \\ -\sin \chi & \cos \chi & 0 \\ 0 & 0 & 1 \end{bmatrix}$  - transformation matrix from local to global coordinate system.

## III. RESULTS AND DISCUSSION

In this section are presented the main results of the simulation process carried out in MATLAB for the UAV autonomously controlled motion in presence of external disturbances along an open trajectory pattern in terms of stabilization and positioning accuracy properties. The parameters of the trajectory pattern considered in [Table I](#) correspond to the coordinates of the waypoints  $P_i$  ( $i = 1-5$ ), time intervals and boundary conditions.

TABLE I  
UAV TRAJECTORY DESIGN PARAMETERS

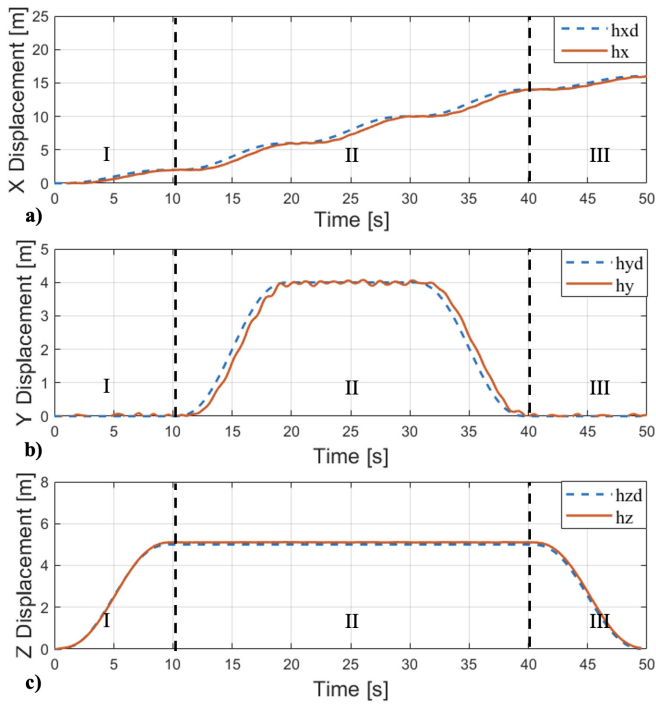
Stage	Time Interval [s]	Trajectory Points [m]	Intermediate Points [m]	Velocity [m/s]	Acceleration [m/s <sup>2</sup> ]
Take off (I)	$t_0 = 0$	$P_0(0,0,0)$	-	$P_0 = 0$	$P_0 = 0$
	$t_1 = 10$	$P_1(2,0,5)$	-	$P_1 = 0$	$P_1 = 0$
Cruise (II)	$t_1 = 0$	$P_1(2,0,5)$	$P_2(6,4,5)$	$P_1 = 0$	$P_1 = 0$
	$t_4 = 40$	$P_4(14,0,5)$	$P_3(10,4,5)$	$P_4 = 0$	$P_4 = 0$
Landing (III)	$t_4 = 40$	$P_4(14,0,5)$	-	$P_4 = 0$	$P_4 = 0$
	$t_5 = 50$	$P_5(16,0,0)$	-	$P_5 = 0$	$P_5 = 0$

Based on the information about boundary conditions and equation 18, a vector of coefficients  $\vec{c}_i$  is generated in concordance with the desired values for position  $\vec{P}_i^d$ , velocity  $\vec{p}_i^d$  and acceleration  $\vec{p}_i^d$  on each segment of the trajectory. In addition, the deviation vectors and control signals are determined at each iteration during the modeling process by integrating the differential equations of the UAV model, represented by the equation 11 using the Euler numerical integration method with a fixed step of 0.001s. Besides, during the simulation process parameters, such as dimensional, mass-inertial and electromechanical main characteristics of the UAV are considered ([Table II](#)).

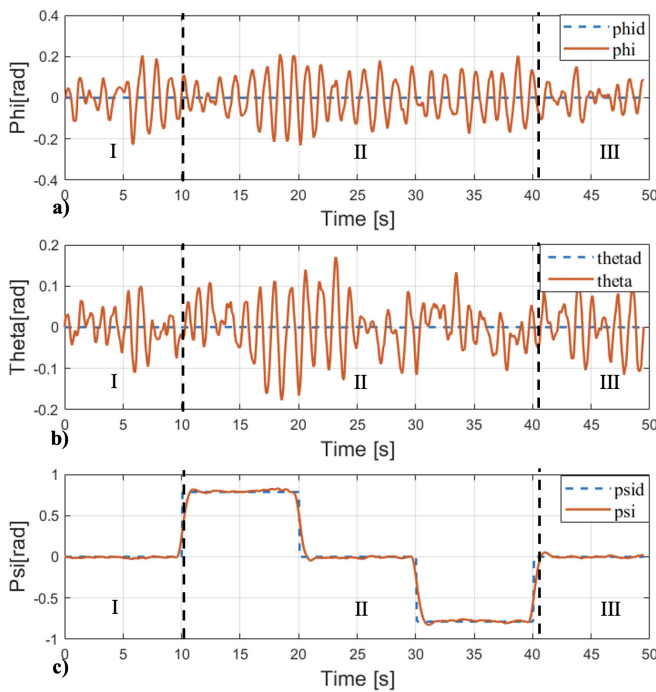
TABLE II  
UAV PARAMETERS

Parameter	Value	Unit
Mass	1.5	kg
Arm length	0.225	m
Lift coefficient	$8.048 \times 10^{-6}$	Nms <sup>2</sup>
Resistance coefficient	$2.423 \times 10^{-7}$	Nms <sup>2</sup>
Inertia matrix	$\begin{bmatrix} 0,0035 & 0 & 0 \\ 0 & 0,0035 & 0 \\ 0 & 0 & 0,005 \end{bmatrix}$	kg.m <sup>2</sup>

At the first stage, the adequacy of the selected synthesis method of the controller operating by an adaptive PID based MPC control system during aerial surveillance missions must be performed. The main results are shown in figures 9 to 12.

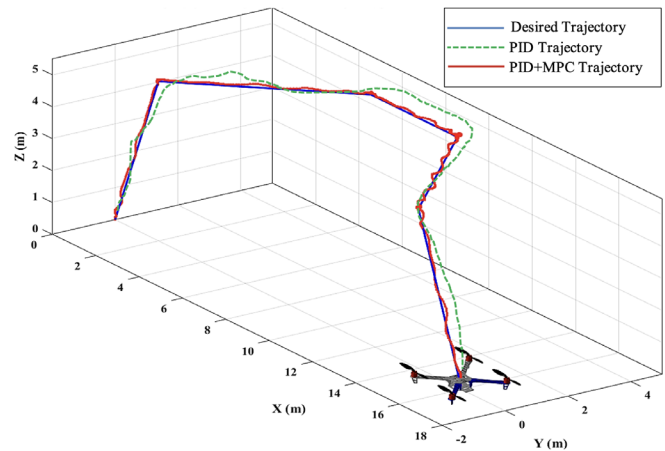


**Fig. 9.** Diagrams of the UAV center of mass deviation from the desired coordinates: a, b, c – UAV displacement along OX, OY, OZ axes; d, e, f – variation of the aircraft angles  $j, q, y$ ; I, II, III – take off, cruise flight and landing stages respectively.



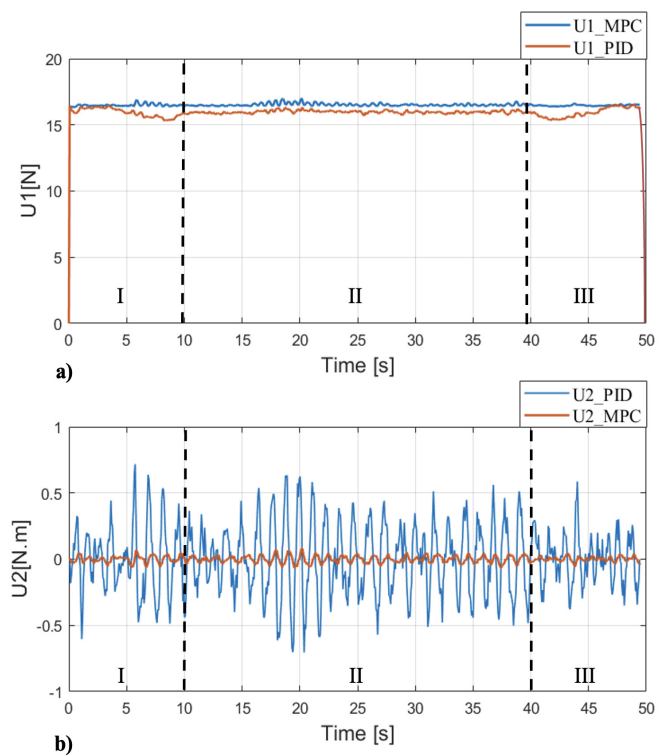
**Fig. 10.** Diagrams of the UAV center of mass deviation from the desired angular orientation: a, b, c – UAV deviation relative to OX, OY, OZ axes by aircraft angles  $j, q, y$ ; I, II, III – take off, cruise flight and landing stages respectively.

In figure 11 is presented a comparative analysis between PID and Adaptive PID based MPC control system capabilities in terms of stabilization and positioning accuracy properties during open loop trajectory pattern.



**Fig. 11.** 3D open trajectory pattern tracking

From results obtained in figures 9 to 11 becomes possible to state that the average deviation of the coordinates of the UAV center of mass along OX, OY, OZ axes is in range 0.025; 0.01 and 0.043 m, respectively. In addition, the average deviation from the UAV desired angular orientation corresponds to 0.08 rad. (relative to OX, OY axes) and 0.06 rad (relative to OZ axis). Therefore, the proposed control strategy ensures high accuracy in terms of positioning the UAV center of mass relative to a given trajectory by optimizing the vector of control signals  $\bar{U}$  (figure 12).



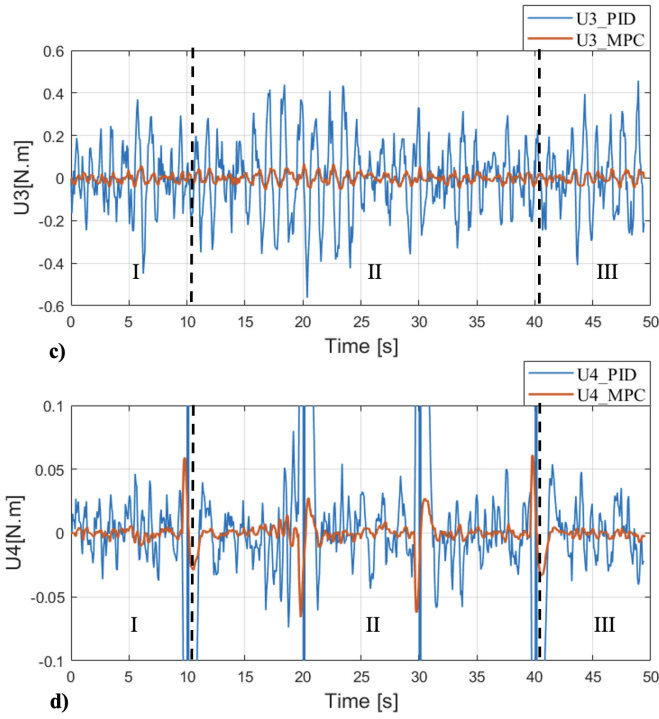


**Fig. 12.** Diagrams of the UAV controlled states: a – lift force  $U_1$ ; b, c, d – external moments  $U_2, U_3, U_4$  along OX, OY, OZ axes respectively.

From figure 12 follows that the average value of the lifting force  $U_1$  is 18.43 N when changing the angular velocity of the  $i$ -th rotor in a range from 5042 to 5077 rpm, depending on the trajectory section and UAV maneuvers. In addition, the average value of the control signals  $U_2, U_3$  is 0.03 Nm, while signal  $U_4$  varies in a range up to 0.06 Nm. Besides, the results confirm that the introduction of the MPC strategy suppresses jumps changes in  $\bar{U}^{PID}$  parameters and provides smoother characteristics in transient process by optimizing the parameters of the controller. Thus, the UAV model can be used as a virtual simulator to study the influence of wind loads on the desired behavior and performance of the aerial platform during flight missions along coastal line. The simulation of wind loads behavior represents a complex task, which requires a set of observations corresponding to a certain time interval, climatic and geographical features of a specific area. With the aim to increase the reliability of the results of wind loads influence on UAV aerodynamics characteristics and adequacy of the designed control system during autonomous surveillance missions, a study of the UAV disturbed motion has been conducted considering a sample of several wind loads observations in the coastal territories of Ecuador. The information was extracted from the database of meteorological stations of the Oceanographic and Antarctic Institute of the Ecuadorian Navy, and National Institute of Meteorology and Hydrology [20], [21].

TABLE III  
NON-DETERMINISTIC WIND LOAD PARAMETERS

Wind load disturbance model	Wind disturbance effect, $\Phi$ [N]	Time interval, $t$ [s]	Velocity range, $V_B$ [m/s]
	$\Phi(t) = [0 \ \Phi^Y \ 0]^T$	$0 < t < t_1$ , $t_4 < t < t_5$	$V_B^X = 0$ ; $V_B^Y = 0, \dots, 3$ ; $V_B^Z = 0$
$\bar{V}_B(t) = V_0 + V_B \sin \Omega t$	$\Phi(t) = [\Phi^X \ \Phi^Y \ 0]^T$	$t_1 < t < t_2$ , $t_3 < t < t_4$	$V_B^X = 0, \dots, 2$ ; $V_B^Y = 0, \dots, 1$ ; $V_B^Z = 0$
	$\Phi(t) = [0 \ 0 \ \Phi^Z]^T$	$t_2 < t < t_3$	$V_B^X = 0$ ; $V_B^Y = 0$ ; $V_B^Z = 0, \dots, 5$ ;

At the first stage of the investigation, have been considered the non-deterministic wind load parameters described in Table III, as well as the continuous random function with normal Gaussian distribution of the equation 7. According to the results shown in figures 13 to 15 the distribution of the wind load in the specified time sections leads to a change in the nature of the deviation of the aircraft angles  $\varphi, \theta, \psi$  in a range up to 0.2; 0.45 and 0.44 rad. Consequently, this affects the UAV positioning accuracy, resulting in deviations of 0.1; 0.28 and 0.13 m along each axis in the specified intervals.

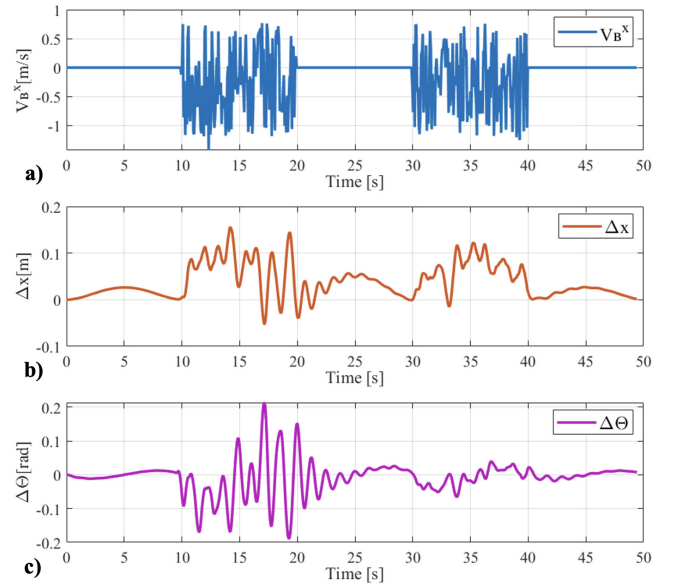


**Fig. 13.** Diagram of the variation in the deviation of the UAV center of mass along the X axis: a – Wind load distribution along the X axis; b – deviation of the UAV movement along the X axis; c – deviation of the UAV center of mass by the pitch angle  $\theta$ .

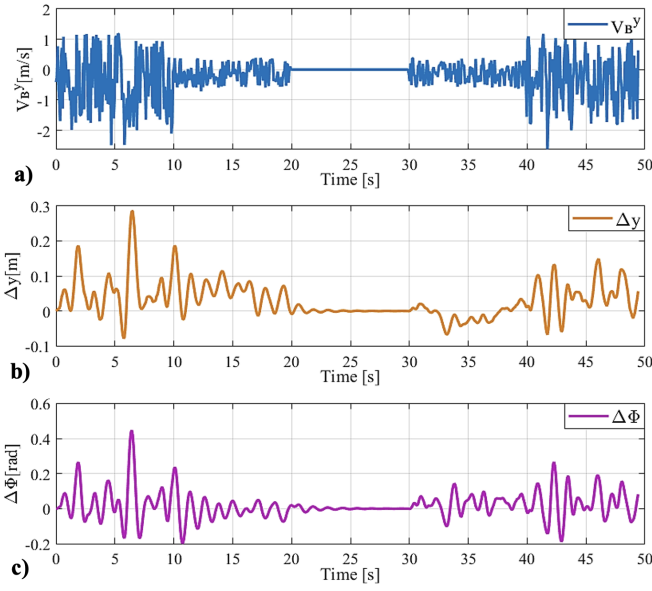


**Fig. 14.** Diagram of the variation in the deviation of the UAV center of mass along the Y axis: a – Wind load distribution along the Y axis; b –deviation of the UAV movement along the Y axis; c –deviation of the UAV center of mass by the roll angle  $\phi$ .

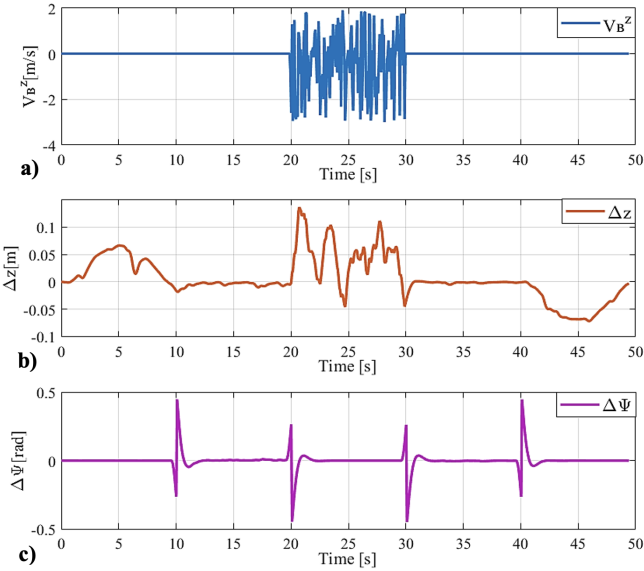


**Fig. 15.** Diagram of the variation in the deviation of the UAV center of mass along the Z axis: a – Wind load distribution along the Z axis; b –deviation of the UAV movement along the Z axis; c –deviation of the UAV center of mass by the yaw angle  $\psi$ .

At the second stage of the investigation, the wind loads deterministic behavior is simulated according to the parameters described in Table IV, including equations 8 to 10.

TABLE IV  
DETERMINISTIC WIND LOAD PARAMETERS

Wind load disturbance model	Wind disturbance effect, $\Phi[N]$	Period T [c]	Duty Cycle %	Velocity range, $V_B$ [m/s]
$V_B(t) = k_1(t)V_0$	$\Phi(t) = [0 \ \Phi^x \ 0]^T$	$t_1 < t < t_2$ , $t_3 < t < t_4$	40, 60	$V_B^x = 1$ ; $V_B^y = 0$ ; $V_B^z = 0$
$V_B(t) = k_2(t)V_0$	$\Phi(t) = [0 \ \Phi^y \ 0]^T$	$t_1 < t < t_2$	100	$V_B^x = 0$ ; $V_B^y = 2$ ; $V_B^z = 0$
$\bar{V}_B(t) = \frac{V_0}{2} + \sum_{n=0}^N V_n \sin(n\omega_0 t)$	$\Phi(t) = [0 \ \Phi^y \ \Phi^z]^T$	$t_1 < t < t_2$ , $t_3 < t < t_4$	10	$V_B^x = 0$ ; $V_B^y = 1.5$ ; $V_B^z = 2$

In accordance with the results presented in figures 16 to 18, the considered wind loads deterministic models represent a significant atmospheric disturbance on UAV performance. However, the UAV control system demonstrates the capability to maintain the center of mass positioning accuracy relative to the specified trajectory within deviations of 0.056; 0.36; 0.27 m along the  $OX$ ,  $OY$ ,  $OZ$  axes, respectively.

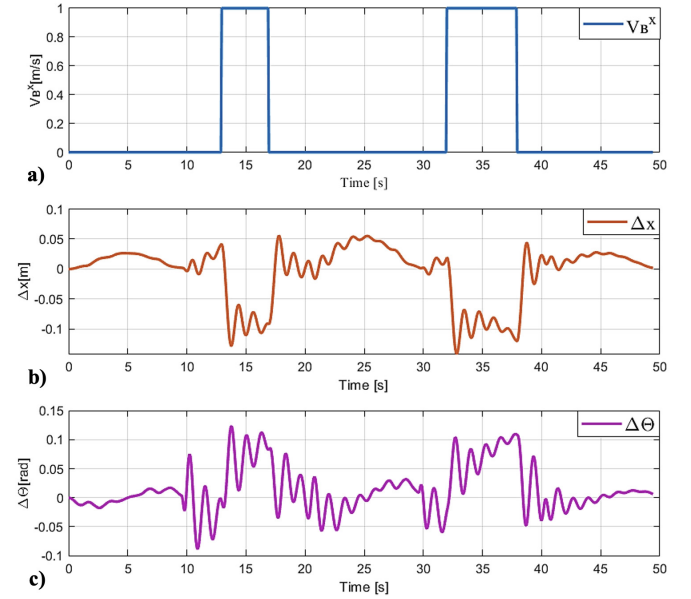


**Fig. 16.** Diagram of the variation in the deviation of the UAV center of mass along the X axis: a – wind load stepwise effect along X axis; b – deviation of the UAV movement along the X axis; c –deviation of the UAV center of mass by the pitch angle  $\theta$ .

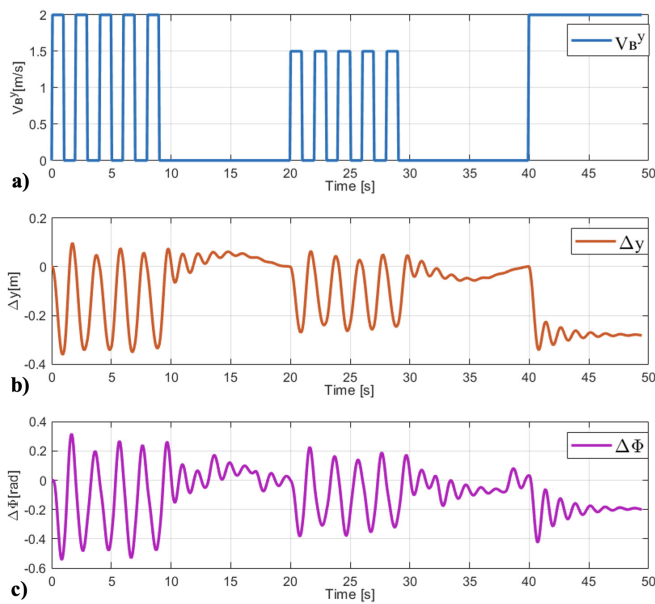


**Fig. 17.** Diagram of the variation in the deviation of the UAV center of mass along the Y axis: a – wind load stepwise effect along Y axis; b – deviation of the UAV movement along the Y axis; c – deviation of the UAV center of mass by the roll angle  $\phi$ .

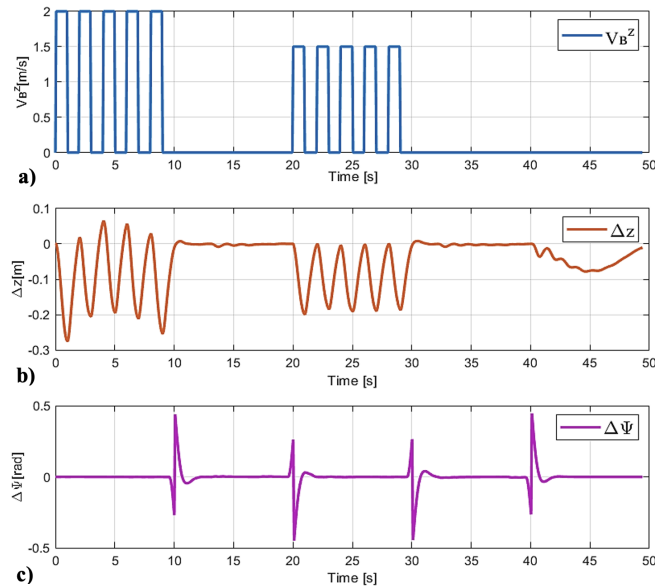


**Fig. 18.** Diagram of the variation in the deviation of the UAV center of mass along the Z axis: a – wind load stepwise effect along Z axis; b – deviation of the UAV movement along the Z axis; c – deviation of the UAV center of mass by the yaw angle  $\psi$ .

#### IV. CONCLUSIONS

This paper addresses the technical monitoring challenges faced by national security services in the coastal territories of Ecuador and proposes the use of an autonomous robotic aerial platform to enhance the efficiency of remote surveillance missions conducted along the coastline. The use of a hierarchical control structure, composed of an adaptive PID based MPC control strategy, optimizes the flight dynamics retaining UAV

robust performance features. Based on the conducted study evaluating the influence of wind load disturbances on UAV controlled motion, it was revealed that deterministic models have a stronger effect on UAV flight dynamics. However, for both models (random and deterministic), the use of the Gaussian normal function and Fourier series decomposition method, respectively, represents a more reliable strategy for simulating the dynamics of air mass movement in a specific territory based on a priori information from meteorological service observations. The introduced wind disturbance models contribute to positioning accuracy deviations up to 0,1; 0,36; 0,27 m along  $OX$ ,  $OY$ ,  $OZ$  axes respectively. Additionally, a delay in the response of the control system to external disturbances at transient values of up to 5 seconds has been registered.

#### REFERENCES

- [1] X. Wang, Z. Huang, G. Sui, H. Lian, "Analysis on the Development Trend of Future UAV Equipment Technology," *Academic Journal of Engineering and Technology Science*, vol. 2, no. 1, pp. 114-121, 2020.
- [2] A.S. Martinez, L.M. Mosquera, O. Emelyanova, "Control System of Small-Unmanned Aerial Vehicle for Monitoring Sea Vessels on Coastal Territory of Ecuador," *Frontiers in Robotics and Electromechanics*, vol. 329, pp. 295-314, 2023.
- [3] B. Fan, Y. Li, R. Zhang, Q. Fu, "Review on the Technological Development and Application of UAV systems", *Chinese Journal of Electronics*, vol. 29, no. 2, pp. 199-207, 2020.
- [4] S. Jatsun, O. Emelyanova, P. Bezmen, A. S. Martinez-León and L. M. Mosquera-Morocho, "Hardware/Software Architecture for Research of Control Algorithms of a Quadcopter in the Presence of External Wind Loads," *Electromechanics and Robotics*, vol. 232, pp. 165-177, 2022.
- [5] A. Correia, P.B. Água, R. Graça, "Machine Learning in Coastal Incident Detection, Identification and Classification with UAV's," in *16th Iberian Conference on Information Systems and Technologies (CISTI)*, 2021, pp. 1-6.
- [6] D.R. Green, J. J. Hagon, C. Gómez, B. L. Gregory, "Using Low-Cost UAV's for Environmental Monitoring, Mapping, and Modelling: Examples from the Coastal Zone," *Coastal management. Academic Press*, pp. 465-501, 2019.
- [7] M. Zurita, W. Aguilar, V. Enríquez, "Toward the Development of Surveillance and Reconnaissance Capacity in Ecuador: Geolocation System," *Developments and Advances in Defense and Security: Proceedings of MICRADS 2019*, pp. 123-136, 2019.
- [8] A. Flores, D. Scipión, C. Saito, J. Apaza, M. Milla, "Unmanned Aircraft System for Andean Volcano Monitoring and Surveillance," in *International Symposium on Safety, Security, and Rescue Robotics (SSRR)*, 2019, pp. 297-302.
- [9] E. A. Valencia, K. A. Palma, I. D. Changoluisa, V. H. Hidalgo, P. J. Cruz, C. E. Cevallos, P. J. Ayala, D. F. Quisi, N. G. Jara, "Wetland Monitoring Through the Deployment of an Autonomous Aerial Platform," *IOP Conference Series: Earth and Environmental Science*, vol. 32, no. 1, 012002, 2019.
- [10] H. Loya, V. Enríquez, F. Salazar, C. Sánchez, F. Urrutia, J. Buele, "Analysis and Determination of Minimum Requirements of an Auto-pilot for the Control of Unmanned Aerial Vehicles (UAV)," in *International Conference on Computer Science, Electronics and Industrial Engineering (CSEI)*, pp. 129-142, 2019.
- [11] D. Mellinger, V. Kumar, "Control and Planning for Vehicles with Uncertainty in Dynamics," *IEEE International Conference on Robotics and Automation (ICRA)*, 2010, pp. 960-965.
- [12] N. Bao, X. Ran, Z. Wu, Y. Xue, K. Wang, "Research on Attitude Controller of Quadcopter Based on Cascade PID Control Algorithm," in *IEEE Information Technology, Networking, Electronic and Automation Control Conference (ITNEC)*, 2017, pp. 1493-1497.
- [13] A. Zenkin, I. Berman, K. Pachkouski, I. Pantiukhin, V. Rzhvskiy, "Quadcopter Simulation Model for Research of Monitoring Tasks," *26th Conference of Open Innovations Association*, 2020, pp. 449-457.

- [14] S. Jatsun, L.M. Mosquera-Morocho, O. Emelyanova, A. S. Martínez-León, "Controlled Adaptive Flight of a Convertiplane Type Tricopter in Conditions of Uncertainty for Monitoring Water Areas," in *2020 International Multi-Conference on Industrial Engineering and Modern Technologies (FarEastCon)*, 2020, pp. 1-7.
- [15] I. Krzysztofik, Z. Koruba, "Analysis of Quadcopter Dynamics During Programmed Movement Under External Disturbance," *Nonlinear Dynamics and Control*, pp. 177-185, 2020.
- [16] S. Jatsun, O. Emelyanova, A.S. Martínez, "Design of an Experimental Test Bench for a UAV Type Convertiplane", *IOP Conference Series: Materials Science and Engineering*, vol 714, no. 1, pp. 012009, 2020.
- [17] A.S. Martínez, S. Jatsun, O. Emelyanova, "Control of the Electric Drives of a Multirotor System Type Convertiplane," *Fundamental and Applied Problems of Technics and technology Journal*, vol. 1, pp. 83-93, 2020.
- [18] S. Jatsun, S. Efimov, O. Emelyanova, A. S. Martínez-León, P. J. Cruz-Dávalos, "Modeling and Control Architecture of an Autonomous Mobile Aerial Platform for Environmental Monitoring," in *2019 International Conference on Information Systems and Computer Science (INCISCOS)*, pp. 177-182, 2019.
- [19] O. Doukhi., A.R. Fayjie, D.J. Lee, "Intelligent Controller Design for Quadrotor Stabilization in Presence of Parameter Variations," *Journal of Advanced Transportation*, 4683912, 2017.
- [20] National Institute of Meteorology and Hydrology INAMHI, (2024, Feb 02) "Aplicativos Web". [Online]. Available: <https://inamhi.website/aplicaciones-web/>
- [21] Oceanographic and Antarctic Institute of the Ecuadorian Navy INOCAR, (2024, Feb 02) "Reporte Meteorológico". [Online]. Available: <https://www.inocar.mil.ec/web/>
- [22] R. Casado, A. Bermúdez, "Simulation Framework for Developing Autonomous Drone Navigation Systems," *Electronics*, 7, 2021.
- [23] B. Lindqvist, S. S. Mansouri, A. Agha-Mohammadi, "Nonlinear MPC for Collision Avoidance and Control of UAV's with Dynamic Obstacles," *Robotics and Automation Letters* vol. 4, pp. 6001-6008, 2020.
- [24] I. Nascimento, A. Ferramosca, L. Pimenta, G. Raffo, "NMPC Strategy for a Quadrotor UAV in a 3D Unknown Environment," in *19th International Conference on Advanced Robotics (ICAR)*, pp. 179-184, 2019.
- [25] A. Ryhlov, "Analysis of Different Distribution Laws Using for Wind Speed Leveling," *Proceedings of Saratov University: Earth Sciences Series*, vol. 10, no. 2, pp. 25-30, 2010

# Evolution of the Polygon of the Protected Natural Area “Parque Nacional Sistema Arrecifal Veracruzano” Due to the Expansion of the Port of Veracruz, Mexico

Xóchitl Citlalli Hernández-Silva<sup>1</sup>, María del Refugio Castañeda-Chávez<sup>2</sup>, Mario Díaz-González<sup>3</sup>, Ángel Morán-Silva<sup>4</sup>, Fabiola Lago-Reynoso<sup>5</sup>, Olaya Pirene Castellanos-Onorio<sup>6</sup>, Jesús Montoya-Mendoza<sup>7</sup>, Manuel Alberto Susunaga-Mirada<sup>8</sup>

**Abstract** — The Port of Veracruz, Mexico was artificially built at the beginning of the 21st century, dredging the sea floor and removing reefs to allow the entry of large ships, which led to a growth in the traffic of goods and people through it, making it the largest commercial port in all of Mexico. In 1992 the Government of Mexico decreed the area of coastal reefs near the Port of Veracruz as a protected natural area with the name of the Parque Nacional Sistema Arrecifal Veracruzano (PSNSAV). In 2013, with the demand of international trade, the decision was made to expand the port, generating job growth in the area and an increase in the flow of containers and automobiles, also have a greater capacity to transport cereals, minerals and fuels. In contrast to the disagreements of the society due to the loss of protected space, the Parks polygon had to be modified. This work try to demonstrated that the construction of the port expansion began previous the presentation to the environmental authorities of the Environmental Impact Statement and the change in the protected limits with the disappearance of the Punta Gorda reefs and the dredging of Vergara Bay for the arrival of deep draft vessels. Through a systematic mapping of the scientific literature combined with satellite mapping and visual interpretation of images, and documentary analysis, we determined the damage to the reef system, which has protected species according to Mexican national regulations.

**Keywords** — PNSAV; Port of Veracruz; Docklands; Mapping; Satellite.

**Resumen** — El Puerto de Veracruz, México fue construido de manera artificial a principios del siglo XXI, dragando el suelo marino y removiendo arrecifes para permitir la entrada de buques de gran tamaño, lo que conllevó a un crecimiento en el tráfico de mercancías y personas a través de él y convirtiéndolo en el mayor puerto comercial de todo México. En 1992 el Gobierno de México decretó en la zona de arrecifes litorales cercanos al Puerto de Veracruz como un área natural protegida con el nombre de Parque Nacional Sistema Arrecifal Veracruzano (PSNSAV). En 2013, con la demanda del comercio internacional, se tomó la decisión de ampliar el puerto, generando un incremento de empleo en la zona y un aumento del flujo de contenedores y automóviles, además de tener una mayor capacidad para transportar cereales, minerales y combustibles. Frente a las disconformidades de la sociedad por la pérdida de espacio protegido, el polígono de Parques tuvo que ser modificado. Con este trabajo se demuestra que la construcción de la ampliación del puerto se inició previa autorización de las autoridades ambientales de la Manifestación de Impacto Ambiental y el cambio en los límites protegidos, lo dicho tuvo inicio con la desaparición de los arrecifes de Punta Gorda y el dragado de la Bahía de Vergara para el arribo de buques de gran calado. A través de un mapeo sistemático de la literatura científica combinado con mapeo satelital e interpretación visual de imágenes, así como el análisis documental, se determinó el daño al sistema de arrecife, el cual cuenta con especies protegidas de acuerdo a la normatividad nacional mexicana.

**Palabras Clave** — PNSAV; Puerto de Veracruz; Zona Portuaria; Mapeo; Satelital.

<sup>1</sup> Tecnológico Nacional de México/Instituto Tecnológico de Veracruz, México. (email: [xochitl.hs@veracruz.tecnm.mx](mailto:xochitl.hs@veracruz.tecnm.mx)). ORCID number <https://orcid.org/0009-0002-5920-7084>

<sup>2</sup> Tecnológico Nacional de México/Instituto Tecnológico de Boca del Río, Boca del Río, Veracruz, México. (email: [mariacastaneda@bdelrio.tecnm.mx](mailto:mariacastaneda@bdelrio.tecnm.mx)). ORCID number <https://orcid.org/0000-0002-9209-0431>

<sup>3</sup> Tecnológico Nacional de México/Instituto Tecnológico Veracruz, México. (email: [mario.dg@veracruz.tecnm.mx](mailto:mario.dg@veracruz.tecnm.mx)). ORCID number <https://orcid.org/0000-0002-9281-2190>

<sup>4</sup> Tecnológico Nacional de México/Instituto Tecnológico Boca del Río, México. (email: [angel.ms@bdelrio.tecnm.mx](mailto:angel.ms@bdelrio.tecnm.mx)). ORCID number <https://orcid.org/0000-0002-7545-2269>

<sup>5</sup> Tecnológico Nacional de México/Instituto Tecnológico de Veracruz, México. (email: [fabiolalango@bdelrio.tecnm.mx](mailto:fabiolalango@bdelrio.tecnm.mx)). ORCID number <https://orcid.org/0000-0001-8359-434X>

<sup>6</sup> Tecnológico Nacional de México/Instituto Tecnológico de Veracruz, México. (email: [olaya.co@veracruz.tecnm.mx](mailto:olaya.co@veracruz.tecnm.mx)). ORCID number <https://orcid.org/0000-0003-3510-2640>

<sup>7</sup> Tecnológico Nacional de México/Instituto Tecnológico Boca del Río, México. (email: [jesusmontoya@bdelrio.tecnm.mx](mailto:jesusmontoya@bdelrio.tecnm.mx)). ORCID number <https://orcid.org/0000-0002-7598-7300>

<sup>8</sup> Tecnológico Nacional de México/Instituto Tecnológico Veracruz, México. (email: [manuel.sm@veracruz.tecnm.mx](mailto:manuel.sm@veracruz.tecnm.mx)). ORCID number <https://orcid.org/0000-0002-5595-0914>

Manuscript Received: 30/11/2023

Revised: 19/02/2024

Accepted: 08/03/2024

DOI: <https://doi.org/10.29019/enfoqueute.1014>

## I. INTRODUCTION

THE City of Veracruz was founded by the Spanish in 1519 [1]. Being in front of a reef area, ships docked at the islet of San Juan de Ulúa located in the reef of La Gallega. Hence, for centuries the process of loading and unloading people and merchandise was carried out in small boats, which allowed the migratory processes and cultural mixing that gave rise to modern Mexico [2]. Between 1880 and 1940, an artificial port with modern infrastructure was built, through the construction of an artificial dock surrounded by jetties and docks, dredging

the seabed to increase the draft and forming a bay. This started a new system of commercial traffic, disappearing the reefs of Caleta and Lavandera, seriously affecting Hornos and Gallega reefs. Between 1940 and 2018, a new expansion of the port facilities was carried out, connecting the Island of San Juan de Ulua with the continental zone, increasing freight transportation capacity. In 2019, the process of port modernization began with the construction of new docking docks to diversify products and services and serve deep-draft ships [3].

On June 1 of 1991, due to the monopoly of loading and unloading operations by the Port Unions, the Government of Mexico requisitions the Port of Veracruz, creating a new state-owned company called *Administración Portuaria Integral de Veracruz S.A de C.V* (APIVER) —currently called *Administración del Sistema Portuario Nacional Veracruz, S.A de C.V* (ASIPONA VERACRUZ)— with which the Secretary of Communications and Transportation (SCT) took administrative and operational control of the country main port, generating free competition and allowing the improvement of services [4].

In July 1993, the Ports Law was published in the Official Gazette of the Federation, which regulates port activities in Mexico in maritime terminals and port facilities, especially their construction, operation, exploitation, and forms of administration, this was reformed in 2021, handing over the administration of ports and port facilities to the Secretary of the Navy of Mexico [5].

In 1992, by decree published in the Official Gazette of the Federation, was established a protected natural area with the category of national park. This was the area of reefs located in front of the coasts of the municipalities of Veracruz, Boca del Río and Alvarado in the state of Veracruz in the waters of the Gulf of Mexico with the name ‘Parque Nacional Sistema Arrecifal Veracruzano’ (PNSAV). Mainly due to its wide biological diversity of great ecological importance, this National Park represents a unique natural resource that provides important ecological, social and economic benefits to the region, but above all to the marine ecosystem of the Gulf of Mexico [6].

Among the environmental services provided by the National Park are, firstly, the provision of food by maintaining nuclei of high biological diversity of great importance for fishing, secondly, cultural and recreational services through activities such as diving, and finally, coastal protection services and infrastructure found in this area. At the same time, it is a buffer for strong meteorological phenomena such as hurricanes and ‘northerns’ that occur in the city and Port of Veracruz and surrounding towns. It is also a regulator of biogeochemical cycles, producing oxygen and capturing carbon dioxide through the fixation of calcium carbonate, a service of great importance in the current climate change scenarios [7].

Mexico is among the 20 largest exporting economies worldwide, which has required having a solid port infrastructure to face the increase in merchandise transportation needs and the diversification of Mexican exports. The Administration of the Port of Veracruz, within the National Port System, presents the greatest diversity of load types, it has seven lines that operate as containers, Agricultural Bulk, Mineral Bulk, General Cargo, Cars, Fluids as Petroleum and Derivatives, which makes it have special characteristics compared to most of the ports in

Mexico. This market brings the greatest diversity of merchandise converges and the greatest variety of cargoes, and a range of vessels with different characteristics, port services and modes transportation, which makes it the main entry and exit of imports and exports to Europe, the Southern United States and South America [8].

The Port of Veracruz is one of the most important ports in Mexico and Latin America, it is the main port of entry and exit for international trade in Mexico and its location is strategic because is located in the Gulf of Mexico and is close to urban and industrial centers from the country [8]. Due to the increasing volume of cargo, the port of Veracruz was overwhelmed in its capacity, it was too small for the demand it had at the time and did not allow the entry of deep-draft container ships. Therefore, in 2014, the project for the construction of a new port began with the aim of increasing its cargo loading management capacity, through a new port for containers, grains and fluids, closest to the existing port area, to a capacity that was projected to handle 4.8 million TEU (twenty-foot equivalent unit) per year, by building new port facilities, such as docks, container yards and railways to connect the new port with the existing one and access roads to the port to avoid the traffic of heavy units in the urban area of the City of Veracruz [9].

The public investment made for the construction of the new Port of Veracruz (which was carried out jointly by the Integral Port Administration and the Government of Mexico during the execution of the project) is public information and may be consulted by those who require it. This investment in Mexican pesos (MXN) was made as follows [10]:

Public Investment:	\$3 895 841 627.00
Studies and Supervision:	\$50 332 635.00
Breakwater:	\$1 289 823 856.00
Dredging:	\$850 000 000.00
Springs:	\$1 037 888 750.00
Highways:	\$31 600 000.00
Services:	\$37 920 000.00
Wastewater treatment plant:	\$25 676 386.00
Maritime signaling:	\$10 000 000.00
River rechanneling:	\$72 600 000.00
Purchase of land for port reserve:	\$400 000 000.00
For damages caused by the new port works:	\$90 000 000.00

The expansion of the port is expected to be complete by 2024 and will cost around 35 billion MXN. With this there are economic and social benefits. In economic terms, the expansion of the port generates greater economic activity and increase local employment. It is estimated that the project will create around 100 000 direct and indirect jobs in the region. This will also increase the competitiveness of the Mexican economy and promote international trade. In social terms, it will have benefits such as the improving the quality of life in the metropolitan area of the city of Veracruz, in terms of economic activity it will have a positive impact on the communities near the port [11].

In a second phase, it is planned to build 35 new berths to provide access capacity for deep-draft vessel, this represents the most important and ambitious work in all of Mexico: ex-

panding the port in an area of 500 hectares in water and 450 on land. This would position Tal as the largest in Mexico, being this project a driver of the economy and generator of thousands of jobs. This is demonstrated in its first months of operations, since there has been a growth in container cargo that has reached 2.3 %, in agricultural bulk approximately 5.7 % and in hydrocarbon cargo it has grown 29.1 % [12]. For the construction of the new Port of Veracruz, the Government of Mexico in 2012 modified the polygonal of the National Park decreed in 1992, with two main purposes: 1) to disincorporate the Punta Gorda reef and Vergara Bay from the PNSAV 2) increase surface area from the park to the south, arguing that both that reef and the bay were immersed in a process of deterioration with no return and should be excluded from legal protection. It is important to mention that the modification of the decree and the PNSAV polygonal in 2012 was also since the port activities were not compatible in any way with the activities permitted in the park in accordance with the 1992 decree. In fact, it is relevant to note that the original polygonal had encapsulated the port of Veracruz, which prevented it from growing (figure 1). With the new polygonal (which disincorporated an important area of the protection polygon adjacent to the port) it was legally allowed for the port to have the necessary area for the execution of the Port of Veracruz Expansion project [3].

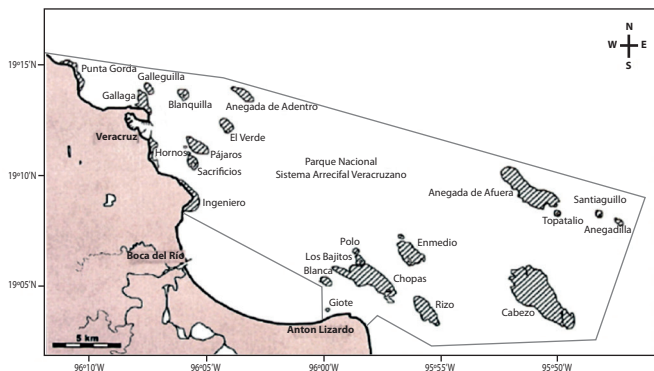


Fig. 1. Original area of PSAV in decree 1992 [12].

The expansion of the Port of Veracruz has generated a series of environmental impacts in the area, which have been the subject of debate and concern among local communities and environmental groups, due to its impact on the environment, the economy and nearby communities [12].

One of the main environmental impacts of the expansion of the Port of Veracruz is the loss of natural habitats in the beach area. The construction of the new container terminal involved the recovery of land that was previously beach areas, which has generated a loss of natural habitats for various species of fauna and flora that inhabit the area. This has been the subject of concern among environmental groups, who have pointed that this

loss of natural habitats can have negative consequences for the ecological balance of the area [13].

Another impact of the port expansion is the increased sedimentation of the marine area. The dredging works carried out to widen the navigation channel and the maneuvering area for ships, which have generated an increase in sedimentation in the marine area, have negatively affected various species of fauna and flora that inhabit the area. This environmental impact indicates that sedimentation can have negative consequences for the marine biodiversity of the area [14]. Another point is the increase in emissions. This expansion increased maritime traffic and land transportation, which generates greater emissions of pollutants into the air and water. This can have negative consequences for the health of the people who live in the area, as well as for the fauna and flora that inhabit it [15].

The purpose of this review is to analyze the four stages of transition from the Port to what is currently the port area. The territory gained from nature for its expansion, its growth and the need to establish environmental indicators are observed. The objective is to control the activities that affect the Veracruz Reef System National Park (PNSAV) and to achieve environmentally friendly port services.

## II. MATERIAL AND METHODS

### A. National Park of the Veracruzano reef System (PNSAV) in Veracruz, Mexico

The National Park named 'Parque Nacional Sistema Arrecifal Veracruzano' (PNSAV) is in the south-central Gulf of Mexico, off the coast of the state of Veracruz, Ignacio de la Llave. Specifically, between the municipalities of Veracruz, Boca del Río, and Alvarado. It consists of 23 individual reef complexes, which are separated by deep channels. The park's coral reefs are home of a great variety of marine life, including more than 700 species of fish, more than 200 species of mollusks, and 11 species of sharks. Additionally, the park is considered one of the most important nesting sites for the hawksbill turtle, which is an endangered species [16].

On November 29, 2012, the decree modifying the 1992 decree was published in the Official Gazette of the Federation, declaring it a Natural Protected Area with the character of National Marine Park. The area called Sistema Arrecifal Veracruzano, with a surface of 52 238 hectares, 91 areas and 50 centimeters, was published on August 24 and 25 of 1992 (its modification took place on November 29 of 2012), in whose First Article it was determined that the total surface of the National Park is 65 516-47-08.05 hectares and includes 28 reefs and six keys or islands. The same as in the Official Gazette of the Federation of November 29, 2012, it is designated as the Veracruzano Reef System National Park (figure 2).

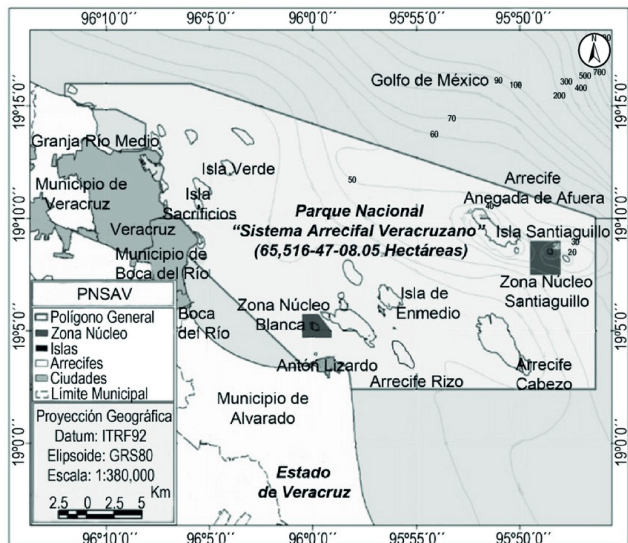


Fig. 2. Location map contained in the decree DOF: 11/29/2012.

It is highlighted that, due to their proximity to the coast, the PNSAV reefs are the most developed reefs in the Gulf of Mexico and are characterized by their resilience to the contribution of fresh water and sediments from the La Antigua, Jamapa and Papaloapan rivers. Coral reefs are the main ecosystem and conservation object of this National Park, they contribute to the mitigation of impacts to the coast caused by storms, hurricanes, and winds such as ‘Nortes’ [17].

*B. Satellite Image Analysis Using gis Tools*

The location of the infrastructure works of the new Port of Veracruz and its coverage area was done through GIS and analysis of satellite images with Google Earth. Some topographic features were also realized through GIS by analyzing satellite images with the use of remote sensing techniques using free-form satellite photographs from Google Earth. For example, available photographs were used with a multi-criteria decision analysis approach (MCDA) (analytical technique that allows identifying several solutions to a problem, using mainly cartographic variables as starting data). Similarly, was used the methodology proposed by Susunaga et al in 2022 [18], due their work observes morphological and area changes, which is useful for this research.

III. RESULTS AND DISCUSSION

*A. Analysis and Observation of Changes in the Polygon of the Protected area Using a Timelapse with the Google Earth Pro tool*

As can be seen in figure 3 (obtained from the Google Earth program with a photographic layer from the year 1992) the polygon decreed in the official journal of the federation of the National Park ‘Parque Nacional Sistema Arrecifal Veracruzano’ included the Punta Gonda reef and the Bay of Vergara, located north of what was once the Port of Veracruz.



Fig. 3. Polygons of the National Park PNSAV in 1992, include Punta Gorda reef and Vergara Bay (Google Earth Pro, historical image with signs).

From 1992 to 2012, the coastal zone of the polygon in the northern zone, which included Vergara Bay, was used as a traditional artisanal fishing zone and as an emerging tourist zone. It was maintained in adequate ecological conditions due to the scarce interconnection with the City of Veracruz. In addition, anthropogenic pollution was scarce, which allowed the observation of migratory birds and coastal fauna such as turtles, crabs and fish in the vicinity of the beach.

For the year 2012, as seen in figure 4, the National Park polygon was modified by decree in the Official Gazette of the Federation. However, the work for the new Port of Veracruz and its expansion had already begun despite this project was not known until 2014. In the figure 4 can see that the Punta Gorda reef was still alive and almost 50 % of it was excluded from the polygon under the argument that it was anthropogenically intervened. In addition, the construction of the port logistics zone had already begun with an area calculated at 1.4 km<sup>2</sup>, and a breakwater had already been built in the northern area of the existing port that allowed it to face the numerous climatological events called ‘Nortes’.



Fig. 4. Polygons of the National Park PNSAV in 2012, exclude Punta Gorda reef and Vergara Bay (Google Earth Pro, historical image with signs).

If we compare the polygon of the original decree of the National Park of 1992 with the modification decreed in 2012 (figure 5) we can determine that the exclusion of Vergara Bay was given to allow the construction work of the new Port of Veracruz. It is called ‘Expansion’, because the project contemplated both rail and logistical interconnection. This park lost a total

area of 11 km<sup>2</sup> in Vergara Bay and in compensation an area was added in the southern zone that included the Pájaros reef, which in total increased the total area of the park.



**Fig. 5.** Comparison of the polygons of the PNSAV National Park, original decree of 1992 and modification of 2012 (Google Earth Pro, historical image with signs).

*B. Analysis and Observation of Changes in the Area of the new port of Veracruz and its Expansion Using a Timelapse with the Google Earth pro tool*

In the first stage of expansion, a growth of 25.8 % has been registered in movements in the port, which denotes that during the period from January to May 2019, 11 million 784 372 tons were registered. While, in the same period, before the expansion 9 million 366 096 tons were recorded, where said entries have been in the categories of agricultural bulk, hydrocarbons, mineral bulk, loose cargo, motor vehicles, non-petroleum fluids, vegetable oils, and others [12].

For this reason, a 10-year period was analyzed, taking the range from 2012 to 2022, and using Google Earth Pro, the modifications that the polygon determined for the nature reserve through the PNSAV were analyzed. The following was observed:

Figure 6 shows the polygon specified in the Diario Oficial de la Federación (delimited in red) off the coasts of the municipalities of Veracruz, Boca del Río and Alvarado. This polygon is formed by a group of 23 coral reefs of great importance due to their scientific, economic, educational, fishing, historical, touristic and cultural value.



**Fig. 6.** Polygon of the PNSAV, with an area of 52,238 ha, whose coordinates are 19°08'N 096°00'W (Google Earth Pro, historical image with signs).

Looking at figure 2, the satellite image from 1992 did not show the beginning of the port expansion works. However, by 2012 (figure 4) can already see the construction of the first logistics areas of the port, which, although they were on land, allow to identify that before the modification of the PNSAV polygon in that year, the port system had already started with the construction of infrastructures, which, when the polygon was modified, were already outside the Arrecifal Marine Park.

Analyzing only the satellite images in the area where the expansion of the Port of Veracruz took place, this process occurred in the area known as North Beach, including the peripheral area of the San Juan de Ulúa Fortress and the PNAV Polygon which is delimited with yellow color (figure 7).



**Fig. 7.** PNSAV polygon and area of the port of Veracruz, Mexico expansion. (Google Earth Pro, historical image with signs, 2012).

In 2012, infrastructure work had not yet begun in the maritime zone, when the relocation of fishermen settled in this area began (figure 7).

By 2013, infrastructure work continued in the ports land area with the construction of more than 1 000 m<sup>2</sup> of new logistics areas, along with the start of construction of the railroad tracks that would connect the port with the rest of the country and the creation of an Environmental Management Unit in a wetlands area that it was decided to conserve (figure 8). It is at this time when access to the beach area was restricted to save peoples safety.



**Fig. 8.** PNSAV Polygon (Google Earth Pro, historical image with signs, year 2013).

In October 2015, can be seen that the expansion of the port works began by filling in the marine area on the Pájaros reef, the construction of the breakwater (which is located within the PNSAV polygon) and the construction of the fluid terminal (figure 9).



Fig. 9. PNSAV Polygon (Google Earth Pro, historical image with signs, year 2015).

In 2016, the construction of 2.5 kilometers of breakwater, the fluids terminal, new docking positions and dredging continued to give greater depth to Vergara Bay for deep-draft vessels (figure 10).



Fig. 10. PNSAV Polygon (Google Earth Pro, historical image with signs, year 2016).

In 2017, filling 550 m<sup>2</sup> began to accommodate the terminals designated in the area for fluid relief (figure 11).



Fig. 11. PNSAV Polygon (Google Earth Pro, historical image with signs, year 2017).

In 2018, the satellite image shows that the filling and growth of said terminal begins, it covers a length of 3.08 km according to the map, and 700 meters from the shore where the beach was inside the sea (figure 12).



Fig. 12. PNSAV Polygon (Google Earth Pro, historical image with signs, year 2018).

In 2019, deforestation is notorious in the area where the expansion works are being carried out. There were complaints in the newspapers about sand reaching the houses near such works. In 2020 and 2021, work continued the land with areas designated for potential assignees to establish their offices at the port (figure 13).



**Fig. 13.** PNSAV Pentagon (Google Earth Pro®, historical image with signs, year 2021).

It can be seen in the satellite image of the year 2021 that the new port of Veracruz begins its operations with the accommodation of vessels and containers.

According to the order presented in the figures, it is shown that the transition stages of the Port from 2011 to 2023 to what is currently the area of the port zone, the territory gained on the shore of the beach (called North Beach) has a total of 2.14 km. This is indicated with a white polygon and the distance with a yellow line (figures 12 and 13), in addition to participating in nature for its expansion and growth. Derived from this, there are deforested spaces, and part of what belonged to the PNSAV Polygon has been taken for works, of which there is no public documentation where it is known whether the mitigation measures specified in the Manifest of Environmental Impact have been followed, where are described preventive measures for the ‘fauna’ indicator (Chapter VI, Page 3, Table 4). It is essential to establish environmental indicators to control the activities that impact the Veracruzano Reef System National Park (PNSAV) and achieve environmentally friendly port services [15].



**Fig. 14.** PSAV Pentagon, Space Mark with construction in Polygon made in yellow, no construction or work for expansion (Google Earth Pro, historical image with signs, year 2023).

Although it is true that Punta Gorda had a decimated coral community with less than 1 % coverage, this should have been evaluated based on the service it provides to the environmental system. It means, be a buffer zone and a sediment trap, which prevents the rest of the reefs from being buried [3].

The construction and expansion of the Port of Veracruz has brought a series of new companies given the growth of international trade by sea, which has also caused conflicts in the metropolitan area of the City of Veracruz. Among, can be mention the increase in the flow of vehicles that transport containers on the entrance highways, since it is an artificial port exposed to inclement weather, it is closed to navigation in some periods, which delays the shipment of goods, requiring the construction of parking lots for cargo vehicles. Additionally during the year 2023 more than one million cars were exported, which have required the construction of logistics zones that have impacted the coastal ecosystem, since most of them are concrete or asphalt slabs, which has created heat islands that have generated the increase in the temperature of the microclimate of the area, which harms the parks reefs, which significantly damages the ecosystem that has been incorporated since 2006 by the United Nations Educational, Scientific and Cultural Organization (UNESCO) to the World Network of the Program Man and the Biosphere (MAB), “Reserve of the Biosphere”.

#### IV. CONCLUSION

This national park is a popular destination for both local and international tourism, which comes to explore the natural beauty of the reef system, its biodiversity with permitted activities such as recreational diving and snorkeling, as well as sport fishing. This place is of utmost importance for scientific research, since scientists from all over the world come to study the ecosystems that exist within the park.

Observing the mapping carried out, the port works, and in accordance with what is specified in the environment impact manifestation initial, have not been completed, since the 3,500-meter-long eastern breakwater still needs to be built. The damage that the PNSAV has received is unknown. In the present analysis with the use of the Google Earth Pro tool, is observed that there is an invasion in the polygon that is registered as a PNSAV protected area, also is observed that there are constructions that affected not only the beaches and reefs that were in the area, but also the flora and fauna of the beaches where the work is carried out are denoted as deforested. It would be important to do one more study on the different consequences that may be generated in the environment, not only due to this expansion but also to know what other factors are affecting it.

One of the most important conclusions of this work is that although the Environmental Impact Statement of the Construction and Expansion of the Port was prepared in 2013, with a project that was planned for 2014. The Comprehensive Port Administration of Veracruz (today ASIPONA See) had already made progress in these works, contravening what is stipulated in the General Law for Ecological Balance and Environmental Protection of Mexico, which establishes that this Environmental Impact Statement must be carried out prior to the start of the works of any project.

This park faces several challenges, including pollution, over-fishing and climate change, which threaten the health and resilience of its coral reefs and the ecosystems that depend on them. Conservation efforts continue, with a focus on reducing pollution, regulating fishing practices, and implementing measures to mitigate the effects of climate change.

Observing the progress over time of the construction work of the new Port of Veracruz and its expansion, we can determine that an artificial bay was created in order to allow the entry of deep draft ships with a considerable number of containers, which will harm the future the vitality of the reefs that are still within the polygon, affecting the reef flora and fauna, since in recent years due to this increase in load, accidents have occurred within the Reef Park.

## REFERENCES

- [1] J. L. Soberanes-Fernández, "Frente a dos aniversarios: XX de Cuestiones Constitucionales y 50. centenario del primer ayuntamiento de México," Cuestiones Constitucionales. *Revista Mexicana de Derecho Constitucional*, vol. 1, no. 46, pp. 383–394, Jun. 2022, doi: 10.22201/ijj.24484881e.2022.46.17063
- [2] P. C. López-Romero, "El huracán que pasó por la ciudad de Veracruz y el puerto de San Juan de Ulúa, Nueva España 1552. La construcción de un 'desastre' en la época virreinal." *Teoría Praxis*, no. 29, pp. 75–88, Dec. 2016, doi: 10.5377/typ.v0i29.6349
- [3] CEMDA, (2024, Feb 28), "El Sistema Arrecifal Veracruzano, Reporte de un Área Natural Protegida Amenazada," [Online]. Available: [https://www.cemda.org.mx/wp-content/uploads/2011/12/PNSAV.Final\\_.pdf](https://www.cemda.org.mx/wp-content/uploads/2011/12/PNSAV.Final_.pdf)
- [4] J. T. Hiskey, "Political Entrepreneurs and Neoliberal Reform in Mexico: The Salinas Requisa of the Port of Veracruz," *Latin American Politics and Society*, vol. 45, no. 2, pp. 105–132, 2003, doi: 10.1111/j.1548-2456.2003.tb00242.x
- [5] C. M. Peyrelongue, "Hub Ports in Mexico: Limitations and Opportunities," *CEPAL Review*, vol. 2002, no. 76, pp. 117–134, 2002, doi: 10.18356/51af2330-en
- [6] I. Winfield, S. Cházaro-Olvera, G. Horta-Puga, M. Arenas-Fuentes, "Macrocrustáceos incrustantes en el Parque Nacional Sistema Arrecifal Veracruzano: biodiversidad, abundancia y distribución," *Revista Mexicana de Biodiversidad*. 81. 165-175. 2010, doi: 10.22201/ib.20078706e.2010.0.219
- [7] P. C. Reyna-González, J. Bello-Pineda, L. Ortíz-Lozano, H. Pérez-España, P. Arceo, J. Brenner, "Incorporating Expert knowledge for Development Spatial Modeling in Assessing Ecosystem Services Provided by Coral Reefs: A Tool for Decision-Making," *Revista de Biología Marina y Oceanografía*, vol. 49, no. 2, pp. 279–292, 2014, doi: 10.4067/S0718-19572014000200008
- [8] A. I. González-Rivera, V. Mugica-Álvarez, R. Sosa-Echeverría, P. Sánchez-Álvarez, V. Magaña-Rueda, G. Vázquez-Cruz, A. Retama, "Air Quality and Atmospheric Emissions from the Operation of the Main Mexican Port in the Gulf of Mexico from 2019 to 2020," *Journal of Marine Science and Engineering*, vol. 11, no. 2, 2023, doi: 10.3390/jmse11020265
- [9] A. Barrero, F. Liaño-Carrera, J. I. Ramírez-Macías, C. Guzmán-Ricardo, "Nuevo Puerto de Veracruz: los sistemas de gestión ambiental como herramienta para el control y seguimiento de los aspectos ambientales en la construcción de megaproyectos de infraestructura," in: *CÁDIZ: del Floreciente S.VIII al Port of the future del S.XXI*, Editorial Dykinson, 2018, pp. 629-367, doi: 10.2307/j.ctv6gqx5t.46
- [10] V. ASIPONA, (2023, Aug 20), "Primer Puerto de México," Veracruz, México: ASIPONA VERACRUZ. [Online]. Available: <https://www.puertoveracruz.com.mx/wordpress/blog/primer-puerto-de-mexico/>
- [11] APIVer, (2023, Sept 14), "Análisis costo-beneficio de la ampliación natural del Puerto de Veracruz en la Zona Norte," Veracruz, México: Administración Portuaria Integral de Veracruz, S.A. de C.V. [Online]. Available: [https://www.puertoveracruz.com.mx/apiver/archivos/IFAI/2012/Libros\\_Blanco/Archivos/Anexos/Docs/GICO3107/CB%20Ampliacion%20Jul%2008.pdf](https://www.puertoveracruz.com.mx/apiver/archivos/IFAI/2012/Libros_Blanco/Archivos/Anexos/Docs/GICO3107/CB%20Ampliacion%20Jul%2008.pdf)
- [12] R. E. Cabello-Pérez, M. G. Andrade-Estrada, J. S. López-Morales, "Situación actual del sector portuario y los objetivos del desarrollo sostenible (ODS): el caso del puerto de Veracruz, México," *Estudios sociales. Revista de alimentación contemporánea y desarrollo regional*, vol. 32, no. 60, pp. e221267, 2022, doi: 10.24836/esv32i60.1267
- [13] Á. J. Fernández, "Crónica del puerto de Veracruz," *Ulúa Revista de Historia, Sociedad y Cultura*, vol. 21, no. 42, pp. 2790, 2023, doi: 10.25009/urhsc.v21i42.2790
- [14] M. Cortez-Huerta, R. Sosa-Echeverría, G. Fuentes-García, R. Durán, P. Sánchez-Álvarez, V. Magaña, A. Retama, "Influence of Particulate Matter on Air Quality due to 'Nortes' Events in the Gulf of Mexico," *Atmospheric Pollution Research*, vol. 14, no. 10, p. 101889, 2023, doi: 10.1016/j.apr.2023.101889
- [15] V. ASIPONA, (2023, Sept 04), "Manifestación de Impacto Ambiental," Secretaría de Medio Ambiente y Recursos Naturales. [Online]. Available: <https://www.gob.mx/profepa/articulos/manifestacion-de-impacto-ambiental-mia>
- [16] L. F. Del Moral-Flores, E. López-Segovia, and T. Hernández-Arellano, "Nuevos registros de peces para el área marina del Parque Nacional Sistema Arrecifal Veracruzano, suroeste del Golfo de México," *Novitates Caribaea*, no. 16, pp. 169–176, 2020, doi: 10.33800/nc.vi16.236
- [17] F. R. Castañeda-Rivero and J. Pech, "Percepción social sobre el Parque Ecológico Estatal Kabah, Cancún, Quintana Roo," 2021. [Online]. Available, doi: 10.13140/RG.2.2.21686.83525
- [18] M. A. Susunaga-Miranda, B. Ortiz-Muñiz, M. del R. Castañeda-Chávez, F. Lango-Reynoso, and M. del C. Hernández-Berriel, "Abandoned Solid Waste Final Disposal Sites in the Sotavento Region of the State of Veracruz, Mexico, Using GIS Tools", *Revista Enfoque UTE*, vol. 13, no. 4, 2022, doi: 10.29019/enfoqueute.853